Landschaftsökologie

Fogwater fluxes above a subtropical montane cloud forest

Inauguraldissertation

zur Erlangung des Doktorgrades der Naturwissenschaften

im Fachbereich Geowissenschaften

der Mathematisch-Naturwissenschaftlichen Fakultät

der Westfälischen Wilhelms-Universität Münster

Vorgelegt von

Eva Beiderwieden

aus Mülheim an der Ruhr

2007

Table of contents

List of figures

List of tables

Chapter 1

Introduction

1.1   Motivation for the project

1.1.1   Montane cloud forest ecosystems

Montane cloud forests are tropical or subtropical evergreen forests that are frequently covered by cloud or mist (Stadtmüller 1987). They typically occur at an altitudinal range between 1200 m and 2500 m above sea level where cloud belts are formed by moist ascending air masses. The average annual rainfall is greater than 2500 mm and the air humidity is mostly near its saturation point. The daily temperature ranges between 12 °C and 21 °C depending on latitude, altitude, aspect, and exposure (Zadroga 1981).

Montane cloud forests are characterized by an extremely high biodiversity with respect to herbs, shrubs, and epiphytes, including high rates of endemic species. The trees of montane cloud forests are generally shorter and heavily stemmed, and the high air humidity promotes the development of mosses, bryophytes, and ferns. Epiphytes play an ecologically important role in cloud interception processes. In addition to that, epiphytes such as "tank" bromeliads and moss "balls" are recognized to have very high water storage capacities and to release the gathered water slowly (Bruijnzeel 2001). The soils of montane cloud forests are typically wet and close to saturation resulting in slow decomposition of organic matter and a peaty and acidic topsoil (Bruijnzeel and Proctor 1995).

The hydrological significance of montane cloud forests is, among other factors, due to the net gain of moisture through cloud water interception by the vegetation and the reduction of evapotranspiration (Hutley et al. 1997). As fog diminishes the solar radiation reaching the vegetation, and the saturation deficit of the foggy air is extremely small, the transpiration rates of montane cloud forests are low (Zadroga 1981). During fog events, the temperature gradients in the canopy profile tend to be more uniform, stable, and generally cooler which might also affect the plant's physiology (Hutley 1997).

Cloud forests became one of the most rapidly disappearing forest ecosystems as the land is continuously being deforested and converted to for example cropland and grazing land (Zadroga 1981; Bruijnzeel and Hamilton 2000; Bruijnzeel 2001; Cayuela et al. 2006). Furthermore, montane cloud forests are threatened by global warming of the atmosphere (Bruijnzeel 2001). The lifting of cloud condensation level affects the

hydrological cycle and has an impact on the ecological scale as well, since the organisms are subjected to extreme changes of their living conditions.

The recognition of montane cloud forests as endangered ecosystems of high ecological significance induced the establishment of several networks such as the "Tropical Montane Cloud Forest Initiative" founded by the World Conservation Union, WWF International, the World Conservation Monitoring Centre, and the UNESCO International Hydrological Programme. The objectives of this initiative are the implementation of an international cooperation on cloud forest conservation and research activities with a special emphasis on the preservation of water catchments and biodiversity (Bruijnzeel 2001).

1.1.2   The Chilan research site

The measurements for this study were carried out at the Chilan research station at 24°35'N and 121°25'E at an altitude of 1650 m above sea level next to the Yuan Yuang Lake nature preserve in north-eastern Taiwan. The area around the study site consists of an old-grown cypress forest (the yellow cypress *Chamaecyparis obtusa* var. *formosana* and the red cypress *Chamaecyparis formosenis*) which constitutes one of the high-quality wood production areas of Taiwan. Around the 1960s, a patch of the old growth was cut down, and the stands were left for regeneration. Within that regenerated plantation, a 1 ha stand was established as a research site in 2002 (Chang et al. 2006).

The Chilan study site is part of the long-term ecological research program sponsored by the Taiwan National Science Council in cooperation with the Taiwan Forest Research Institute, the Institute of Botany of the Academia Sinica in Taipeh, the National Dong Hwa University, and other universities. The goal of the program is to assess the biogeochemical cycles of the ecosystem with an emphasis on the role of fog deposition and its effects on the endemic cypress forest. The yellow cypress is the predominant tree species. It accounts for 82 % of the total basal area and has a density of 1820 stems per hectare. The average tree height is 13.7 m and the cypress plantation is characterized by a homogeneous canopy structure (Figure 1.1). The study site was chosen as a long-term research site due to the even-aged stand and the relatively homogeneous topography (the plantation slopes gently with an angle of 14° towards southeast), which is rare at that altitude in Taiwan (Chang et al. 2006). Hsia et al. (2004) point out that due to its excellent fetch conditions, the Chilan research site is well suited to study atmosphere-canopy-interactions using micrometeorological methods.

Fog occurs almost every day at the study site. The highest duration of fog with an average of 14.2 hours per day is observed in November, and the lowest fog duration is found in July with 2.7 hours per day (Chang et al. 2006). Liao et al. (2003a) report that the reduction of solar radiation through fog droplets as well as the constant exposure to the acidic fog water represent important ecological factors for the growth of the cypress forest.

The climate of the study site is characterized as temperate heavy moist (Chou et al. 2000). The air temperature is relatively low with an annual mean of 13 °C. The annual rainfall is on average greater than 4000 mm (Hwang et al. 1996).

Much effort has been taken to study the distribution of the cypress forest since both *Chameacyparis* species are highly appreciated in Taiwan (*e.g.*, Su 1984; Jen 1995). On the one hand, the hardwood is of great economic value due to its strong resistance against termites and fungi (Kuo et al. 2004) and its typical purple-pink coloring (red cypress). On the other hand, the wood has symbolic significance in the Taiwanese heritage and culture. According to pollen analysis, the cypress forest around the Yuan Yuang Lake nature preserve exists for at least 4000 years (Chen and Wu 1999).

Figure 1.1: Aspect of the homogeneous cypress plantation at the Chilan research site.

1.2   Objectives of this study

The scope of this study is to research the ecological conditions of the Yuan Yuang Lake nature preserve with a special emphasis on fog as the key factor determining the vegetation structure. The endemic appearance of both *Chamaecyparis* species at the mid-altitudes (1000 m to 2000 m above ground level) in the subtropical montane cloud forests of Taiwan is not fully understood. The light environment of the cloud forest is strongly influenced when fog is present due to the reduction of solar radiation. Fog may thus be the decisive factor in the ecological competition of the forest vegetation.

In order to investigate the specific role of fog water in the hydrological and nutrient cycle of the montane cloud forest ecosystem, the thesis is focused on the following aspects:

- Direct measurements of fogwater fluxes from the atmosphere to the forest canopy,

- the influence of fog on the energy budget of the ecosystem,

- the collection of fog water samples and its chemical analysis,

- the quantification of the nutrient input through occult deposition,

- and the relevance of nutrient input through occult deposition (fog water) compared to wet deposition (rain).

1.3   Structure of this thesis

This thesis consists of five papers that all address the question of how fog water influences the ecological processes of a montane cloud forest in Taiwan. The collected papers have been accepted for publication or submitted to peer-reviewed journals or conference proceedings. Each paper emphasizes a different research question. All aspects taken together provide a comprehensive investigation of the impact of fog on the ecological conditions of the cypress forest.

Chapter 1 provides a general introduction to the ecosystem "montane cloud forest" and presents the Yuan Yuang Lake nature preserve where the field work for this study was performed. Furthermore, some fundamentals about the characteristics of atmospheric turbulence are mentioned. Based on that, the eddy covariance method to determine the turbulent fogwater fluxes is explained. The actual introductions to the individual research topics and approaches follow in the respective papers.

Chapter 2 deals with the influence of fog water on the energy budget of the Yuan Yuang Lake nature preserve. In the paper, two experimental periods (11 days with clear weather and 5 days with foggy conditions) at the Chilan research site were compared with regard to the energy budget of the ecosystem.

Chapter 3 concentrates on the study of simultaneous evapotranspiration and deposition of fog droplets. By using two different methods (the Bowen ratio method and the eddy covariance method), positive water vapor fluxes were measured despite saturated conditions. The interlinking of the water fluxes and the energy budget of the ecosystem is shown by means of a representative fog event.

Chapter 4 deals with the nutrient input through occult and wet deposition into the cypress forest. The event based nutrient input during the 47-day experimental period was calculated and evaluated with regard to its relevance for the ecosystem. The path of the air masses during the last 120 hours before reaching the study site was computed by the help of backward trajectories.

Chapter 5 is focused on the pattern of fog events and the quality of the eddy covariance data. The regime of the fog event was analyzed with an emphasis on the energy balance and the radiation balance of the ecosystem. The data quality was evaluated by means of micrometeorological parameters.

Chapter 6 concentrates on the influence of fog water on the CO_2 and water vapor fluxes of the forest ecosystem. The response of the CO_2 and water vapor fluxes as a function of the light conditions of the cypress forest was studied. Additionally, the light use efficiency of the *Chamaecyparis* species and other environmental conditions to perform photosynthesis during foggy conditions were analyzed.

Chapter 7 provides a general synthesis of the study. The results of the different research aspects are linked together, and an outlook for further research is given.

1.4 Working hypotheses

Considering former studies performed in cloud forests or comparable ecosystems, the following working hypotheses are suggested:

- The appearance of both endemic *Chamaecyparis* species is supposedly related to the occurrence of fog.

- The reduction of solar radiation during fog is assumed to affect the energy budget of the cypress forest.

- The ion concentrations of fog water are expected to be higher than those of rain.

- The chemical composition of the fog water is presumably influenced by the pathway of the air masses.

- The nutrient input through occult deposition is assumed to provide a significant contribution to the nutrient budget of the ecosystem.

1.5 Fog water deposition

1.5.1 Fog water

Fog water is recognized to be the key factor sustaining the ecological functions of montane cloud forests. It accounts for a significant hydrological and nutrient input to forest ecosystems (Weathers and Likens 1997; Chang et al. 2006) and may influence the biogeochemistry of the ecosystem (Dawson 1998). It has been widely reported that the concentration of chemical compounds is several times higher in fog water than in precipitation (Schemenauer et al. 1995; Igawa et al. 1998; Bridges et al. 2002; Beiderwieden et al. 2005). Many studies have shown that fog water exhibits particularly high concentrations of ions related to anthropogenic activity such as H^+, NH_4^+, NO_3^-, and SO_4^{2-} (*e.g.,* Klemm and Wrzesinsky 2007). The differences of ion concentrations between fog water and rain are assumed to result from the altitude of the formation

processes. Fog, also referred to as a stratocumulus cloud with contact to the surface, represents the lower layer of the atmosphere which is more strongly influenced by surface emissions. Rain droplets originate at higher altitudes where the atmosphere is less polluted from ground-based emissions (Bridges et al. 2002). Another reason for the concentration differences may be the droplet size. Rain droplets are normally much larger than fog droplets and therefore they may be more diluted or less concentrated, respectively.

The deposition by means of fog droplets has been defined as "occult" precipitation since it is not recordable by standard rain gauges and is thus not included in precipitation measurements (Dollard et al. 1983). The quantification of fogwater deposition is still a challenge in the field of atmospheric research due to its instrumental requirements and methodological difficulties. Different methodological approaches such as the modeling of fogwater deposition (Lovett 1984; Pahl 1996; Weathers et al. 2000; Chang 2006), the estimation of the fogwater deposition by weighing plants before and after the fog event (Trautner and Eiden 1988; Chang et al. 2002), water balance methods (Bruijnzeel 2001) or other indirect methods were applied to quantify the fogwater deposition. In recent studies, a direct micrometeorological technique to measure the deposition fluxes of fog water has been realized, *i.e.* the eddy covariance method (Beswick et al 1991; Vong and Kowalski 1995; Kowalski and Vong 1999; Vermeulen et al. 1997).

1.5.2 Atmospheric turbulence

In the planetary boundary layer, the horizontal transport of quantities such as moisture, heat, momentum, and pollutants is dominated by the mean wind (advection), and in the vertical direction by turbulent exchange. The turbulence of the planetary boundary layer is principally generated by forcings from the ground, such as thermal turbulence due to solar heating of the surface (buoyancy effects as a result of air density variations with height) or mechanical turbulence as a result of frictional drag. The strength of the mechanical turbulence depends on the wind speed and the surface roughness. Turbulent elements are defined as irregular, quasi-random variations or gusts that last for durations of seconds to minutes (Stull 1988). By averaging, for example, the instantaneous horizontal wind speed U measured over a certain time period (*e.g.*, 30 minutes intervals), we can differentiate a mean wind and a turbulent part of the wind:

$$U(t) = \overline{U} + u'(t) \qquad\qquad\qquad (1.1)$$

Turbulent elements are defined as a type of motion (Stull 1988). As temperature, moisture, and atmospheric scalars are carried by these turbulent movements, their measurements can be divided into a mean and a turbulent component:

$$c = \overline{c} + c' \qquad\qquad\qquad (1.2)$$

These short term variations (the turbulent component of Equation 1.2) are induced by small-scale swirls of motion, *i.e.* eddies. The intensity of such eddies depends on the wind velocity, the characteristics of the surface, and the stratification of the atmosphere (Liljequist and Cehak 1990). The superposition of many eddies of various scales accounts for the atmospheric turbulence (Stull 2000).

1.5.3 Estimation of fogwater fluxes

The deposition of fog water to the ecosystem is based on two processes, the turbulent deposition and the gravitational settling. The importance of both deposition processes depends on the droplet size as well as on the wind speed and the characteristics of the vegetation cover. In general, the turbulent deposition is higher over forest canopies than over grasslands due to the more pronounced roughness of the forest canopy. Additionally, the leaf area index of trees, especially of conifers, is larger than of grass promoting the impaction of fog droplets (Trautner 1988; Thalmann 2001).

Since the estimation of fogwater fluxes is the fundamental method used in this study, the basic concept is explained in the following section.

1.5.3.1 Gravitational settling

Sedimentation, *i.e.* the gravitational settling of fog droplets, was calculated using the Stoke's sedimentation velocity v_s (Beswick 1991) according to

$$v_s = \frac{g d^2 (\rho_{water} - \rho_{air})}{18 \eta_{air}} \qquad (1.3)$$

where g is the acceleration due to gravity [m s^{-2}], η the dynamic viscosity [kg m^{-1} s^{-1}], d the droplet diameter [m], and ρ the density [kg m^{-3}].

The gravitational settling contribution D_{sed} [kg m^{-2} s^{-1}] was determined by multiplying the sedimentation velocity v_s [m s^{-1}] by the liquid water content LWC [kg m^{-3}]:

$$D_{sed} = \sum_i v_{s,i} \cdot LWC \qquad (1.4)$$

1.5.3.2 Turbulent deposition

The turbulent deposition of fog droplets, driven by the turbulent exchange between the forest canopy and the atmosphere, was calculated by means of the eddy covariance method. The eddy covariance approach is based on the assumption that each air parcel moving due to turbulent motion carries air scalar properties such as momentum, temperature, gases, aerosols, and liquid water, *e.g.* fog droplets.

Applying Reynolds averaging and assuming that $\overline{w'} = 0$ and $\overline{c'} = 0$, the turbulent vertical flux of a scalar c (*e.g.*, the liquid water content) can be expressed as

$$F_c = \overline{w' \cdot c'} \qquad\qquad\qquad (1.5)$$

where F_c is the turbulent flux of the scalar c [*e.g.*, kg m^{-2} s^{-1}], w is the vertical wind component [m s^{-1}], and c is the concentration of the scalar [*e.g.*, kg m^{-3}]. The prime denotes the instantaneous turbulent fluctuation of the individual measurement from its average during the 30 minutes interval. The overbar indicates the time average of the 30 minutes interval. The averaging interval has been chosen to cover all relevant turbulence elements.

For a valid application of the eddy covariance method, some assumptions need to be considered (Stull 1988; Foken 2003):

- Steady state condition of the vertical wind component w and the scalar c during the 30 minutes averaging interval (Foken and Wichura 1996),

- horizontal homogeneity of the underlying surface ensuring that all sensors are located within the same footprint (horizontal exchange processes can thus be neglected and only the vertical transport has to be considered),

- Taylor hypothesis (turbulence elements pass the sensors as "frozen" elements, *i.e.* the horizontal wind speed translates the turbulence elements as a function of time to their corresponding measurement in space) (Stull 1988),

- and the use of fast-response sensors to quantify the respective scalar (temporal resolution of 10 - 20 Hz).

If an adequate technique is available, the measurement of the turbulent fluxes by means of the eddy covariance method is possible for all air components. In recent years, appropriate instruments have been developed for air constituents like CO_2 and water vapor (*e.g.*, the LI-COR 7500), ozone, or methane. Using slower sensors, the turbulent components will be filtered by the instrument response, resulting in incorrect fluxes (Stull 1988). Negative fluxes are directed downward and indicate deposition into the ecosystem. In contrast, positive fluxes are directed upward and indicate emission out of the ecosystem.

1.5.3.3 Total fogwater deposition

The total fogwater deposition D_{total} was calculated by adding the gravitational and the turbulent deposition contributions:

$$D_{total} = D_{sed} + D_{turb} \qquad\qquad\qquad (1.6)$$

The total fogwater input of each 30 minutes interval [kg m^{-2}] was derived by multiplying the fog deposition rates [kg m^{-2} s^{-1}] by 1800 s. The nutrient input through fog deposition [mg m^{-2}] was estimated by multiplying the total fogwater deposition

[L m^{-2}] by the average nutrient concentration of the corresponding fogwater sample [mg L^{-1}].

1.5.4   Experimental

The experimental work for this thesis was carried out during three field campaigns at the Chilan research station. The first campaign took place in February and March 2005. The second experimental phase was carried out in September and October 2005, and the third field experiment was performed in August and September 2006. The plugging diagram (Figure 1.2) shows the schematic arrangement of the instrumental devices.
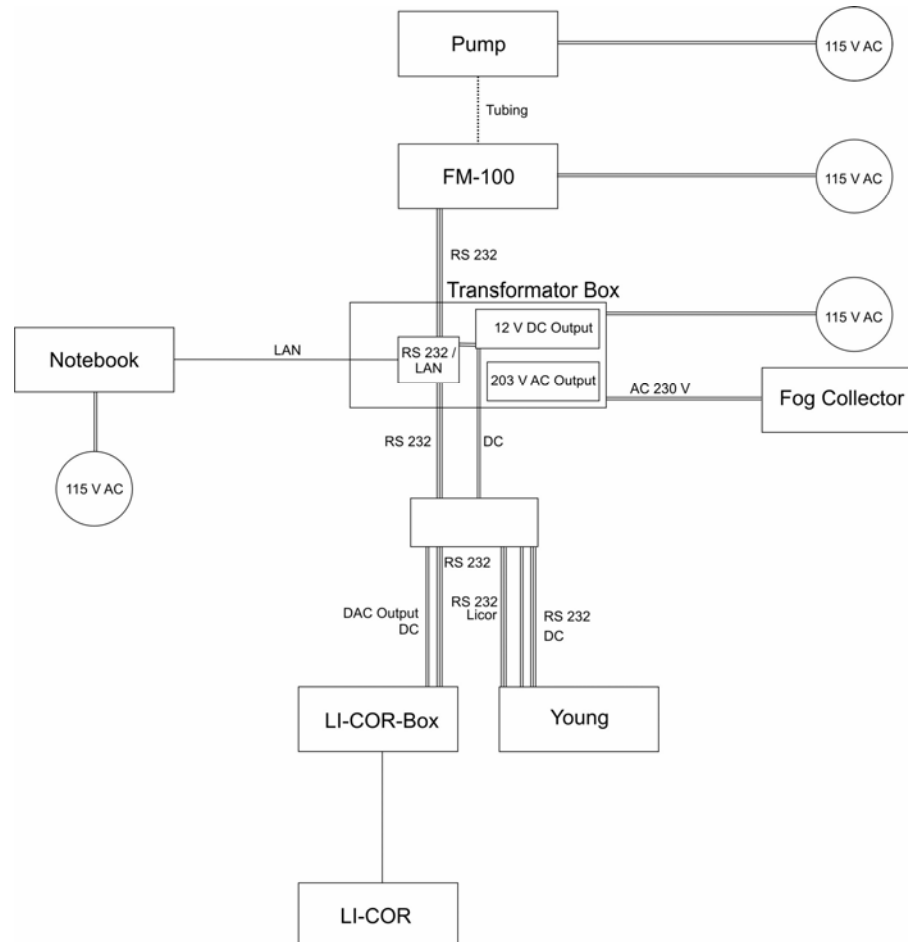
Figure 1.2: Plugging diagram of the instrumentation used to study the fogwater deposition at the Chilan research site.

The experimental setup to measure the fogwater deposition by means of the eddy covariance method and the nutrient input through occult deposition consisted of three main components:

- Fog droplet spectrometer,
- ultrasonic anemometer,
- and fog water collector.

The instruments for the eddy covariance measurements were mounted at 23.4 m above ground level on the uppermost platform (about 10 m above the average tree height) of a meteorological tower within the cypress plantation (Figure 1.3). The meteorological data (*e.g.*, temperature, air pressure, air humidity, visibility, and radiation components) used for this study were taken from the standard instrumentation available at the Chilan research station.

Eddy covariance setup:
- Fog droplet spectrometer,
- ultrasonic anemometer,
- and CO_2/H_2O gas analyzer.

Active fogwater collector
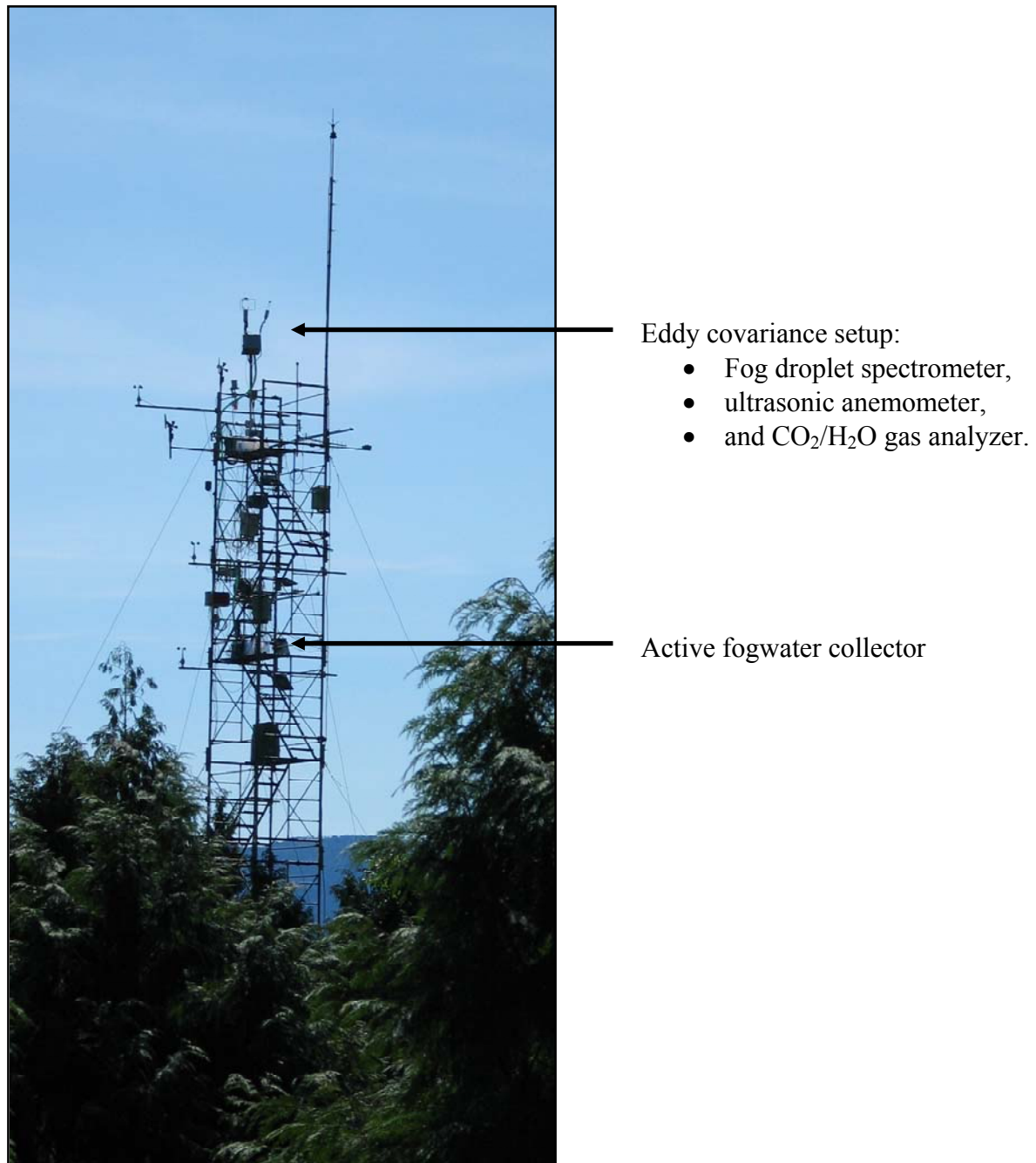
Figure 1.3: Meteorological tower at the Chilan research station

1.5.4.1   Fog droplet spectrometer

A fog droplet spectrometer (model FM-100) developed by Droplet Measurement Technologies (Boulder, Colorado, USA) was used to determine the liquid water content of foggy air (Figure 1.4). The FM-100 detects the number and size of the fog droplets by measuring the light scattering intensity when the air sample passes through a laser beam. The laser beam area of the instrument is 0.285 mm^2. The FM-100 recorded the spectra of fog droplets with diameters ranging from 2 µm to 50 µm within 40 channels. Through a vacuum tubing, the FM-100 was connected to a pump that pulled the foggy air through the instrument. The mean airflow was around 13 m s^{-1}.

Before and after each field campaign, the fog droplet spectrometer was calibrated. For calibration, standard glass beads with a specified diameter of 14.5 µm were injected into the measuring section of the instrument. The diameter distribution of the calibration beads always showed the expected maximum.
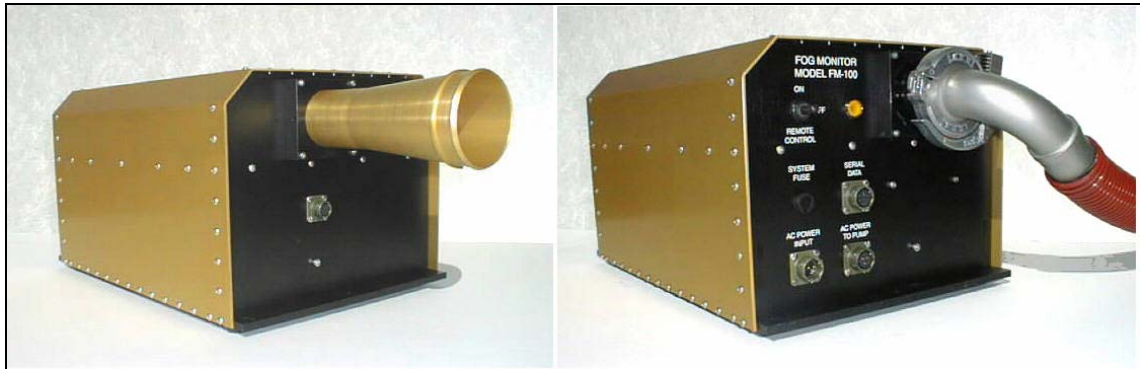
Figure 1.4: Front and back of the fog droplet spectrometer (FM-100).

1.5.4.2   Ultrasonic anemometer

An ultrasonic anemometer (Model 81000) manufactured by R.M. Young (Traverse City, Michigan, USA) was employed to measure the three-dimensional wind speed, *i.e.* the *u*, *v*, and *w* wind components (Figure 1.5). It operates at wind velocities from 0 m s^{-1} to 40 m s^{-1} within a temperature range from -50 °C and +50 °C. The resolution of the anemometer is 0.01 m s^{-1}. During the field campaigns, the anemometer was operated at a frequency of 12.5 Hz. The instrument measures the travel time of ultrasonic signals between the three sensor pairs. The time between sending and receiving a signal pulse depends on the wind speed and the air density.

Figure 1.5: Ultrasonic anemometer (Young 81000) to measure the three-dimensional wind velocity.

1.5.4.3 Fog water collector

In order to collect fogwater samples for the analysis of the chemical composition, an active strand fogwater collector was used (Figure 1.6) (Wrzesinsky 2000). The foggy air was pulled through the instrument by a fan with a consistent velocity of 8 m s^{-1}. Due to their inertia, the fog droplets impacted on the collection harps. The collected fog water flowed along a tube downward into an automated ISCO-sampler (Lincoln, New England, USA). The sampling area of the fog collector was 650 cm^{-2}. Fog collection was triggered by visibility measurements at the meteorological tower. Whenever the visibility was below 1000 m (foggy conditions), the fog collector was switched on and operated.

Figure 1.6: Active fogwater collector mounted at the meteorological tower.

Chapter 2

The impact of fog on the energy budget of a subtropical cypress forest in Taiwan

E. Beiderwieden[*1], O. Klemm[1], and Y.-J. Hsia[2]

[1]Institute for Landscape Ecology, University of Münster, Robert-Koch-Str. 26, 48149 Münster, Germany.

[2]Graduate Institute of Natural Resources, National Dong Hwa University, Shoufeng, Hualien 974, Taiwan.

[*]corresponding author

Abstract

Results of energy balance measurements during an 11 day period under clear weather, and a 5 day period under foggy conditions are presented. The single most important factor discriminating the two periods was the intensity of solar radiation. During fog, a reduction of incoming shortwave radiation of up to 95 % was found. Using the eddy covariance method, turbulent fluxes of CO_2, latent heat E, and sensible heat H, were measured. The energy balance EB was positive (26 W m^{-2}) under clear conditions, resulting in a gain of energy for the ecosystem. In contrast, during the presence of fog, EB remained negative (-15 W m^{-2}) indicating a loss of energy. For both situations, EB was not completely closed. Possible reasons for this finding are discussed. The ratio of available energy and the sum of turbulent fluxes E, H, and soil heat flux S during the clear and foggy period was examined for daytime and nighttime conditions. The CO_2 flux exhibited a diurnal cycle with negative fluxes in the daytime associated with CO_2 uptake by the vegetation. The average CO_2 fluxes of -7.8 μmol m^{-2} s^{-1} during clear conditions and -3.2 μmol m^{-2} s^{-1} during foggy conditions indicate that the ecosystem benefits from clear weather conditions.

Key words: eddy covariance, energy balance, fog, forest ecosystem, radiation balance, cypress forest.

霧對亞熱帶扁柏林能量收支的影響

Eva Beiderwieden*[1], Otto Klemm[1], 夏禹九[2]

摘要

本文陳述棲蘭山扁柏天然更新林11天晴日及5天霧日的能量收支量測結果。晴日及霧日最大的差異為日輻射強度；當霧籠罩之際，日輻射量最低會減少95%。使用渦度相關法量測的二氧化碳、可感熱及蒸發潛熱，顯示晴日之時能量平衡值為正值（+26 W m^{-2}），林分獲得能量。相反的在霧日，能量平衡值為負值（-15 W m^{-2}），林分喪失能量。不論在晴日或霧日能量都未完全平衡，本文對此一結果有進一步的討論，並分別檢視白天及夜間淨輻射量與可感熱、蒸發潛熱及土壤熱通量三者總和之比率。二氧化碳通量則呈現日變化，自天為負值，亦即此一林分吸收二氧化碳。在晴日二氧化碳通量平均為 -7.8 μmole m^{-2} s^{-1}，而有霧時則僅達 -3.2 μmole m^{-2} s^{-1}，因此晴日對此一林分的能量收支而言是有利的。

關鍵詞：渦度相關法、能量平衡、霧、森林生態系、輻射能平衡、扁柏森林。

2.1   Introduction

Exchange of CO_2 and energy fluxes, such as latent and sensible heat fluxes across the biosphere/atmosphere interface, are climatic factors of essential importance. Particularly in the tropics and subtropics, where the solar radiation is of larger magnitude than in the temperate zone, the energy budget of an ecosystem is strongly influenced by the latent and sensible heat fluxes. Yet, minor changes in solar radiation and cloudiness have a strong impact on the radiation budget and, consequently, on the energy balance of an ecosystem. The reduction of shortwave radiation during fog events is suggested to be a crucial ecological factor determining vegetation composition.

Due to intensive instrumental requirements and complex ambient conditions, only a few direct measurements of fog water and gas fluxes in montane ecosystems exist. In the present study, we compare eddy covariance flux data collected in November 2005 during clear weather conditions with those obtained in September 2002 during foggy conditions (Klemm et al. 2006) to assess the influence of fog water in the closure of energy balance. The experiments were carried out within an endemic cypress cloud forest in Taiwan. Understanding of structure and function of forest ecosystems is of major interest for Taiwan since 52 % of the island is covered by forest (Chou et al. 2000). In cloud forest ecosystems, fog water is a significant contribution to the hydrological cycle and an important source of nutrients and pollutants (Elias et al. 1995; Cavellier et al. 1997; Bruijnzeel and Veneklaas 1998; Clark et al. 1998; Dawson 1998; Weathers et al. 2000; Chang et al. 2002). Water input through fog deposition is estimated to comprise up to 30 % (Schatzmann 1999) or 48 % (Holder 2004) for mountainous ecosystems, depending on cloud characteristics, wind speed, and vegetation structure (Bruijnzeel and Veneklaas 1998). For the experimental site Chilan, fog deposition comprises 10 % of the total hydrological input (Chang et al. 2006), and is estimated to contribute > 50 % to the total nutrient input (Chang et al. 2002). Frequent and continuous occurrence of fog deposition yields the complex functioning of the hydrological cycle and energy budget of this montane cloud forest. Fog water is therefore suggested to play a dominant role in these biogeochemical cycles. We compare two typical but different weather periods, with the objective to elucidate the impact of fog in the energy budget and CO_2 flux of an endemic cypress forest.

2.2   Materials and methods

2.2.1   Study site

The present study was carried out within the Chilan Nature Preserve in the northeastern part of Hsinchu County in a subtropical montane forest in Taiwan. The Chilan research site is located at 24°35'N, 121°24'E at 1650 meters a.s.l. on the eastern slope of the Syue-Shan Mountain Range. The measurements were performed on a 23.4 m high

meteorological tower (10 m above maximum canopy height) within a 300 hectare homogeneous yellow cypress plantation (*Chamaecyparis obtusa* var. *formosana*) with a slope of 15° towards SE (120°). The canopy is virtually closed and uniform, tree heights range from 10 to 13 m (Hsia et al. 2004). *Chamaecyparis obtusa* var. *formosana* and *Chamaecyparis formosensis* are the predominant tree species, and *Rhododendron formosanum* prevails in the understory of the cypress-forest.

The Chilan site has a temperate heavy moist climate (Chou et al. 2000). It is characterised by high annual rainfall of more than 4000 mm (Chen and Chiu 2000) and a mean annual temperature of 13 °C. No apparent wet and dry seasons occur. Heavy clouds are frequent and the average fog duration is 4.7 to 11.0 hours per day (Chang et al. 2002). The annual frequency of fog occurrence often exceeds 350 days (Chang et al. 2006). At the experimental site, two main wind directions exist, namely winds from SE and N/NW (Figure 2.1).
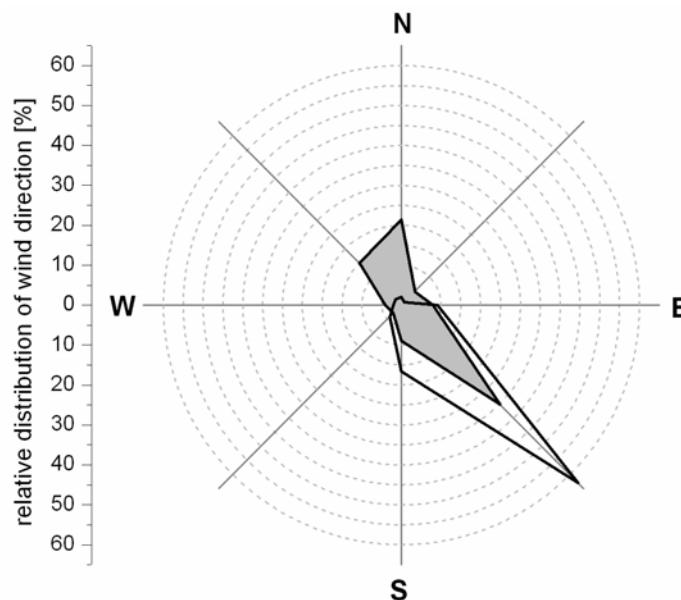
Figure 2.1: Relative distribution of wind direction [%] at the experimental site Chilan measured from March through November 2005. Grey shaded area: average wind direction of the entire period; transparent area: average wind direction during fog events.

The wind regime proceeds in a well pronounced regular diurnal cycle. During daytime, winds from SE persist for several hours. Fog occurs typically during the afternoon hours (Figure 2.2) and is quite strictly associated with winds from SE. At night, downhill winds from N and NW prevail (Hsia et al. 2004; Klemm et al. 2006). Solar radiation at the study site is reduced notably by the presence of fog (Chang et al. 2002; Liao et al. 2003b) influencing the energy budget of the cypress forest.
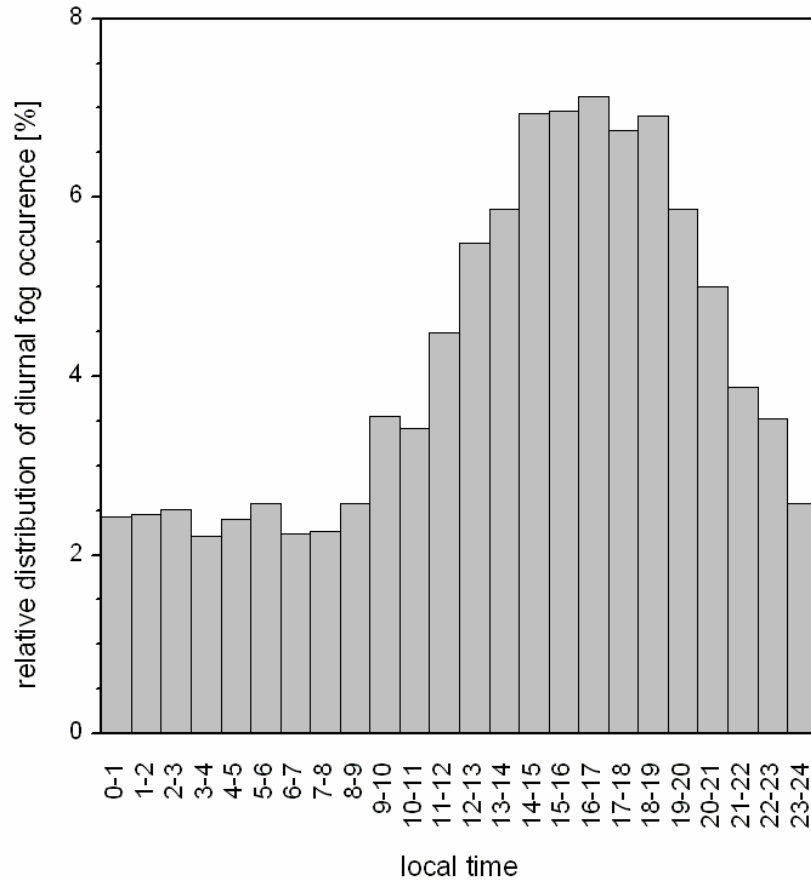
Figure 2.2: Distribution of the diurnal cycle of fog occurrence at the Chilan site from September through November 2005 using 10-minutes averages.

2.2.2   Instrumentation

The experimental setup was installed at the Chilan site to study the CO_2 flux, latent heat, and sensible heat fluxes within a subtropical cypress forest. It consisted of a Young ultrasonic anemometer, and an open path LI-COR 7500 combined infrared CO_2/H_2O-analyzer. The Young ultrasonic anemometer (Model 81000)[1] records three-dimensional wind speed (u, v, w) data from 0 to 40 m s^{-1}, the sonic temperature from -50 °C to +50 °C. The LI-COR 7500 open path CO_2/H_2O-analyzer[2] operates at temperatures ranging from -25 °C to +50 °C and was synchronized with data from the sonic anemometer. The radiation components (*i.e.*, the incoming and reflected solar radiation plus the incoming and emitted long wave radiation) were measured employing a Kipp & Zonen CNR 1 net radiometer. Standard meteorological data (*e.g.*, temperature, air humidity, and visibility) and soil heat flux data were taken from the routine data acquisition by the Dong Hwa University at Hualien.

---

[1] R. M. Young Company, 2801 Aeropark Drive, Traverse City, Michigan 49686, USA

[2] LI-COR Biosciences, 4421 Superior Street, P. O. Box 4425, Lincoln, NE 68504, USA

2.2.3   Data processing

The eddy covariance data were collected by a portable computer at 12.5 Hz sampling frequency. The meteorological data were stored every 10 minutes by using a data logger and reflect the average value over each time interval. The experimental tower was equipped with 115 V AC power supply. Communication of the Young anemometer and the computer was performed via a RS 232 serial interface.

The turbulent deposition was determined with the eddy covariance technique. In the present study, the eddy covariance method was applied for the calculation of vertical turbulent fluxes F_x of CO_2, latent heat, and sensible heat. Following the Reynolds averaging, the flux F_x on an entity x can be quantified as

$$F_x = \overline{w'x'} \tag{2.1}$$

where w' is the short term deviation of vertical wind speed w and x' is the concentration fluctuation of scalar x from their average. The primes denote the deviations from the mean values and the overbar indicates the time average of the sampling interval (*e.g.*, 30 minutes).

Raw data were recorded continuously using the in-house software "Aquisio". After the removal of apparent outliers resulting from technical problems, data were computed by the in-house software "DANA". The following processing steps were conducted:

- Coordinate rotation of u, v, and w wind components using the planar fit method,
- detrending of the data sets calculating the moving averages (1200 sec intervals) of the scalar data,
- Webb correction (Webb et al. 1980),
- determining time lag values by cross correlation,
- and computing turbulent fluxes.

2.2.4   Data quality

All flux data were subjected to strict data limits to reject implausible values. The eddy covariance method requires the following assumptions: stationarity of the observed time series (30 min), horizontal homogeneity, and a well developed turbulence regime due to stationarity of atmospheric conditions. To test the stationarity of each 30-minute interval, the variance $w'x'$30 min was computed and compared with the variance of the six 5-minute intervals $w'x'$5 min of the same time period (Foken and Wichura 1996). If the deviation was less than 30 %, the averaging interval was assumed to be stationary. Following the classification of data quality by the steady state test (Foken et al. 2004), averaging intervals with a deviation up to 50 % can be used for fundamental research. Time series which are determined not to be in steady-state (stationarity > 50 %) were excluded from further analyses. The spatial homogeneity of the surface is a given due to the area of 300 hectares of the cypress plantation with a uniform canopy (Hsia et al.

2004). The friction velocity u_* characterizes the development of the turbulence regime. Particularly during night time, atmospheric layering can be stable and turbulence may not be pronounced. For the calculation of the turbulent fluxes, only data with $u_* > 0.1$ m s^{-1} were considered. Overall, daytime data were of better quality than those of night time due to a better developed turbulence regime.

2.2.5   Energy balance

Closure of the energy balance may be used to evaluate the quality of eddy covariance measurements at a given site (Aubinet et al. 2000; Wilson et al. 2002; Foken et al. 2004; Klemm et al. 2006). Former studies (Klemm et al. 2006) confirmed the suitability of the study site for these measurements. The energy balance residual EB, is expressed in terms of the net radiation Rn, soil heat flux S, sensible heat flux H, and the latent heat flux E:

$$EB = Rn - S - H - E \ [W\,m^{-2}] \tag{2.2}$$

The net radiation balance Rn is the sum of incoming solar radiation $SW\downarrow$ (wavelength $\lambda < 4$ µm), reflected solar radiation $SW\uparrow$, incoming long wave radiation $LW\downarrow$ (4 µm $< \lambda < 50$ µm), and emitted long wave radiation $LW\uparrow$:

$$Rn = SW\downarrow - SW\uparrow + LW\downarrow - LW\uparrow \ [W\,m^{-2}] \tag{2.3}$$

Formulation of the energy balance of an ecosystem assumes that the available energy Rn is larger or equal to the sum of sensible heat flux, latent heat flux, and soil heat flux. Here, the closure of energy balance EBC is calculated after (Foken 2003)

$$EBC = \frac{EB}{(-Rn - S)} \ [\%] \tag{2.4}$$

Another method to evaluate the energy balance closure was applied computing the energy balance ratio EBR (Marth 1998; Gu et al. 1999; Wilson et al. 2002):

$$EBR = \frac{\sum (E + H)}{\sum (Rn - S)} \tag{2.5}$$

2.3   Results

The incoming shortwave radiation was reduced notably during foggy conditions (Figure 2.3 and Figure 2.4). Over the sampling periods in September 2002 and November 2005, a reduction of shortwave radiation of up to 95 % during foggy conditions was detected (the mean reduction during foggy conditions was 34 %). This severe reduction of available short wave radiation is enhanced through an increase of the albedo from the value of 0.10 for clear conditions to 0.12 for foggy conditions. Figure 2.3 and Figure 2.4 show *EB, H, H, S, Rn*, temperature, visibility, and wind direction for two clear and two foggy days, respectively. After sunrise, *Rn* became positive and accordingly after sunset, *Rn* decreased to negative values. This transition also coincided with the change of wind direction from SE to N. The wind regime is imbedded into a large land-sea-breeze-circulation. After noon, warm and water vapour saturated air masses from SE reached the study site. An additional regional scale mountain-valley wind system, caused by thermal heating on the slopes, intensified the advection of clouds that formed during adiabatic rise. The formation of fog during wind from SE is consequently of orographic nature, being a result of forced lifting and cooling of air during the uphill transport. In contrast, during night time, downhill winds from the N and NW prevail. This advection of relatively dry and cool air led to dissipation of fog by adiabatic warming. The coherency of fog and wind direction during the experimental period was tested using a binary logistic regression. In 69 % of the cases, the occurrence of fog was correctly predicted by wind direction (from southern and eastern direction). The presence of fog at the Chilan site is thus strongly associated with wind from SE. Figure 2.1 confirms the predominance of SE winds during the presence of fog.

In Table 2.1, the results of *EB, EBC*, and *EBR* of the clear (2005) and foggy (2002) period are shown. The average net radiation is 115 W m^{-2} during clear conditions, whereas during foggy conditions *Rn* was only 91 W m^{-2}. The average *EB* was 26 W m^{-2} during the clear period and had a negative value of -15 W m^{-2} during foggy conditions. The turbulent fluxes *E, H*, and *S*, respectively, were slightly higher compared to those during the clear situation.

Energy flux data were tested statistically. A Kolmogorov-Smirnov test led to rejection of the hypothesis that *E, H, S*, and *EB* are normally distributed and hence, the non-parametric Mann-Whitney test was applied. Differences of *EB* between clear and foggy conditions were found to be significant ($p < 0.05$), whereas those of *E, H*, and *S* are statistically not significant.
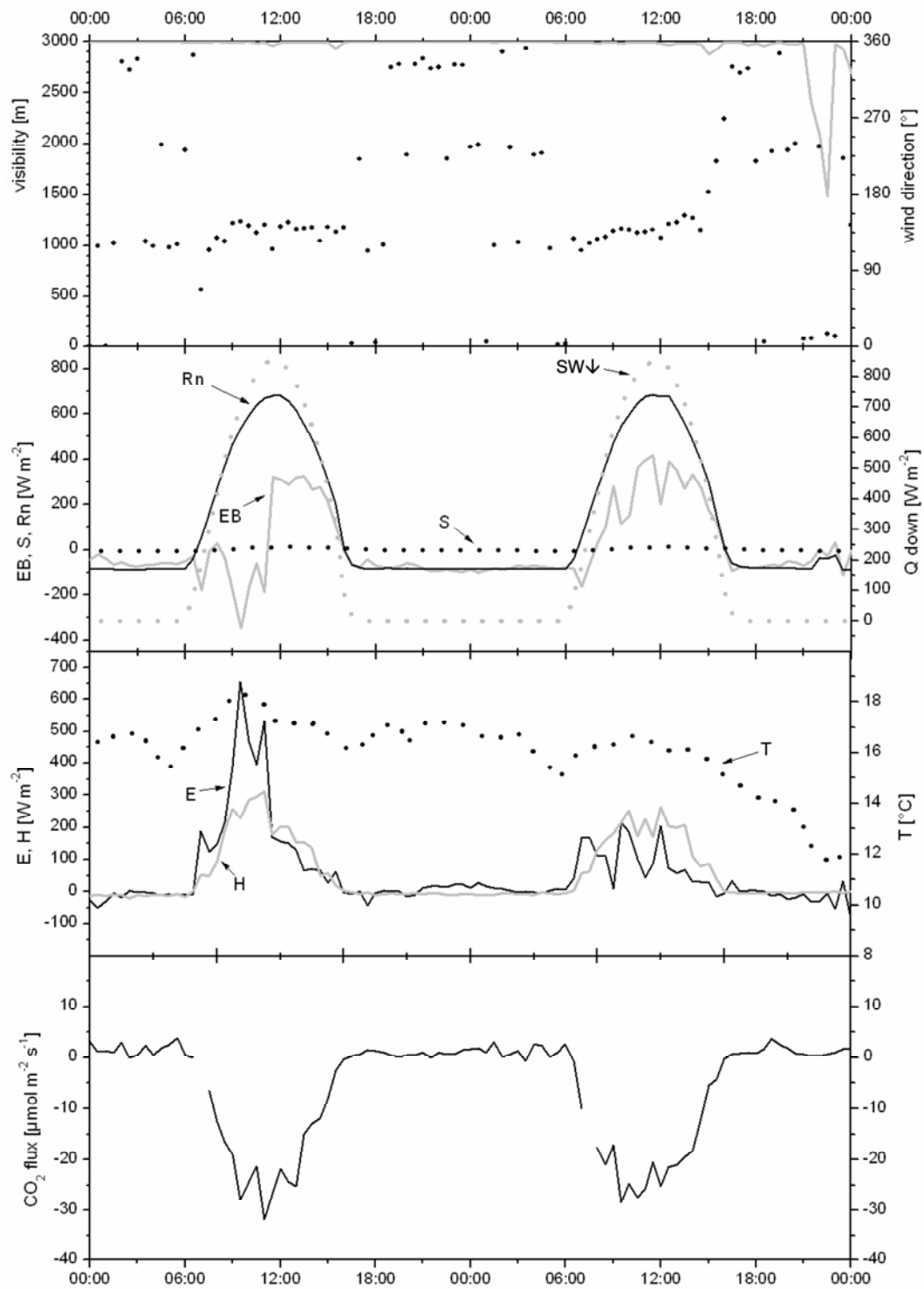
Figure 2.3: Typical diurnal variations of visibility and wind direction (top panel), energy balance, soil heat flux, radiation balance, and incoming shortwave radiation (second panel), latent heat, sensible heat, and temperature (third panel), and the CO_2 flux (bottom panel) during two clear days (03/11/2005 and 04/11/2005, Chilan site).
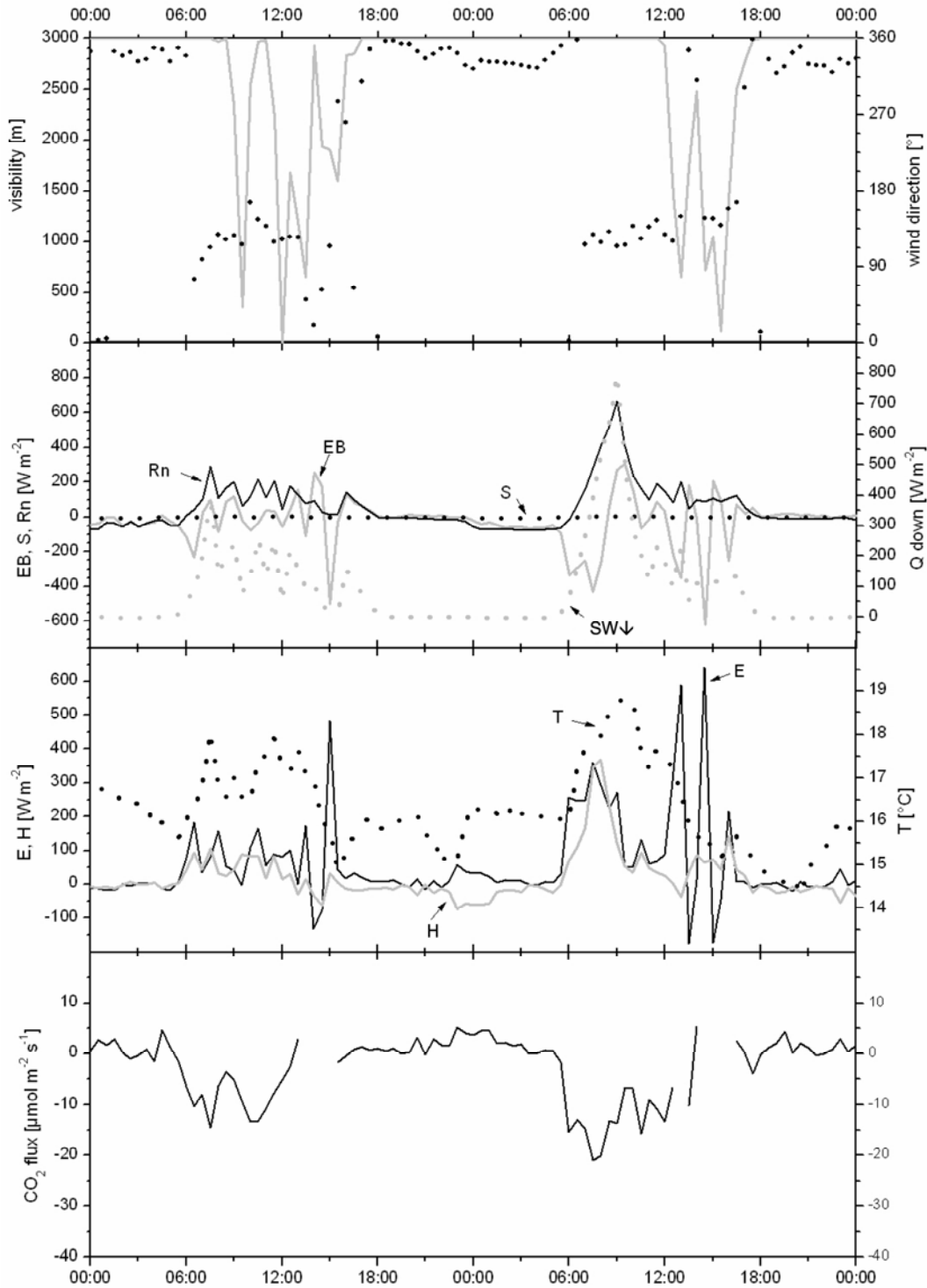
Figure 2.4: Typical diurnal variations of visibility and wind direction (top panel), energy balance, soil heat flux, radiation balance, and incoming shortwave radiation (second panel), latent heat, sensible heat, and temperature (third panel), and the CO_2 flux (bottom panel) during two foggy days (01/09/2002 and 02/09/2002, Chilan site).

Table 2.1: Mean values of radiation balance Rn, latent heat flux E, sensible heat flux H, soil heat flux S, sum of E+H+S, energy balance residual EB, energy balance closure EBC, and energy balance ratio EBR measured at the Chilan site.

Parameter	Unit	Clear 11 days	Foggy 5 days
Rn	W m^{-2}	115	91
E	W m^{-2}	49	61
H	W m^{-2}	41	46
S	W m^{-2}	-1	-1
EB	W m^{-2}	26	-15
EBC	%	-22	17
EBR	−	0.8	1.2

During the clear period, *EBC* was -22 % and *EBR* was 0.8. Under foggy conditions, *EBC* was 17 % and *EBR* was 1.2. Differences in the relation of the available energy *Rn* to *E+H+S* subdivided into daytime (6 a.m. to 6 p.m.) and nighttime (6 p.m. to 6 a.m.) as well as into clear and foggy conditions are summarized in Table 2.2. Figure 2.5 presents the ratio of *Rn* to the sums of the turbulent fluxes *E, H*, and *S* graphically, the 1:1-lines denote the equilibrium of both parameters.

Table 2.2: Relation of Rn to E, H, and S under clear and foggy conditions at daytimes and at night.

Time	Weather condition	Rn [W m^{-2}]	E+H+S [W m^{-2}]	Relation of Rn to E+H+S
daytime	clear	291	192	Rn>E+H+S
daytime	foggy	223	226	Rn≤E+H+S
nighttime	clear	-66	-13	Rn<E+H+S
nighttime	foggy	-53	-23	Rn<E+H+S

During clear conditions in daytime, available energy *Rn* was substantially larger than the sum of turbulent fluxes *E, H,* and *S*. In daytime under foggy conditions, the relation of *Rn* to *E+H+S* was more or less balanced, even though *Rn* was lower. The imbalance of energy budget was most pronounced during nocturnal periods. At night as well as during foggy conditions, the sum of turbulent fluxes was higher than the net radiation *Rn*.

The average air temperature was 16.6 °C and rather stable during the foggy period. In contrast, for the clear period, the average temperature was 13.3 °C, with more pronounced variation.

The CO_2 fluxes within the cypress forest exhibit diurnal behavior with CO_2 deposition during daytime and upward fluxes at night under clear as well as foggy conditions. During the clear period, the average CO_2 flux into the cypress forest was -7.8 µmol m^{-2} s^{-1} (Figure 2.3) while during foggy conditions, the average CO_2 flux was -3.2 µmol m^{-2} s^{-1} (Figure 2.4).
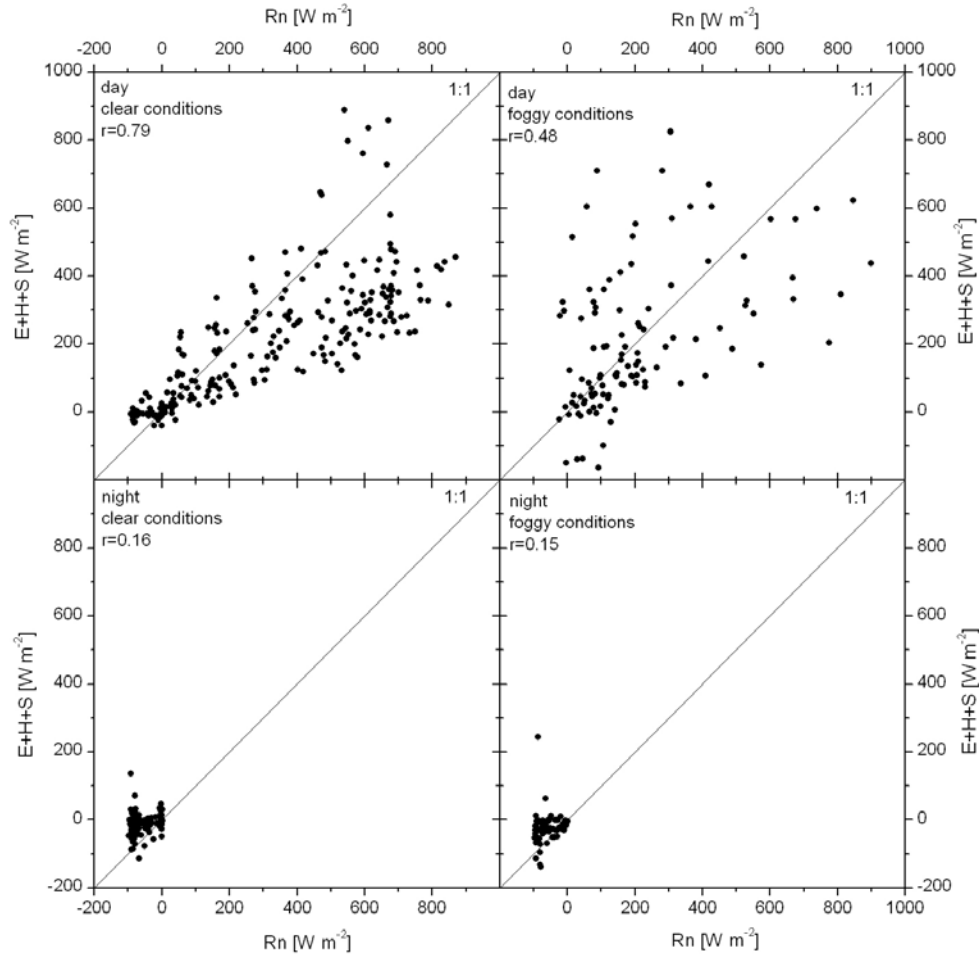
Figure 2.5: Ratio of the sum of turbulent fluxes E, H, and S to available energy Rn during clear conditions at daytime (6 a.m. to 6 p.m.), foggy conditions at daytime, clear conditions at night time (6 p.m. to 6 a.m.), and foggy conditions at night time. The 1:1-line and the correlation coefficient r are given in each section.

2.4   Discussion

Results of energy balance measurements during an 11 day period under clear weather and a 5 day period under foggy conditions were compared. The prime issue of this study was to estimate the impact of fog in the energy budget of a subtropical forest ecosystem. Due to the naturally sufficient availability of water and nutrient supply, solar radiation input is presumed to be a key factor determining the productivity of subtropical forests. The energy balance and the CO_2 flux were examined to evaluate the effect of fog on the ecosystem.

The shortwave incoming radiation was reduced heavily due to reflection and absorption of solar radiation by fog. Less radiation energy is available to the ecosystem. We found that the available radiation energy *Rn* remarkably exceeds the sum of *E, H,* and *S* only during daytime when there is unrestricted solar radiation without fog. It is striking that during periods of reduced solar radiation due to fog, *Rn* was lower than *E+H+S*. These

conditions are normally just typical for the night time. In other words, the advection of warm and saturated air masses from SE, associated with the formation of fog, leads to a turnover of the energy budget for the ecosystem at the Chilan site.

The loss of energy from the ecosystem was most pronounced during nocturnal periods (Figure 2.5) when Rn was negative as a result of the absence of solar radiation and net upward longwave radiative cooling (Stull 1988).

During the clear period, EB was positive and EBC negative signifying a gain of energy for the cypress forest. The ecosystem warmed up and retained energy by temporal storage in the vegetation and, to a lesser degree, the soil.

It is remarkable that the average latent heat flux E is larger during the foggy period than the clear one. The little higher value for latent heat flux E during foggy conditions is suggested to result from re-evaporation of deposited and intercepted fog water. The data in Figure 2.4 show that typically at the end of a fog event E increased noticeably and at that time, the EB became negative. This fact demonstrates the influence of E on EB.

After the strict data quality control procedure, the experimental site Chilan appeared appropriate for energy balance measurements with the eddy covariance method. The friction velocity u_* stated a pronounced turbulence regime, especially in the daytime. The calculated EBC for both the clear and foggy period match those of other studies that state values for EBC between 10 % and 37 % (Foken 2003) and show that EB was better closed under foggy conditions. Differences in EBC of -22 % for clear and 16 % for foggy conditions are therefore suggested to be considerable but the absolute values remain in the same order of magnitude. The lack of energy balance closure is considered to be on the order of approximately 15 % to 30 % by different authors and surfaces (Wilson et al. 2002; Foken 2003). The dimensions of the absolute values of EBR also agree well with literature data (Wilson et al. 2002). Potential reasons for the energy balance closure problem are widely discussed (Foken and Oncley 1995; Wilson et al. 2002; Culf et al. 2004; Foken et al. 2004; Heusinkveld et al. 2004) and different explanations are offered. Instrumentation errors of the measurement technique are supposed to be influencing variables for non-closure of the energy balance. For example, the accuracy of net radiometers influences the calculation significantly, as the net radiation comprises a large portion in the energy balance (Foken et al. 2004). Another problem is the exact determination of the soil heat flux S (Foken et al. 2004; Heusinkveld et al. 2004) due to the difficult measurement of heat storage in the soil. Other approaches attribute the problem of energy balance closure to land surface heterogeneity (Panin et al. 1998; Raabe et al. 2002). The typical averaging interval of 30 minutes for eddy covariance measurements may possibly not be adequate in heterogeneous landscapes such as montane forests to detect advection due to longer wavelengths. The advection in homogeneous terrain is assumed to be marginal (Heusinkvfeld et al. 2004). For this study, flux divergences due to horizontal advection could not be quantified since only one meteorological station was available. As the study site is located in mountainous terrain, an influence of advective fluxes on the

residuals in energy balance closure cannot be ruled out. Methodological problems such as different scales and balance layers may also generate inaccuracies. Furthermore, the observed time period may not be appropriate because of seasonal or diurnal effects. The concept of energy balance requires closure over longer periods such as a vegetation period, or an annual cycle. The data basis for this study, a 5- and an 11-day period, respectively, may not be fully representative for an evaluation of the energy balance closure. The consideration of a short-time period may cause temporal storage and energy sinks in the vegetation or soil.

We recognized the difficulties of energy balance measurements and considered the aforementioned constraints. Nevertheless, the application of correction methods and rigorous data quality control minimize the influence of measurement errors and lead to a plausible data set. Our focus lies in the comparison of a clear with a foggy period under otherwise identical conditions (site, instrument setup), so that many potential sources of inaccuracy are not relevant for this comparison. Moreover, in forest ecosystems with dense canopy layers such as the cypress forest studied here, little solar radiation reaches the surface and energy storage due to soil heat storage is of low significance (Culf et al. 2004). Figure 2.3 and Figure 2.4 show that the diurnal cycles of soil heat flux at the Chilan site were not very pronounced and closely balanced in the course of a day. Furthermore, the relatively homogeneous canopy height of the cypress plantation should minimize the generation of additional turbulent structures leading to inhomogeneities in the data sets. Overall, the difference of *EB* between foggy and clear days is statistically different.

The CO_2 flux is assumed to be a criterion to evaluate the energy input of an ecosystem. During daytime, plants open the stomata, assimilate, and metabolize carbon dioxide; the vegetation acts as a sink of CO_2. Photosynthesis is driven by shortwave radiation and increases with light intensity. Therefore, the rate of assimilation and CO_2 uptake is strongly related to solar radiation. The comparison of the CO_2 fluxes also indicates the gain for the ecosystem during clear conditions. During foggy conditions, the average CO_2 flux was smaller. Lower net radiation led to reduced photosynthesis and thus, less CO_2 uptake by the forest. The actual photosynthesis rate depends on the characteristics of the cypress in respond to the photosynthetic active radiation. Furthermore, fog water might cover the leaf surface that the pathway of CO_2 is blocked and no gas exchange occurs. Additional experiments are needed to prove the metabolism.

2.5   Conclusions

The present energy balance study accounts for a more detailed understanding of micro-meteorological processes of cloud forest ecosystems. The comparison of energy balance during clear and foggy conditions revealed the high significance of fog in the energy budget of the cypress forest at the Chilan site.

Although the closure of the energy balance was within acceptable limits for the clear and foggy conditions, the systematic differences between both states were striking. Under clear conditions, which may be associated with clouds at higher altitudes, the forest ecosystem apparently gained energy: the fluxes of sensible heat (H), latent heat (E), and into the soil (S), did not balance out the net radiation. During foggy conditions, the flux of solar radiation was limited. The incoming longwave radiation was higher during the foggy conditions because the fog itself was relatively warm. However, the total incoming radiation was considerably lower than during non-foggy conditions. In fog, H and E were reduced, but in total higher than Rn.

It is not clear what this net energy loss during fog means for the metabolism of the plants. We suspect that some species may be adapted better to these circumstances than others and that the energy budget may be one important factor leading to specific plant communities in the mountainous tropical cloud forest ecosystems.

It is known that forests act as CO_2 sinks, above all in the case of unrestricted solar radiation and unlimited availability of water. During foggy conditions, less CO_2 deposits into the cypress forest. In cloud forests, water is suggested not to be a limiting factor and therefore, the amount of radiation is assumed to be limiting for CO_2 assimilation.

More detailed experiments should be conducted to estimate the energy balance of these sensible ecosystems in more detail. Such studies should be conducted over a longer time period. Additional instrumentation is required to better quantify the energy storage in the ecosystem and the soil flux. Furthermore, the role of horizontal advection should be analyzed in more detail. In 2006, a second experimental tower will be set up at the Chilan site.

Chapter 3

It goes both ways: measurements of simultaneous evapotranspiration and fog droplet deposition at a montane cloud forest

E. Beiderwieden[*1], V. Wolff[1,2], Y.-J. Hsia[3], and O. Klemm[1]

[1]Institute for Landscape Ecology, University of Münster, Robert-Koch-Str. 26, 48149 Münster, Germany.

[2]now at Max-Plank-Institute (Otto-Hahn-Institiute), Johann-Joachim-Becher-Weg 27, 55128 Mainz, Germany.

[3]Graduate Institute of Natural Resources, National Dong Hwa University, Shoufeng, Hualien 974, Taiwan.

[*]corresponding author

Abstract

Fluxes of latent heat, sensible heat, and water vapor, including turbulent deposition of fog droplets, were measured for two months in autumn 2005 within a subtropical montane cypress forest in Taiwan. The goal of the study was to determine whether significant evapotranspiration can occur during foggy conditions. Water vapor fluxes, Q_w, as determined with the Bowen ratio method, were compared to those simultaneously measured with the eddy covariance method. The median Bowen ratio was 1.06, and the median Q_w flux was $5.2 \cdot 10^{-5}$ kg m^{-2} s^{-1}. The vertical gradients of temperature and water vapor pressure over the forest, ΔT and Δe, peaked around noon during days without fog, and were reduced during foggy conditions. For 66 % of the data points, ΔT and Δe were negative, corresponding to positive (upward) fluxes of sensible heat Q_H and latent heat Q_E. Q_H, Q_E, and Q_W varied with wind direction. Average Q_W and Q_E for winds from S to SE were more than twenty times higher than those of north-easterly winds, while the average Q_H was about four times higher for the same wind direction. Partitioning of the available energy during a 24 hour period showed that during the daytime Q_H dominated, while at nighttime Q_E was dominant. A Monte Carlo simulation proved that statistically significant evapotranspiration rates, *i.e.* upward water vapor fluxes, occurred during fog. At the same time, deposition fluxes of fog droplets

occurred. Our results show that even during fog events, significant evapotranspiration may occur.

Key words: Bowen ration, eddy covariance, fog, evapotranspiration, Monte Carlo simulation.

3.1   Introduction

Mountain cloud forests are considered to be extremely fragile ecosystems, because they play an important role in biodiversity conservation and ecological integrity of high altitude areas (Stadtmüller 1987). They host many endangered species and have very high rates of endemism (Bubb et al. 2004). Their unique structure and function is created by, among other factors, the frequent occurrence of fog. Fog affects the micro-climate drastically by reducing the amount of incoming shortwave radiation (Klemm et al. 2006), causing less energy to be available for photosynthesis and evapotranspiration, and through high air humidity, which influences the physiological conditions of plants. Montane cloud forests typically occur over an elevation range of about 500 m, but there is considerable variation in the altitude at which they are found (Bubb et al. 2004). In the tropics, cloud forests are mainly located between 1200 and 2500 m above sea level (a.s.l.), where cloud belts are formed by ascending moist air masses. The hydrology, ecology, and soil properties of cloud forests are also strongly influenced by a significant contribution of water input from fog deposition (Stadtmüller 1987). In mountainous ecosystems, water input through fog deposition is estimated to contribute up to 48 % (Holder 2004) of the water balance. Up to 50 % of the nutrient input may also result from water stripped from clouds by epiphytes such as mosses and ferns (Benzing 1998; Chang et al. 2002).

Evapotranspiration from vegetation is important not only for the water balances of eco-systems and single plants, but also for the energy balance (Arya 2001). Considerable amounts of energy are required for the phase change of water from liquid to vapor phase, and this energy is transferred to the atmosphere via the transport of water vapor. Evapotranspiration may thus be considered as a process of energy transference (Houghton 1985) and a key process in the earth's energy budget. On a global scale, eva-potranspiration accounts for 75 % of the turbulent energy transfer from the earth to the atmosphere (Chapin et al. 2002). However, water vapor flux is difficult to quantify (Peacock and Hess 2004) and the related measurements are complicated by large diffi-culties, particularly in humid environments. For example, optical and sonic techniques for measuring water vapor and wind vector, which are fast enough for the application of the eddy covariance method, are often prevented by water droplets on the sensing devices. Gradient techniques, such as the Bowen ratio method, also encounter diffi-culties due to small vertical gradients of the water vapor concentration.

Research and conservation needs for cloud forests were identified during various international workshops (Hamilton et al. 1995; Aldrich 1998). One of the overall goals is the quantification of the hydrological properties of cloud forests (Bubb et al. 2004). The objectives of this study are to measure evapotranspiration in a montane cypress forest and to analyze whether evapotranspiration of water can, in fact, occur during the extremely humid conditions associated with fog. It is well documented that turbulent deposition of fog droplets onto vegetation occurs during foggy conditions (Gallagher et al. 1992; Vong and Kowalski 1995; Kowalski and Vong 1999; Vermeulen et al. 1997; Thalmann et al. 2002; Eugster et al. 2006; Holwerda et al. 2006). However, defining the relationships between evapotranspiration of water vapor and turbulent deposition of liquid water and discovering whether these processes can occur simultaneously will improve the general understanding of hydrological processes and energy flux partitioning in these ecosystems.

3.2   Methods

3.2.1   Study Site

The Chilan study site is located in north-eastern Taiwan in the Yuan Yuang Lake Nature Preserve, Hsinchu County. It comprises the uppermost head water of the Tahan River watershed, at an elevation between 1650 and 2432 m a.s.l. (Chou et al. 2000). The experimental site is part of Taiwan's Long Term Ecological Research (LTER) program, which is supported by the Taiwan National Science Council in cooperation with the Taiwan Forest Research Institute. The scope of this program is to study the ecological processes with regard to hydrological and nutrient fluxes within the ecosystem. The present study was carried out in the partially-managed forest surrounding the nature preserve.

The predominant tree species of the forest are *Chamaecyparis obtusa* var. *formosana* (yellow cypress) and *Chamaecyparis formosensis* (red cypress). The understory consists mainly of *Rhododendron formosanum* and is rich in epiphytes due to high humidity. To support the preservation of both endemic *Chamaecyparis* species in the middle-altitude (1000-2500 m a.s.l.) of the cloud forests of Taiwan, a special effort, as part of this study, is undertaken to investigate their limiting ecological factors.

The canopy of the cypress forest is considerably closed and uniform. The tree heights range between 11 to 14.3 m, the average height is 13.7 m. The cypress stand comprises an area of 300 ha and is situated within a valley on a relatively flat section which slopes with an angel of 15° towards south-east (approximately 120°). Due to the homogenous canopy layer, this location is well suitable for micrometeorological measurements. The experimental tower is situated at 24°35'27.4''N and 121°29'56.3''E at 1650 m a.s.l.. The uppermost platform is at 23.4 m above ground level and thus approximately 10 m above the average canopy height.

The climate of the study site is categorized as temperate heavy moist. The average annual temperature is 13 °C, and the annual rainfall averages over 4000 mm (Klemm et al. 2006). The abundant frequency of fog accounts for a significant reduction of incoming solar radiation, and thus is an important ecological aspect for the growth of the endemic cypress forest (Hwang et al. 1996; Chang et al. 2002). The fog duration ranges from 4.7 to 11 hours per day (Chang et al. 2002). The presence of fog is strongly associated with wind directions from SE and S, and it is formed orographically as a result of adiabatic cooling during uphill transport (Klemm et al. 2006).

3.2.2   Experimental setup

From September 23 through November 10 in 2005, an instrument array to study the fluxes of latent heat, sensible heat, and water vapor was installed at the meteorological tower at the Chilan study site. The Bowen Ratio setup consisted of two Frankenberger psychrometers, a Kipp & Zonen CNR 1 net radiometer, and five Hukseflux thermal soil heat flux sensors (Table 3.1). For flux-profile relationships, the relative precision of the sensors is more important than their absolute accuracy. For this reason, inter-calibration of the psychrometer sensors was performed prior the experiment both in the laboratory and at the study site. The data were stored every 10 minutes and reflect the average value over each time interval. At the same time, an eddy covariance setup comprising of a Young 81000 ultrasonic anemometer in combination with a LI-COR 7500 open path infrared CO_2/H_2O analyzer and a fog droplet spectrometer (model FM-100, Droplet Measurement Technologies, Boulder, USA) was used to determine the turbulent vertical fluxes of CO_2, water vapor, latent heat, sensible heat, and fog water (12.5 Hz sample frequency) on the basis of 30 minute averages. The spectrometer detects the number and sizes of fog droplets using the scattering of a laser beam, and records the spectra of fog droplets with diameters from 2 μm to 50 μm within 40 channels. Further meteorological data were taken from the standard instrumentation available at the meteorological station.

Table 3.1: Instrumentation used to measure water vapor, sensible heat, and latent heat fluxes over a two month period in a subtropical montane cloud forest in Taiwan.

Method	Instrument	Height
Bowen ratio	psychrometer (Frankenberger)	15.05 m
	psychrometer (Frankenberger)	23.12 m
	Kipp & Zonen CNR 1 net radiometer	22.50 m
	Hukseflux thermal sensors	-0.10 m
Eddy covariance	Young 81000 ultrasonic anemometer	23.40 m
	FM-100 fog droplet spectrometer	23.20 m
	LI-COR 7500 CO_2/H_2O analyzer	23.40 m

3.2.3   Flux measurement theory and data analysis

The Bowen ratio method (*e.g.*, Stull 1988) was applied to the data collected during this study in order to determine the fluxes of sensible heat (Q_H) and latent heat (Q_E). The Bowen ratio *Bo* is an estimate of the ratio between latent and sensible heat fluxes (Oke 1987)

$$Bo = \frac{Q_H}{Q_E} \tag{3.1}$$

In order to put *Bo* into context of this study, an energy budget equation *EB* is used. It is expressed in terms of net radiation R_{net}, soil heat flux H_{soil}, sensible heat flux Q_H, and latent heat flux Q_E following

$$EB = R_{net} - H_{soil} - Q_H - Q_E \tag{3.2}$$

Assuming that the turbulent eddy exchange coefficients for heat and water vapor are equal, only the measurements of temperature (*T*) and water vapor pressure (*e*) at two levels (ΔT and Δe, respectively) within the surface layer are required to determine *Bo* with a simplification of the flux gradient similarity (Arya 2001; Foken 2003):

$$Bo = \frac{c_p \cdot \Delta T}{L_v \cdot \Delta e} \tag{3.3}$$

where c_p *is* the specific heat capacity of the air, and L_v is the heat of evaporation for water. Now, Q_H and Q_E can be calculated as

$$Q_H = (R_{net} - H_{soil}) \cdot \frac{Bo}{(1 + Bo)} \tag{3.4}$$

$$Q_E = \frac{(R_{net} - H_{soil})}{(1 + Bo)} \tag{3.5}$$

In addition to ΔT and Δe, only the radiation balance R_{net} and the soil heat flux H_{soil} need to be measured. The water vapor flux (Q_W) is simply determined using

$$Q_W = \frac{Q_E}{L_v} \tag{3.6}$$

The distance between the sensor heights should be as large as possible, in order to obtain substantial, large temperature and water vapor pressure gradients. Further, micrometeorological gradient techniques such as Bowen ratio measurements should be performed within the inertial sublayer where fluxes are constant with height. Monteith and Unsworth (1990) define the lower limit of the inertial sublayer by

$$z_m - d = z_0 \tag{3.7}$$

where z_m is the measurement height, d is the displacement height, and z_0 is the ground level. They further postulate for the measurement height z_m that

$$z_m - d > 10 \cdot z_0 \tag{3.8}$$

The displacement height d was calculated by analyzing logarithmic wind profiles (Arya 2001); it was found to be 6.65 m. For this study, the psychrometers were installed at 15.05 m (8.40 m above d) and 23.12 m (16.47 m above d).

In order to insure data quality by excluding potentially erroneous counter gradient fluxes, a strict data quality assurance routine was applied. Data were rejected when the inequality

$$\frac{L_v \cdot \Delta q + c_p \cdot \Delta T}{R_{net} - H_{soil}} < 0 \tag{3.9}$$

was not valid (Ohmura 1982), where q is the specific humidity [g kg^{-1}].

Profile gradient measurements require resolvable differences of measured scalars between the installation heights. In other words, Δq and ΔT must be significantly different from zero. Therefore, the differences between T_{dry} and T_{wet} for the upper and lower psychrometers were tested by establishing their 95 % confidence interval. Only data points for which these intervals of the upper and lower sensor pairs do not overlap, were accepted. To ensure that only time periods with well developed turbulence regime are analyzed, data with wind speeds < 1 m s^{-1} were rejected from further analyses. Because the calculation of the latent and sensible heat flux after Formula (3.4) and Formula (3.5) for Bo equals -1 (which occurs when Q_H and Q_E are of equal magnitude but with opposite signs) has no numerical meaning (Payero et al. 2003), Ohmura (1982) introduced a criterion for rejecting such data when it fulfills the inequality

$$-\frac{L_v}{c_p} \cdot \Delta q - 2\left[\frac{L_v}{c_p} \cdot E(q) + E(T)\right] < \Delta T < -\frac{L_v}{c_p} \cdot \Delta q + 2\left[\frac{L_v}{c_p} \cdot E(q) + E(T)\right] \tag{3.10}$$

$E(q)$ is the limit of resolution for specific humidity q and $E(T)$ the limit of resolution for temperature T.

We used a Monte Carlo type simulation (MCS) to analyze the statistical significance of the water vapor fluxes measured during fog conditions by using the Bowen ratio method. The MCS uses random numbers to permute subsamples of the original psychrometer T_{dry} and T_{wet} data. For randomly chosen data sets, a probability distribution was simulated (Legendre and Legendre 1998): For an individual data set of the lower psychrometer, 10,000 normally distributed random numbers were generated for each T_{dry} and T_{wet} data point. The actual values were used as arithmetic means, and the standard deviations were taken from intercalibrations between sensor pairs. For each

pair of simulated T_{dry} and T_{wet}, the Bowen ratio Bo, and the water vapor fluxes were computed, resulting in 10,000 simulated Bo's and fluxes. The mean and standard deviation of these calculated fluxes are independent of the number of simulations if a large enough number of simulations was performed (Legendre and Legendre 1998). The simulated mean water vapor fluxes were tested with a single value t-test against zero to prove if they are statistically significant.

The eddy covariance method (*e.g.*, Stull 1988) was applied to calculate the turbulent vertical fluxes of fog water Q_F, Q_W, Q_H, and Q_E. Following the Reynolds averaging, the turbulent flux Q_x of an entity x (*e.g.*, water vapor) can be quantified as

$$Q_x = \overline{w'x'} \qquad\qquad (3.11)$$

where w is the vertical wind speed and x is the magnitude of the scalar (in the unit mol m^{-2} s^{-1} for the water vapor flux and kg m^{-2} s^{-1} for the fog water flux). The primes denote the deviation of individual measurements from the mean (*e.g.*, 30 min averaging period) and the overbar indicates the time average of the 30 min averaging interval.

The raw data were recorded and computed by using in-house software. The following processing steps were conducted: (1) coordinate rotation of *u, v,* and *w* wind components by using the planar fit method, (2) de-trending of data by calculating moving averages (1200 s), (3) Webb correction (Webb et al. 1980), (4) determination of the time lag, using a cross-correlation, and (5) computation of the turbulent vertical fluxes. Only data from steady-state conditions during the averaging interval, simultaneously exhibiting a well developed turbulence regime, were used for the calculation. The extent of atmospheric turbulence was determined using the friction velocity u_*.

3.3   Results and discussion

During the 49-day experimental period, the weather generally exhibited sunny conditions during the morning hours and decreasing temperatures with fog during the afternoon hours. The wind speeds were low, with a mean of 1.5 m s^{-1}. Approximately 30 % of the time, the wind speeds were less than 1 m s^{-1}. The dimensionless stability parameter z/L (calculated from aerodynamic height z and Obukhov length L) was used to classify the atmospheric stability conditions (Stull 1988). During the night time, the wind was typically from the N to NW, and low wind speeds and stable conditions led to a poorly developed turbulence regime. Neutral conditions mainly occurred during the transition times, when wind direction changed during the late morning and early night hours. Over the day, unstable conditions associated with valley winds from the S and SE dominated, namely, the advection of air masses ascending along the slopes. During 42 % of the study period, the conditions were foggy (visibility < 1000 m). The occurrence of fog was strongly related to daytime upslope winds from S to SE, which advected warm and humid air masses, and was thus defined as advective and orographic fog. Adiabatic cooling and subsequent condensation led to the formation of the fog. The

dissipation of the fog corresponded to mountain winds from the N to NW, which carried relatively cool and dry air masses.

During times without fog, temperature differences between the two measurement levels increased and reached a maximum at noon, and ΔT and Δe ranged between -1.95 and +4.98 °C and -4.01 and +1.90 hPa, respectively. Both, ΔT and Δe, had negative signs in 66 % of the valid data, representing higher temperatures and higher water vapor pressures at the lower psychrometer and thus positive (upward) fluxes of latent and sensible heat. During fog, differences between T_{dry} and T_{wet} dropped to a minimum because of the high air humidity. Values for ΔT and the differences of water vapor pressure between upper and lower psychrometers (Δe) ranged between -1.01 and +0.55 °C and between -0.83 and +0.59 hPa, respectively. The water vapor pressure saturation deficit also decreased to a minimum due to the high relative humidity. The standard deviations of ΔT_{dry} and ΔT_{wet} were 0.22 °C and 0.56 °C for times without fog and 0.08 °C and 0.07 °C during fog. These values were used to calculate the Bowen ratios.

The median Bowen ratio determined in this study using the valid data is 1.06 for the subtropical cloud forest. The 25 %-quartile of Bo is 0.47 and the 75 %-quartile is 1.64. This shows that for half of the data set (data between the 25 % and the 75 % quartiles, $0.47 \leq Bo \leq 1.64$), the sensible and latent heat fluxes were of the same direction and of similar size. Water vapor fluxes determined with Bowen ratio ranged between -2.4·10^{-5} kg m^{-2} s^{-1} and +1.8·10^{-4} kg m^{-2} s^{-1}; the median water vapor flux was +5.2·10^{-5} kg m^{-2} s^{-1} and the average was +5.3·10^{-5} kg m^{-2} s^{-1}. During fog, the median water vapor flux was +5.6·10^{-5} kg m^{-2} s^{-1} and during no-fog conditions it was +5.3·10^{-5} kg m^{-2} s^{-1}. Mean water vapor flux increased during the daylight hours, with a peak just before noon, after which the flux gradually decreased until sunset (Figure 3.1 A). Individual water vapor flux measurements were generally higher and showed greater variability during daylight hours than during nighttime hours (Figure 3.1 A). Sensible heat flux, latent heat flux, and net radiation followed the same trend as the mean water vapor flux (Figure 3.1 B). These trends are controlled primarily by the diurnal variation in solar radiation, which causes a diurnal variation in the overall energy budget. During the daytime, the Q_H (associated with winds from the S to SE) was much greater than Q_E. At night, the Q_E was smaller, but still positive, while Q_H was negative (downward heat flux) (Figure 3.1 B). Q_H follows the same trends as the net radiation, which indicates the importance of Q_H for the local energy budget during the day. On the basis of median values, the Bowen ratio divided the available energy into 56 % Q_H and 44 % Q_E.

However, the magnitude of Q_H, Q_E, and Q_W also varied with wind direction (Figure 3.2 A and Figure 3.2 B). The fluxes of Q_H, Q_E, and Q_W associated with winds from S to SE were considerably higher than those from the N to NW. The overall average fluxes of Q_E and Q_W were more than twenty times higher, while Q_H was about four times higher (Table 3.2). Since winds from the N to NW occurred principally during the night

time, the observed fluxes were noticeably smaller because of the absence of solar radiation. Under these conditions, Q_H was negative (Figure 3.2 A).

In order to determine whether there were statistically significant water vapor fluxes during foggy conditions, the MCS was applied to 17 sets of foggy weather data that fulfilled the quality requirements. The simulated water vapor fluxes were then tested by a t-test to show that the mean value is significantly different from zero. For all tested data sets, the t-test showed a statistically significant difference between the averages and zero at the $p < 0.01$ level. Thus, an upward water vapor flux or evapotranspiration did, in fact, occur during foggy conditions, and further analysis of the collected data, as follows, is warranted and useful.
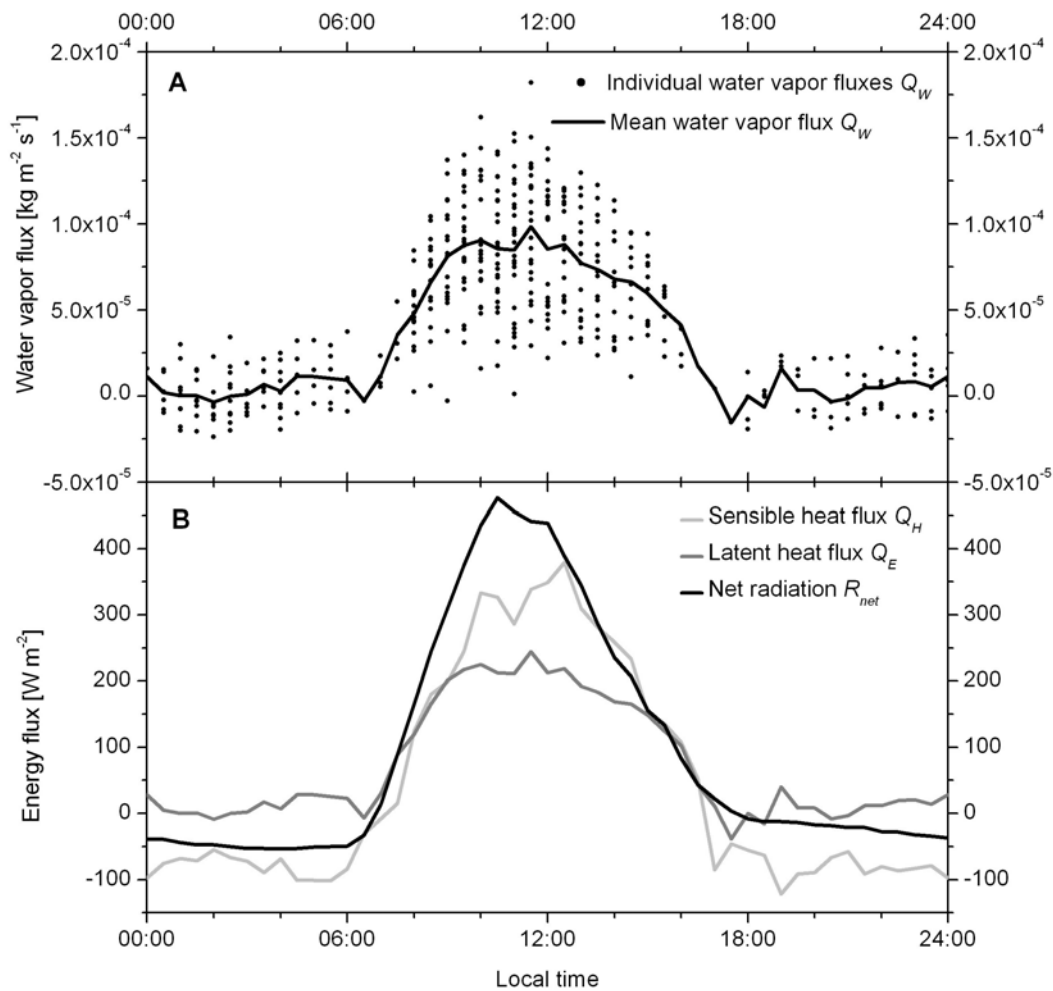
Figure 3.1: (A) Individual diurnal water vapor flux measurements [kg m^{-2} s^{-1}] and mean diurnal water vapor flux Q_w [kg m^{-2} s^{-1}], and (B) mean diurnal sensible heat flux Q_H [W m^{-2}], latent heat flux Q_E [W m^{-2}], and net radiation Rn [W m^{-2}], for the experimental period from September through November 2005.
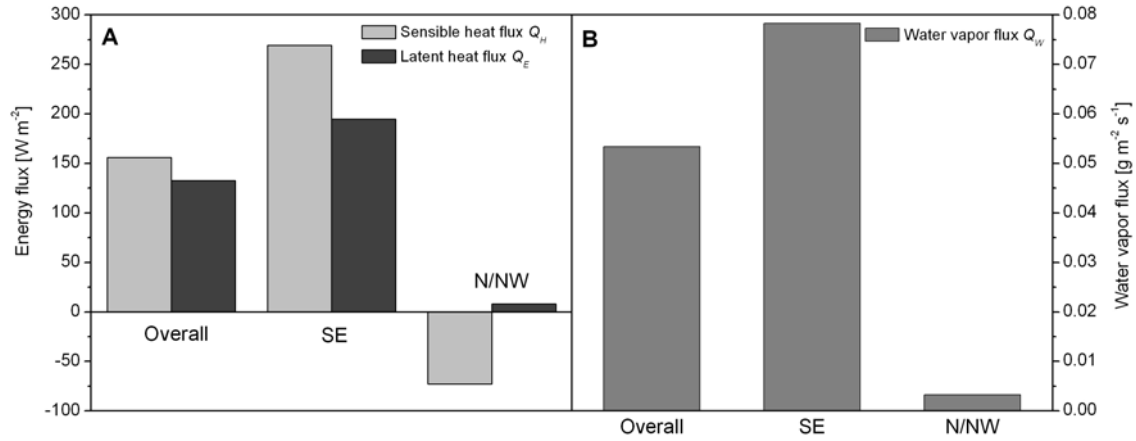
Figure 3.2: Average energy fluxes (sensible heat flux Q_H [W m^{-2}], latent heat flux Q_E [W m^{-2}]), and (B) water vapor flux Q_W [g m^{-2} s^{-1}] for the prevailing wind directions.

Table 3.2: Sensible heat fluxes Q_H, latent heat fluxes Q_E, and water vapor fluxes Q_W determined with the Bowen Ratio method categorized by wind direction and meteorological conditions.

Parameter		All data	S to SE	N to NW	No fog	Fog
	Min	-171.2	21.0	-171.2	-171.2	41.8
Q_H [W m^{-2}]	Max	771.3	771.3	4.3 10^{-3}	771.3	211.6
	Average	156.0	269.1	-72.7	157.3	95.5
	Median	165.6	258.3	-77.2	175.0	85.5
	Min	-59.6	-7.4	-59.6	-59.6	59.8
Q_E [W m^{-2}]	Max	454.1	454.1	136.8	454.1	218.2
	Average	132.8	194.7	8.1	133.1	139.2
	Median	130.0	194.2	5.7	131.2	140.7
	Min	-2.4 10^{-5}	-2.9 10^{-6}	-2.4 10^{-5}	-2.4 10^{-5}	2.4 10^{-5}
Q_W [kg m^{-2} s^{-1}]	Max	1.8 10^{-4}	1.8 10^{-4}	5.5 10^{-5}	1.8 10^{-4}	8.7 10^{-5}
	Average	5.3 10^{-5}	7.8 10^{-5}	3.3 10^{-6}	5.4 10^{-5}	5.6 10^{-5}
	Median	5.2 10^{-5}	7.8 10^{-5}	2.3 10^{-6}	5.3 10^{-5}	5.6 10^{-5}

The actual water vapor flux calculated with the eddy covariance method ranged between -6.0·10^{-5} kg m^{-2} s^{-1} and +3.3·10^{-4} kg m^{-2} s^{-1} with a median flux of +6.5·10^{-6} kg m^{-2} s^{-1}. The study of the turbulent fog water flux Q_F, as measured with the eddy covariance method, also supports that both positive Q_W and negative fog water fluxes Q_F, *i.e.* fog water deposition, occurred simultaneously with evapotranspiration. In Figure 3.3, the trends of the fog water flux, water vapor flux (Figure 3.3 A), sensible heat flux, latent heat flux, energy balance, incoming shortwave radiation (Figure 3.3 B), air temperature T measured at 15.05 m and 23.12 m, wind direction WD (Figure 3.3 C), absolute humidity a [g m^{-3}], and the liquid water content LWC [g m^{-3}] (Figure 3.3 D) during a representative fog event (2005-11-01, 6:00 to 21:00 hrs local time) are presented. Similar patterns were observed during almost all analyzed fog events. The following discussion describes the conditions that occurred during one such typical fog event.

After sunrise (*e.g.*, 6:30 hrs local time; first vertical line, Figure 3.3), incoming short-wave radiation Q_{down} increased along with evapotranspiration, which corresponded to a positive Q_W (and Q_E) and increased absolute humidity. At the same time, valley-winds from SE advected saturated and foggy air into the study area. The turbulent fog water deposition flux was up to -0.008 g m^{-2} s^{-1}, and the *LWC* was up to 0.18 g m^{-3} (at 9:30 hrs local time). Figure 3.4 shows that fog droplets with diameters of 5 μm to 40 μm deposited to the ecosystem.

At 11:00 hrs local time (second vertical line, Figure 3.3), Q_w and Q_E both peaked, while Q_H and *EB* were both positive, but had not reached their peaks. Just before noontime, both Q_{down} and Q_W reached their highest daily value. The comparison of the temperature at the 15.05 m and 23.12 m measurement levels confirmed static instability and thus likely upward turbulent transport of sensible heat. Over the course of the day, the forest canopy is warmed by absorbing solar radiation (albedo = 0.08). This resulted in a higher air temperature at 15.05 m than at 23.12 m throughout the fog event. The temperature difference between the measurement levels was largest (1 K) when the incoming solar radiation was highest (at 11:30 hrs local time; third vertical line, Figure 3.3). The absolute humidity at 15.05 m was likely higher than that at 23.12 m, due to higher water absorption capacity of warmer air under saturated conditions (100 % relative humidity during the entire fog event; not shown in Figure 3.3). Thus, concentration differences and a measurable upward water vapor transport occurred despite such saturated conditions. As a result, evapotranspiration and fog droplet deposition processes are confirmed to have occurred simultaneously during the fog event. The energy needed to evaporate the water involved in evapotranspiration, which led to a positive Q_w, came from the incoming shortwave radiation.

At 11:30 hrs local time, the *LWC* decreased to 0.004 g m^{-3} and the fog water flux was reduced (-0.001 g m^{-2} s^{-1}) but still present. Around 12:30 hrs local time (fourth vertical line, Figure 3.3), the *LWC* and the fog water flux increased again temporarily and fog droplets with mean diameters between 5 μm and 25 μm were deposited (Figure 3.4). After noon, the incoming solar radiation and overall *EB* began decreasing due to the normal diurnal variation, as well as, the absorption and reflection of shortwave radiation by the fog layer above the vegetation and above the experimental setup. As a consequence, the air temperature decreased and differences between 15.05 m and 23.2 m narrowed. Q_W remained positive until 17:30 hrs local time (fifth vertical line, Figure 3.3). The change of the mean wind direction from SE to N/NW after sunset induced the advection of drier and warmer air by down-slope winds and eventually led to the dissipation of the fog.
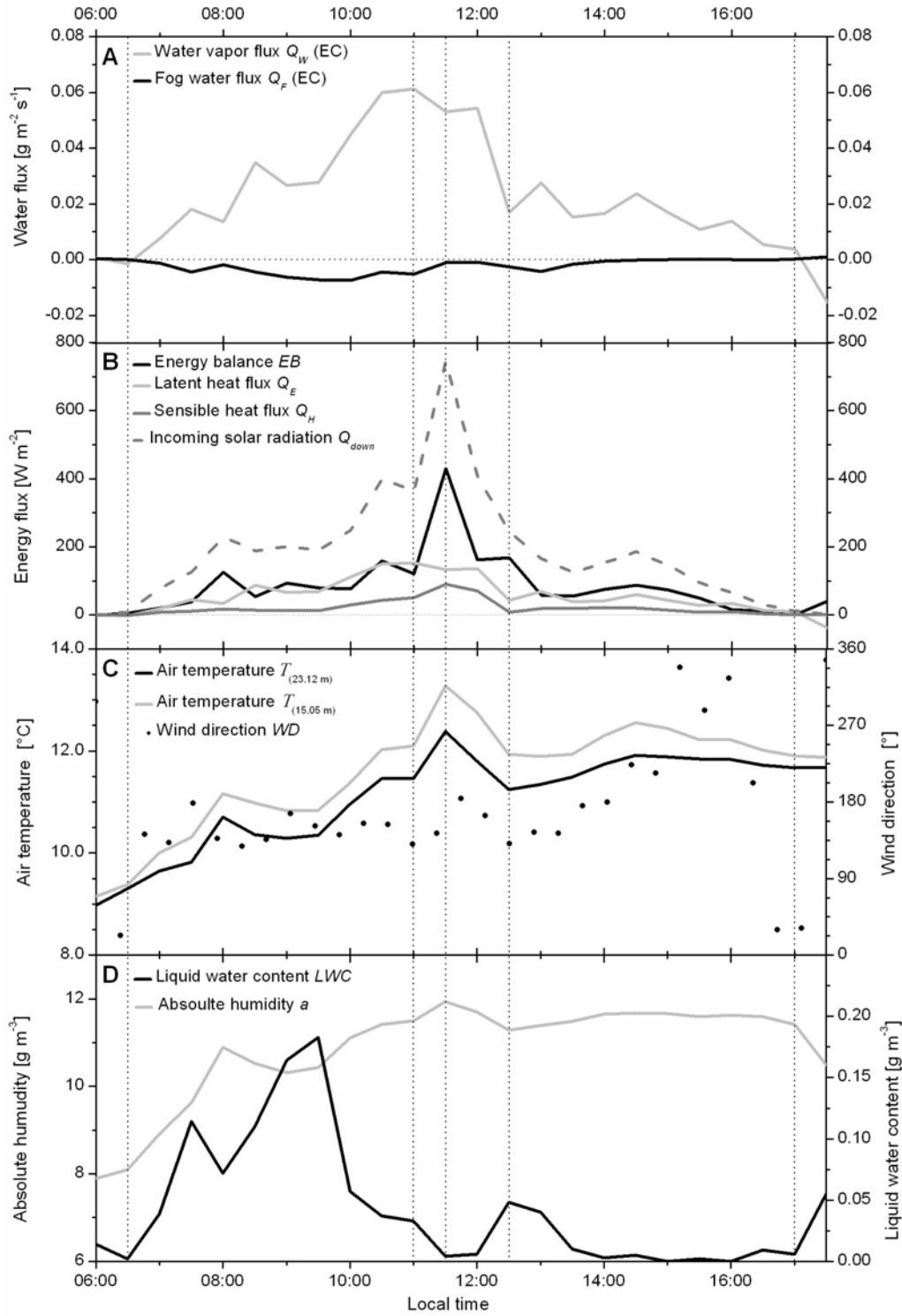
Figure 3.3: Courses of (A) turbulent fog water flux Q_F [g m^{-2} s^{-1}], water vapor flux Q_W [g m^{-2} s^{-1}], (B) sensible heat flux Q_H [W m^{-2}], latent heat flux Q_E [W m^{-2}], incoming shortwave radiation Q_{down} [W m^{-2}], energy balance EB [W m^{-2}], (C) air temperature T (15.06 m and 23.12 m) [°C], wind direction WD [°], (D) absolute humidity a [g m^{-3}], and the liquid water content LWC [g m^{-3}] during a representative fog event measured at the Chilan site (2005-11-01, 6:00 to 17:30 local time). The turbulent fog water flux and the water vapor flux were measured by using the eddy covariance method. Q_W and Q_E translate into each other by use of the factor 2465 (with the employed units). Vertical lines indicate times of interest as discussed in the text.
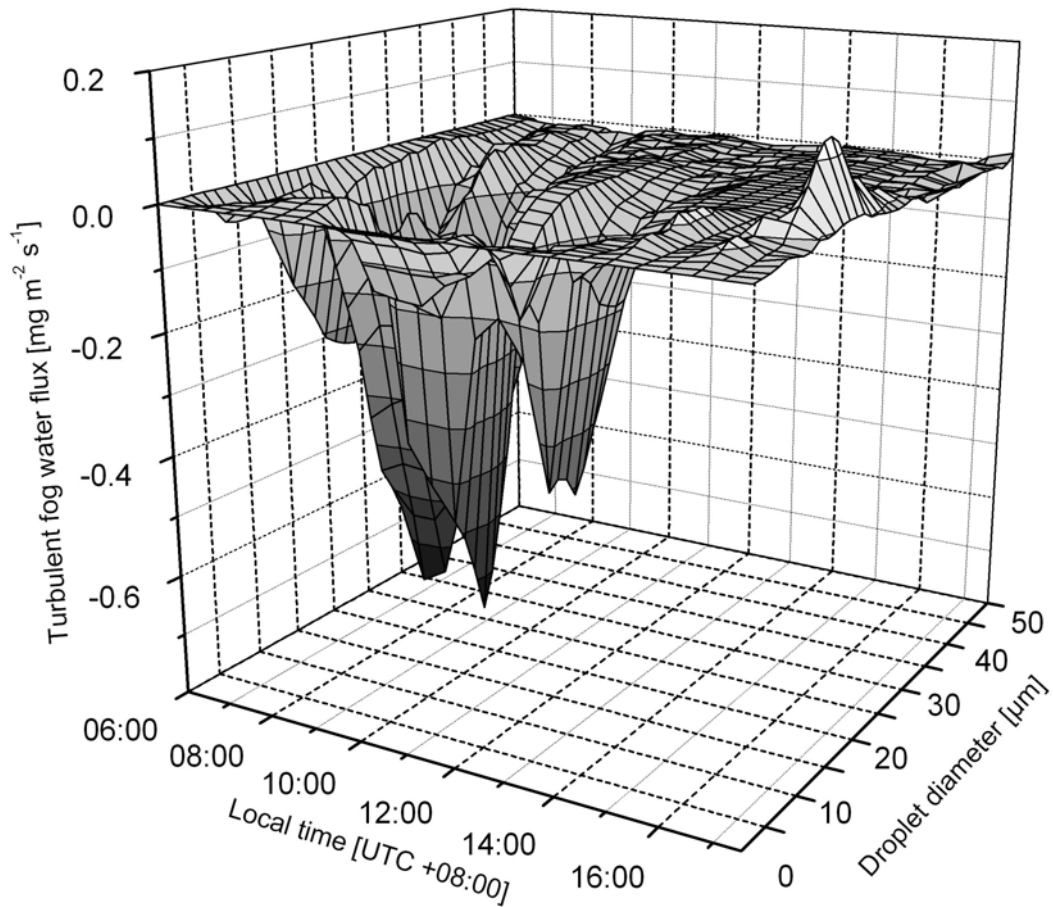
Figure 3.4: Relationships between turbulent fog water flux [mg m^{-2} s^{-1}] and fog droplet diameter [µm] over time for a representative fog event, using a 30 minute averaging interval on data measured with the eddy covariance method at the Chilan site (2005-11-01, 6:00 to 17:30 local time.

3.4   Conclusions

During this study, we successfully measured positive water vapor fluxes even during foggy conditions. This fact contradicts the conventional assumption that foggy air is so saturated with water vapor that evaporation is not possible. However, the occurrence of these simultaneous fog droplet deposition and evapotranspiration was shown by using two different and independent methods, *i.e.* the Bowen ratio method and the eddy covariance method. Using the Monte Carlo simulation (in combination with a single value t-test), we confirmed that evapotranspiration is possible during foggy conditions. In the micrometeorological context, the application of the Monte Carlo type simulation is innovative and new. Such a MCS was useful in showing that statistically significant evapotranspiration in conjunction with fog droplet deposition is possible during foggy conditions. The MCS supports the results of actual water vapor flux measurements.

The relationships between water fluxes and energy budget, measured with eddy covariance, were well-defined by the representative fog event. The same patterns were

repeated during most of the fog events. Therefore, it is concluded that our observations involve existing interaction but no artifacts. Both the Bowen ratio and the eddy covariance measurements thus revealed the operation of evapotranspiration during foggy conditions.

A comparison of the Bowen ratio and eddy covariance methods showed that the measured water vapor fluxes corresponded well for both methods. The Spearman rank correlation confirms a significant correlation ($r = 0.77$) of the 30 min water vapor fluxes determined with the Bowen ratio and eddy covariance methods on the $p < 0.01$ level. Nevertheless, the Bowen ratio setup yielded fewer gaps in its data set than the eddy covariance setup. Since rain droplets caused technical problems and failures resulting in a heterogeneous, patchy data set, eddy covariance data were not available for the entire experimental period. Under difficult meteorological conditions such as heavy rain, the instrumentation for the Bowen ratio method performed more reliably. Thus, the Bowen ratio method was the most suitable approach for studying Q_H, Q_E, and Q_W during the current experimental period, and appeared more suitable for continuous measurements during humid conditions.

We applied a one-dimensional approach since previous studies at the same study site confirmed a well closed energy budget, and thus supported the general applicability of such a method (Klemm et al. 2006). Our results show that minor changes of temperature affect the magnitude and direction of Q_W. Therefore, particular attention should be paid to the thermal structure of the canopy and atmospheric boundary layer.

The Bowen ratio *Bo* is a measure of the strength of the interaction between the energy budget and hydrological cycle, since it is inversely related to the portion of net radiation that drives water loss from ecosystems (Chapin et al. 2002). A median *Bo* of 1.06, indicating sensible and latent heat fluxes with the same order of magnitude, which confirms the strong coupling between the energy budget and hydrological cycle for the study site. The energy source for the observed processes is difficult to specify. However, it is likely that the energy comes from the incoming shortwave radiation, as that is the largest energy source. The advection of dry and warm air into the study area may play a role in the local energy budget, but further measurements, such as approaches that consider the horizontal advection, are needed to study this topic in more detail. Measurements of fog water deposition in combination with the collection of fog water samples may allow the estimation the nutrient input into the ecosystem through occult deposition, and to assess the role of fog water in ecosystem nutrient cycling.

The results of this study provide an important contribution to the understanding of evaporation processes within montane cloud forests, as it confirms that evapotranspiration can occur simultaneously with fog droplet deposition. This phenomenon has important implications for understanding of the hydrological processes of cloud forest ecosystems. Many questions remain, which may be answered using other direct micrometeorological methods, such as the eddy covariance approach. For example, future work will focus on the specific role of fog water in the energy budget with a special

emphasis on the coupling between deposition and evaporation processes. More research is needed to determine the specific effects that simultaneous evapotranspiration and fog droplet deposition have on the ecosystem.

Acknowledgements

Chapter 4

Nutrient input through occult and wet deposition into a subtropical montane cloud forest

E. Beiderwieden[*1], A. Schmidt[1], Y.-J. Hsia[2], S.-C. Chang[2], T. Wrzesinsky[1], and O. Klemm[1]

[1]Institute for Landscape Ecology, University of Münster, Robert-Koch-Str. 26, 48149 Münster, Germany.

[2]Graduate Institute of Natural Resources, National Dong Hwa University, Shoufeng, Hualien 974, Taiwan.

[*]corresponding author

Abstract

Chemical composition of fog and rain water was studied during a 47-day experimental period. The differences between the fog and rain water were found to be significantly for most analyzed ions. H^+, NH_4^+, NO_3^-, and SO_4^{2-} made up 85 % of the total median ion concentration in fog and 84 % in rain water. The total mean equivalent concentration was 15 times higher in the fog than in the rain water. The fog water samples were classified according to their air mass history. The analysis of the 120 hours backward trajectory led to the identification of three advection regimes. Significant differences of ion concentrations between the respective classes were found. Air masses of class I travelled exclusively over the Pacific Ocean, class II were carried over the Philippines, and class III were advected from mainland China. The turbulent fog water deposition was determined by the means of the eddy covariance method. The total (turbulent plus gravitational) fog water fluxes ranged between +31.7 mg m^{-2} s^{-1} and -56.6 mg m^{-2} s^{-1}. Fog water droplets with mean diameters between 15 μm and 25 μm contributed most to the liquid water flux. The sample based nutrient input was calculated on the basis of the occult and wet deposition, and the concentrations of the simultaneously collected fog and rainwater samples, respectively. The nutrient input through wet deposition was about 13 times higher than through occult deposition.

Keywords: Eddy covariance, turbulent fog water fluxes, atmospheric deposition, trajectories, neural network, cypress forest.

4.1   Introduction

Montane cloud forests are defined as forests that are frequently covered in cloud or mist (Stadtmüller 1987; Hamilton et al. 1995). In the tropics, they typically occur between 1200 m and 2500 m above sea level (a.s.l.), where cloud belts are formed by ascending moist air masses. They are recognized as "storehouses" of biodiversity since they host relevant concentrations of the world's species biodiversity as well as high rates of endemism (Hamilton et al. 1995; Aldrich et al. 2000). Cayuela et al. (2006) point out that only 2.5 percent of the total area of the world's tropical forests is specified as "montane cloud forest", but no accurate data are available about the actual worldwide distribution. Cloud forests belong to the world's most endangered ecosystems as they are affected, for instance, by changes of land use such as the conversion to pasture and croplands (Doumenge et al. 1995; Cayuela et al. 2006). Furthermore, the global warming forces a lifting of the condensation level along with a reduction of fog frequency (Lawton et al. 2001). The raise in cloud base and thus the displacement of the minimum level of montane cloud forests cause considerable ecological changes for the organisms adapted to that habitat (Pounds et al. 1999; Bruijnzeel 2001). Bruijnzeel and Hamilton (2000) even stated that with an increase in global warming montane cloud forests are likely to disappear.

During the last decades, an enhanced interest in montane cloud forest is evident (*e.g.*, Hamilton et al. 1995; Cavelier et al. 1996; Cavelier et al. 1997; Bruijnzeel and Veneklaas 1998; Clark et al. 1998; Bruijnzeel 2001; Holder 2003; Bruijnzeel 2004; Holder 2004; Chang et al. 2006; Eugster et al. 2006; Holwerda et al. 2006; Klemm et al. 2006; León-Vargas et al. 2006). The ecological significance of montane cloud forests is, among other factors, due to their unique hydrological conditions. The vegetation gathers water from wind-blown fog and thus captures a significant contribution to the hydrological cycle and nutrient budget. The contribution of fog water as an additional water source to the hydrological budget of forest ecosystems is well documented (Zadroga 1981; Hutley et al. 1997; Zimmermann et al. 1999; DeFelice 2002; Liu et al. 2004). The recognition of the ecological value of montane cloud forests led to the establishment of various international initiatives that aim at the implementation of research, conservation and restoration activities (Aldrich 1998; Aldrich et al. 2000; Bubb et al. 2004). However, few studies are available that focus on nutrient input through fog water deposition, since the simultaneous measurements of fogwater deposition and the chemical composition of the appropriate fog water are required (*e.g.*, Thalmann et al. 2002). The experimental quantification of occult deposition fluxes is still a challenge in atmospheric research due to its technical instrument requirements and methodological difficulties. Different approaches were applied to quantify the fogwater (occult) deposition such as modeling of fog water deposition fluxes (Lovett 1984) or the estimation of the water deposition by weighing plants (Chang et al. 2002). In this study, we present the results of a 47-day experimental period of direct measure-ments of fogwater fluxes at a montane cloud forest in Taiwan. The eddy covariance method was applied in combination with an active fogwater collector to examine the

deposition fluxes of nutrients into the ecosystem. We compared the nutrient input through occult deposition to the deposition of water and nutrients through wet deposition (rain). To our knowledge, this study presents the only measurements of turbulent fogwater fluxes by using the eddy covariance method available for Southeast Asia.

The quantification of the nutrient input through occult and wet deposition will improve the understanding of the biogeochemical cycle functions in montane cloud forests. In this study, we discuss the concentrations of various ions in fog water versus rainwater and evaluate the role of occult and wet deposition into the ecosystem. The overall scope of this study is to illuminate the influence of fog on the endemic appearance of the respective cypress forest. We presume that fog is the key factor that determines the vegetation structure since fog affects the plants' metabolism. Fog reduces photosynthesis through lowering solar radiation and decreased air temperature, as well as reducing the mineral uptake associated with lower transpiration during foggy conditions (Bruijnzeel and Veneklaas 1998).

4.2   Experimental

4.2.1   Site description

The study took place at the Chilan research site (1650 m a.s.l.) in north-eastern Taiwan (Chang et al. 2006; Klemm et al. 2006). The predominant tree species of the cloud forest are *Chamaecyparis obtusa* var. *formosana* (yellow cypress) and *Chamaecyparis formosensis* (red cypress). The appearance of both endemic *Chamaecyparis* species is assumed to be strongly coupled with abundant frequency of fog. The fog duration ranges from 4.7 to 11 hours per day (Chang *et al.* 2002). The reduction of incoming shortwave radiation due to fog as well as the constant exposure to acidic fog water deposition account for important ecological aspects for the growth of the endemic cypress forest (Liao et al. 2003a).

The measurements were carried out in the partly managed forest beside the nature preserve. The canopy layer is considerably closed and uniform; its average height is 9.8 m. The instruments were mounted on an experimental tower (24°35'27.4''N and 121°29'56.3''E) at 23.4 m (eddy covariance setup) and 20.4 m (fogwater collector) above ground, respectively.

4.2.2 Methods

4.2.2.1 Fog deposition measurements

The turbulent fogwater fluxes were determined by means of the eddy covariance method (*e.g.*, Stull 1988). This method is often described as the only direct flux measurement technique for fog (Gallagher et al. 1992; Vong and Kowalski 1995; Burkard et al. 2002). The experimental setup consisted of a Young 81000 ultrasonic anemometer (R.M. Young, USA) in combination with a fog droplet spectrometer (Model FM-100, Droplet Measurement Technologies, Boulder, USA). The sample frequency was 12.5 Hz and the averaging interval was 30 min. The fog droplet spectrometer detected the number and size of fog droplets by scattering of a laser beam and recorded the spectra of fog droplets with mean diameters from 2 μm to 50 μm within 40 channels.

The turbulent flux F_x of an entity x can be quantified as

$$F_x = \overline{w'x'} \tag{4.1}$$

where w is the vertical wind speed and x is, for example, the liquid water content. The primes denote the deviation of individual measurements from the mean (*e.g.*, 30 min averaging period) and the overbars indicate the time average of the 30 min averaging interval. The wind vector coordinates were double rotated to align the main axis with the streamlines and to yield zero average v and w wind components, respectively.

The gravitational deposition $D_{gravitational}$ was determined after the Stokes' settling velocity v_s (Beswick et al. 1991). The total fogwater flux was calculated by adding the turbulent and the gravitational flux. Positive fogwater fluxes are directed upward and negative fogwater fluxes are directed downward. The extent of atmospheric turbulence was characterized by means of the friction velocity u_*.

4.2.2.2 Gap filling

For this study, we used an artificial neural network to fill small data gaps in the fogwater flux time series caused by instrument malfunctions. Artificial neural networks are mathematical modeling tools to cognize and represent arbitrary complex relationships between input and somehow related output values. Due to their ability to learn from given cause-and-effect datasets or ancient time series, artificial neural networks became a useful tool for several problems in the field of statistic, economy and natural sciences (Patterson 1996). The application of artificial neural networks is an approved feature to substitute missing values (Papale and Valentini 2003).

For our purpose, a multi-layer perceptron network (MLP) was trained with available datasets in order to find a mapping rule for the 4-dimensional input values consisting of, in our case, the mean air temperature, incoming shortwave radiation, wind direction, and visibility onto the target value, *i.e.* the measured water deposition fluxes. An MLP

network consists of several connected nodes arranged in layers. These nodes or 'neurons' generate simple functions of the received input values. The input of a single neuron is built of a weighted sum of the outputs from all connected neurons in the previous layer. Due to the multiple connections, a network of such neurons can principally model any non-linear function (Bishop, 1995; Patterson, 1996). This approach bears the advantage that the underlying relationship between the input data and the target values (*i.e.,* the results) are not needed to initialize the model parameters in advance. In contrast to other multivariate gap filling procedures, the artificial neural network is able to learn from available training patterns, which is one the most important differences to other linear or non-linear statistical gap filling procedures (Stauch and Jarvis 2006). The iterative learning process within an artificial neural network is realized by changing the weights and thresholds of the neurons which influence the activation values of the neurons in the following layer (Figure 4.1). The sum of input values is transformed by a logistic, sigmoid activation function (Bishop 1995) representing the activation value of the neuron which is transmitted to the next layer. The adjustable network parameters were set to reach the lowest error E between the real target values in the training data set and the target values reproduced by the network. We calculated the mean squared error calculated from all n deviations to obtain the quality of a neural network:

$$E = \frac{1}{n} \sum_{i=1}^{n} (m_i - y_i)^2 \qquad\qquad (4.2)$$

where n is the number of available training datasets consisting of inputs and corresponding target values, m_i are the measured values, and y_i are the output values calculated by the network. During the optimization process, the *quasi-Newton* method (Bishop 1995; Setiono and Hui 1995) was used to find the minimum error function.
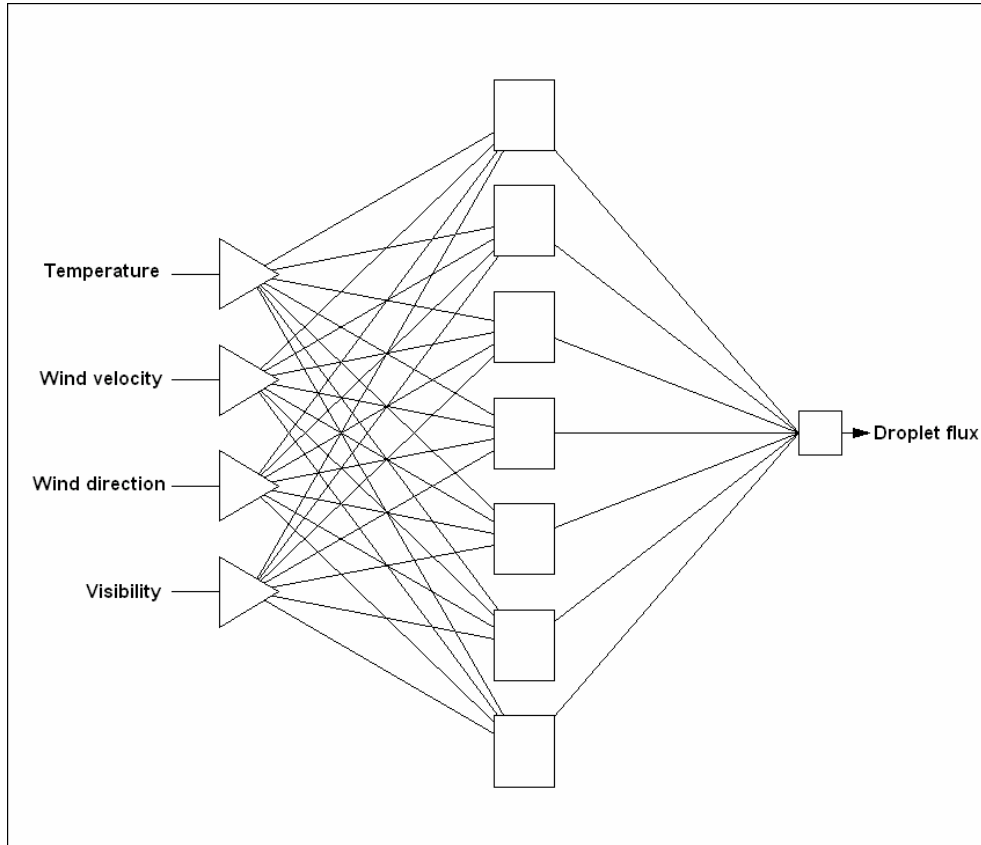
Figure 4.1: Schematic diagram of the 4-7-1 layout of the neural network used for the fog water flux reproduction. The neurons belonging to the first input layer transmit the values to the neurons in the second layer. After summation of all inputs in every neuron, the weighted sum is transformed by a logistic function giving the output of the neuron. Thus, the values building the inputs of the third layer's neurons are transformed non-linearly when finally summed and again transformed linearly or nonlinearly in the output layer (see text).

4.2.2.3 Fog and rainwater collection

For the fogwater collection, an active strand cloud water collector was used (Wrzesinsky 2000). A fan aspirated the foggy air with a consistent velocity of 8.1 m s^{-1}. The fog droplets impacted on the strings (Teflon) due to their inertness and slid along the strings through a tube (Teflon) into an automated sampler (ISCO, USA). The sampling area of the active cloud water collector was 650 cm^2. Whenever the visibility (MIRA visibility sensor 3544, Aanderaa instruments, Norway) dropped below 1000 m, the fog collector was triggered and operated automatically.

The strings as well as all sampling bottles were pre-cleaned with bi-deionised water. The ISCO sampler contained 24 sampling bottles (Polypropylene) of 1 L volume. For most of the time, a new bottle was triggered every one hour to ensure a high sampling resolution. The fog water collected with the ISCO sampler was filled into two 50 mL sampling bottles (high density polyethylene, HDPE). When the sampling volumes were too little, two (or more) bottles were combined.

The amount of precipitation was quantified by a tipping bucket rain gauge (TIC-1, Takeda, Japan). The rain data and other meteorological data were saved at 10 minutes averages. The rain water samples were collected using a self-made bulk precipitation gauge (HDPE funnel and bottle). The rain water was sampled on a per event basis. The rain and fogwater samples were treated in the same way. One 50 mL bottle was frozen immediately to inhibit microbial activity; the other aliquot was used for the measurements of pH and electric conductivity. Additionally, field blanks were taken for the quality control. All used materials that came into contact with the fog and rain water were chemically inert so that contamination of the water can be excluded.

The event based nutrient deposition [mg m^{-2}] was determined by multiplying the total fog (and rain, respectively) water deposition [L m^{-2}] by the mean concentrations of ions measured in the simultaneously collected water sample [mg L^{-1}]. For the quantification of the ion input through occult and wet deposition for a single event, the sample based nutrient input was summed over the respective time period.

4.2.2.4   Analytical procedures

Measurements of pH and electric conductivity were performed on-site, whereas the chemical analysis of NH_4^+, Na^+, K^+, Ca^{2+}, Mg^{2+}, Cl^-, NO_3^-, PO_4^{3-}, SO_4^{2-}, and F^- were performed in the laboratory at the University of Münster, Germany (Table 4.1). The pH electrode was calibrated before use. To examine the data quality, an ion balance was computed by summing up the equivalent concentrations of anions $c_{eq,i-}$ and cations $c_{eq,i+}$ for all fog and rainwater samples respectively. According to the condition of electric neutrality, the sum of $c_{eq,i-}$ should be equal to that of $c_{eq,i+}$ for each sample:

$$\sum_i c_{eq,i-} = \sum_i c_{eq,i+} \qquad\qquad (4.3)$$

Additionally, for each fogwater sample the theoretical electric conductivity $x_{theoretical}$ [µS cm^{-1}] was calculated by adding the products of the specific conductivities $x_{specific,i}$ [µS cm^{-1}] and the equivalent concentrations $c_{eq,i}$ of the respective ion i [µeq L^{-1}] after

$$x_{theoretical} = \sum_{ions} x_{specific} \cdot c_{eq}$$

$$(4.4)$$

Table 4.1: Methods and used instruments for the chemical analysis of the fog and rainwater water samples.

Parameter	Method	Instrument
Conductivity	conductivity electrode	LF 315 (WTW, Germany)
pH	pH electrode	pH 323 (WTW, Germany)
NH_4^+	flow injection analysis	Aquatec Analyzer 5400 (Aquatec, Sweden)
Na^+	flame photometry	PEP-7 (Jenway, UK)
K^+	flame photometry	PEP-7 (Jenway, UK)
Mg^{2+}	atomic absorption spectroscopy	Optima 3000 (Perkin Elmer, USA)
Ca^{2+}	atomic absorption spectroscopy	Optima 3000 (Perkin Elmer, USA)
Cl^-	ion chromatography	DX 100 (Dionex, USA)
NO_3^-	ion chromatography	DX 100 (Dionex, USA)
SO_4^{2-}	ion chromatography	DX 100 (Dionex, USA)
PO_4^{3-}	ion chromatography	DX 100 (Dionex, USA)
F^-	ion chromatography	DX 100 (Dionex, USA)

4.2.2.5 Trajectory calculations

Backward trajectories were calculated to study the advection regime of air masses and the coherency of the origin of air masses and their pollutant concentrations (Klemm et al. 1994; Thalmann et al. 2002; Tago et al. 2006). For every fogwater sample, a backward trajectory was computed using the HYSPLIT model (Draxler and Rolph 2003; Rolph 2003). Each trajectory indicates the path of the respective air mass during the last 120 hours at 1 m above surface level before reaching the fogwater collector.

4.3   Results

4.3.1   Fog and rainwater chemistry

During the experimental period from August 04 through September 20 in 2006, 217 fogwater samples and 20 rain samples were collected. The results of the chemical analysis are presented in Table 4.2. The data quality was examined by considering the ion balances of the single samples and by a comparison of the measured with the calculated electric conductivity. The ion balances indicated a very good agreement between the sum of anions and the sum of cations. The Pearson's correlation test showed a significant correlation on the $p < 0.05$ level ($r = 0.91$ for fog water and $r = 0.83$ for rain water). The median ratio of $\sum$anions / $\sum$cations was 0.97 for fog water and 0.96 for rain water. The agreement between the measured and calculated conductivity was also very high ($r = 0.87$ for fog water and $r = 0.98$ for rain water). The examination of data quality shows that the samples were analyzed with high accuracy.

Table 4.2: Statistical parameters of electric conductivity [μS cm^{-1}], pH, and measured ions [μeq L^{-1}] of all fogwater and rainwater samples collected between 4 August and 20 September 2006 at the Chilan site. "b.d.l." means "below detection limit", σ is the standard deviation.

Parameter	Fog (*n* = 217)					Rain (*n* = 20)				
	Median	Mean	σ	Min	Max	Median	Mean	σ	Min	Max
Conductivity	52	131	198	2	1102	8	12	10	2	35
pH	4.13	3.61	0.79	2.24	6.11	4.94	4.74	0.53	4.24	6.59
H$^+$	74.1	244	496	0.8	5754	11.5	18.2	16.3	0.3	57.5
NH$_4^+$	56.3	235	412	b.d.l.	2469	5	13.2	17.3	0	59.4
Na$^+$	13.2	58.6	124	b.d.l.	732	b.d.l.	1.1	2	b.d.l.	4.4
K$^+$	2.6	10.3	19.5	b.d.l.	139	b.d.l.	b.d.l.	0.6	b.d.l.	2.5
Ca^{2+}	10.5	34.1	63.2	3.5	494	4.7	6	2.6	3	12.5
Mg^{2+}	7	18.8	41.3	1.1	457	2.1	2	0.6	1.1	3.3
Cl$^-$	13.7	42.8	69.9	b.d.l.	399	2.8	2.8	1.7	0.7	6.4
NO$_3^-$	35.5	179	379	0.9	2992	7.7	12.2	11.4	0.8	32.5
PO$_4^{3-}$	8.9	18	19.5	2.4	61.3	b.d.l.	b.d.l.	b.d.l.	b.d.l.	b.d.l.
SO$_4^{2-}$	103	401	759	1.7	6329	17.6	28.6	26	3.2	93.2
F$^-$	2.6	6.9	13.4	b.d.l.	90.9	1.3	1.3	0.1	b.d.l.	1.4

The study of the backward trajectories indicated that three advection regimes, which were well distinguished from each other, existed at the study site. Therefore, the trajectories were grouped into three classes (Figure 4.2). The air masses of class I traveled exclusively over the Pacific Ocean during the last 120 hours before reaching the study site (Figure 4.2 A). The air masses of class II were carried over the Philippines and reached the Chilan site from the south (Figure 4.2 B). The pathway of the air masses of class III were advected from mainland China which is located north/north-westerly to the study site (Figure 4.2 C). The classification of the trajectories led to the hypothesis that systematic differences exist between the three classes concerning their chemical composition. The fog water samples were grouped according to their respective trajectory. The examination of the trajectories yielded 102 fogwater samples classified as class I, 20 samples as class II, and 95 as class III. Table 4.3 shows the statistical parameters of the respective classes.

Statistical tests were applied to examine if the classification of the fogwater samples on the basis of the trajectories was statistically meaningful. A Kolmogorov-Smirnov test confirmed that the pH, electric conductivity, and all analyzed ions (except for K$^+$ and Ca^{2+}) were log-normally distributed. By using a Levene's test, the homogeneity of variances was tested. The variances of the data set were homogeneous ($p < 0.05$) and thus, a one-way analysis of variance (ANOVA) could be applied to test if the differences between the classes are statistically significant (Table 4.4). The variances of the classes were significantly different from each other ($p < 0.05$). The Tukey test was used to examine which classes were significantly different from each other on the

$p < 0.05$ level (Table 4.5). Since K^+ and Ca^{2+} were neither normally distributed nor the homogeneity of variances was given, a non-parametric Kruskal-Wallis ANOVA was applied to test if there are significant differences between the classes (Table 4.4). Afterwards, a Mann-Whitney test was used (Table 4.5).

The statistical analysis arrived at the result that the classification of the fogwater samples on the basis of the pathway of the trajectories was plausible. The differences between class I and class III were throughout extremely significant (highly significant for Na^+, respectively) for all analyzed parameters. The differences between class II and class III were extremely significant for SO_4^{2-}, highly significant for electric conductivity, pH, NH_4^+, and Ca^{2+} as well as significant for Mg^{2+}. For Na^+, K^+, Cl^-, and NO_3^-, the differences were not significant. Class I and class II were not significantly different for any analyzed parameter. The ANOVA did not achieve a result for PO_4^{3-} and F^- since the number of samples of class II was too small due to the low concentrations that ions.

A Kolmogorov-Smirnov test showed that the rainwater samples were log-normally distributed ($p < 0.05$). A single t-test (for the electric conductivity, pH, NH_4^+, Na^+, Mg^{2+}, Cl^-, NO_3^-, SO_4^{2-} and F^-) and a non-parametric Mann-Whitney test (for K^+ and Ca^+, because no Gaussian distribution was given for the fog water) was applied to examine the differences between the fog and rain water. The differences were found to be significant for all parameters (except for K^+ and F^-: not significant) on the $p < 0.05$ level. For PO_4^{3-}, the t-test was not applied as the concentrations were below detection limit. The total mean equivalent concentration of the fogwater samples was 1249 µeq L^{-1} and 86 µeq L^{-1} for the rain water samples. Thus, the total mean equivalent concentration was about 15 times higher in the fog than in the rain water.

For both the fog and rainwater samples, H^+, NH_4^+, NO_3^-, and SO_4^{2-} contributed most to the total equivalent concentration. Those ions made up 85 % of the total equivalent concentration in the fog water and 84 % in the rain water.
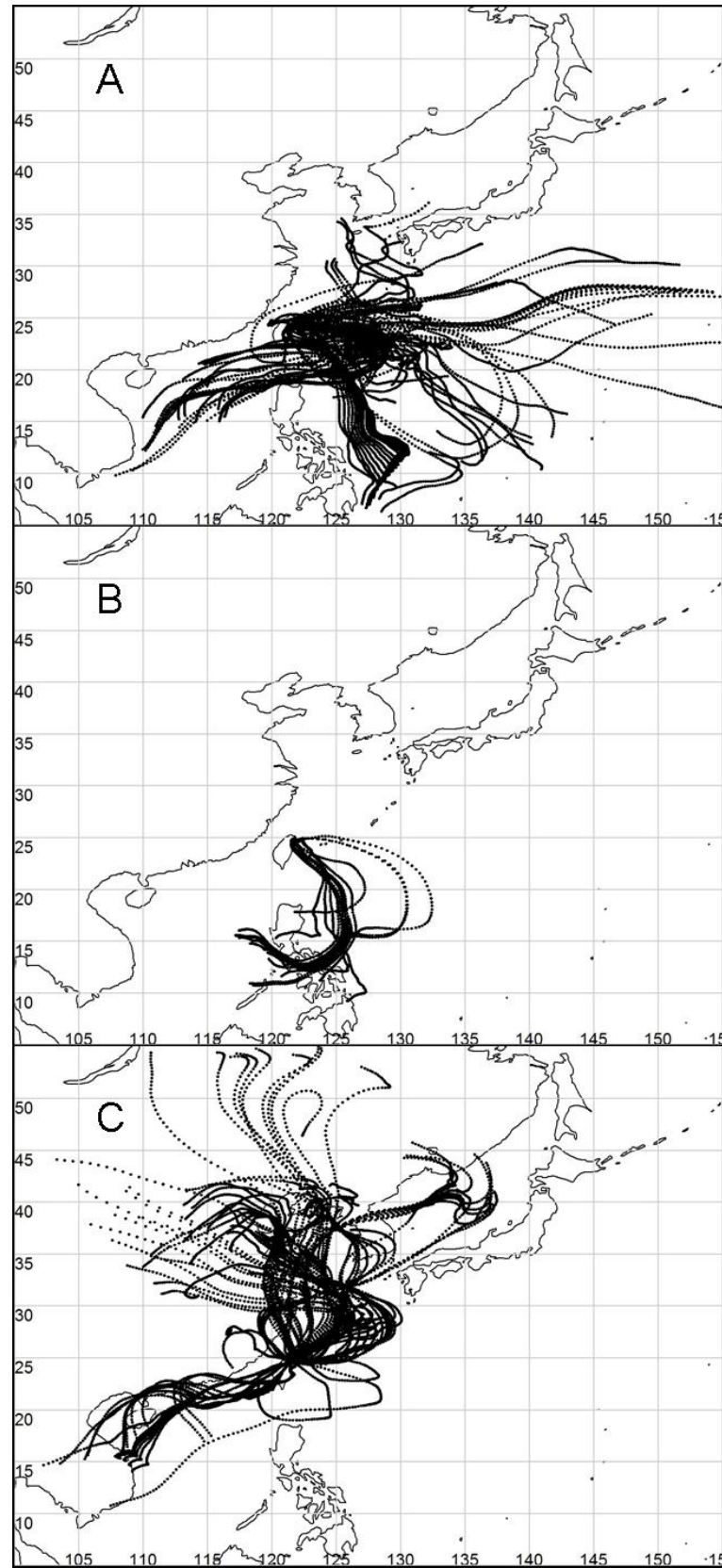
Figure 4.2: Backward trajectories representing the last 120 hours before reaching the Chilan site (24°35'27.4''N and 121°29'56.3''E). A: All trajectories categorized as class I (n = 102). B: All trajectories categorized as class II (n = 20). C: All trajectories categorized as class III (n = 95).

Table 4.3: Median values, averages and standard deviation of the particular classes. Ion concentrations are given in unit µeq L^{-1} and electric conductivity is given in µS cm^{-1}.

Parameter	Class I (n = 102)			Class II (n = 20)			Class III (n = 95)		
	Median	Average	σ	Median	Average	σ	Median	Average	σ
Conductivity	26.2	56.5	84.7	79.2	72.1	58.5	119	214	254
pH	4.43	4.03	0.73	3.85	3.91	0.78	3.69	3.37	0.67
H^+	37.2	87.2	136	141	123	108	204	426	690
NH_4^+	28.7	88.8	179	57.3	60.4	57.2	152	398	505
Na^+	8.7	34.4	78.8	8.7	28.1	42.6	26.3	84.5	156
K^+	2.5	3.8	6	2.5	3	3.9	7.5	18	26.2
Ca^{2+}	8.5	20.9	38.4	10	11.6	7	17	49.1	77.7
Mg^{2+}	4.1	10.3	16.4	6.4	9	9	9.9	28.1	56.9
Cl^-	6.9	24.5	44.7	11.6	29.7	41.5	31.8	62.3	87.1
NO_3^-	23	85.6	193	56.1	78.1	75.8	85.6	270	462
PO_4^{3-}	5.5	11.7	15	b.d.l.	b.d.l.	b.d.l.	18.2	22.2	19.1
SO_4^{2-}	57.3	122	199	89.5	114	110	316	729	1018
F^-	1.4	7	22.4	3.2	3.2	n.d.	5.1	7.1	6.8
∑cations	103			240			455		
∑anions	95			227			442		

Table 4.4: Significance of the differences within the group of all fogwater samples tested using a one-way ANOVA (electric conductivity, pH, NH_4^+, Ca^{2+}, Mg^{2+}, Cl^-, NO_3^-, PO_4^{3-}, SO_4^{2-}, and F^-) and a Kruskal-Wallis ANOVA (K^+ and Ca^{2+}). The level of significance was termed after: n.s. - not significant, * - significant (p < 0.05), ** - highly significant (p < 0.01), *** - extremely significant (p < 0.001). For PO_4^{3-} and F^-, the ANOVA did not achieve a result due to the limited data set of class II.

Parameter	Significance
Conductivity	***
pH	***
H^+	***
NH_4^+	***
Na^+	*
K^+	***
Ca^{2+}	***
Mg^{2+}	***
Cl^-	***
NO_3^-	***
PO_4^{3-}	–
SO_4^{2-}	***
F^-	–

Table 4.5: *Differences between the classes (determined on the basis of the trajectories) tested with a Tukey test (electric conductivity, pH, NH_4^+, Ca^{2+}, Mg^{2+}, Cl^-, NO_3^-, PO_4^{3-}, SO_4^{2-}, and F^-) and a Man-Whitney test (K^+ and Ca^{2+}). The level of significance was termed after: n.s. - not significant, * - significant (p < 0.05), ** - highly significant (p < 0.01), *** - extremely significant (p < 0.001).*

Parameter	Class	Class I	Class II	Class III
Conductivity	Class I	1	n.s.	***
	Class II		1	**
	Class III			1
pH	Class I	1	n.s.	***
	Class II		1	**
	Class III			1
H^+	Class I	1	n.s.	***
	Class II		1	**
	Class III			1
NH_4^+	Class I	1	n.s.	***
	Class II		1	**
	Class III			1
Na^+	Class I	1	n.s.	*
	Class II		1	n.s.
	Class III			1
K^+	Class I	1	n.s.	***
	Class II		1	n.s.
	Class III			1
Ca^{2+}	Class I	1	n.s.	***
	Class II		1	**
	Class III			1
Mg^{2+}	Class I	1	n.s.	***
	Class II		1	*
	Class III			1
Cl^-	Class I	1	n.s.	***
	Class II		1	n.s.
	Class III			1
NO_3^-	Class I	1	n.s.	***
	Class II		1	n.s.
	Class III			1
SO_4^{2-}	Class I	1	n.s.	***
	Class II		1	***
	Class III			1

4.3.2   Occult and wet deposition

During August 04 through September 20 in 2006, 5.77 mm fog water was deposited into the ecosystem by means of turbulent deposition plus gravitational deposition. The total fogwater fluxes ranged between +31.7 mg m^{-2} s^{-1} (emission fluxes) and -56.6 mg m^{-2} s^{-1} (deposition fluxes). The mean liquid water content (*LWC*) as averaged over periods with fog (visibility < 1000 m), was 83.9 mg m^{-3}, and the mean total fog water flux was -4.1 mg m^{-2} s^{-1}. The bimodal pattern of the median normalized droplet number size distribution (Figure 4.3) shows mean droplet diameters *d* with 2 µm < *d* < 6 µm and 9 µm < *d* < 15 µm were the most frequent. Larger fog droplets with mean diameters of 15 µm < *d* < 25 µm contributed most to the total fog water flux. The sedimentation velocity of the fog droplets v_s was calculated. It ranged between 0.007 cm s^{-1} for mean droplet diameters of 1.5 µm and 7.24 cm s^{-1} for mean droplet diameters of 49 µm. The friction velocity u_* is a measure to characterize the development of the turbulence regime (Foken 2003). For a friction velocity $u_* > 0.1$ m s^{-1}, turbulent conditions were assumed. In 18.7 % of the data set, that condition was not fulfilled.
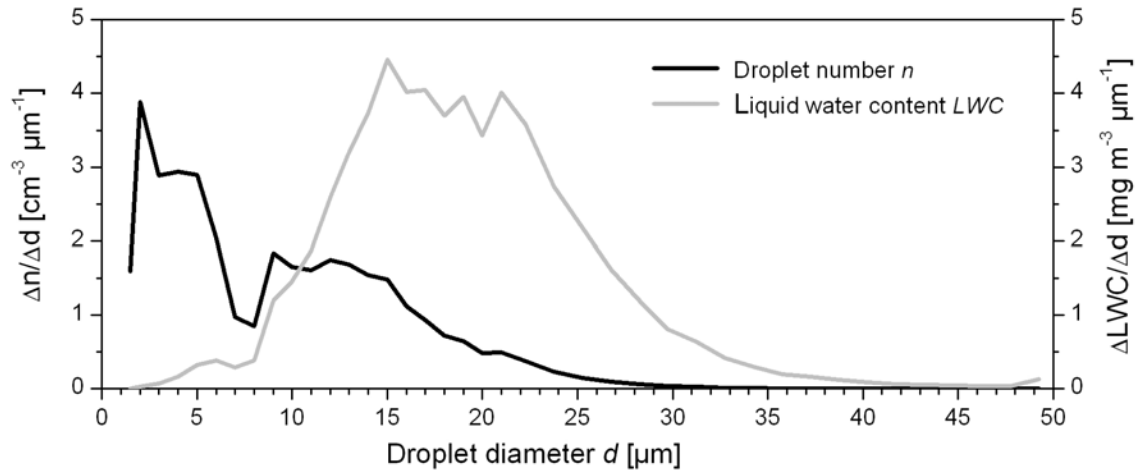
Figure 4.3: Median droplet size distribution of droplet number n (black line) and liquid water content LWC (grey line) on the basis of the medians of all 30-minutes intervals with foggy conditions (visibility < 1000 m) during 4 August 2006 through 20 September 2006 at the Chilan site.

The eddy covariance setup performed as expected, even though small data gaps were inevitable. Large rain droplets caused technical problems and device failures. The experimental site is located in a remote area where the power supply is not permanently guaranteed. In case of heavy thunderstorms, short power failures occasionally occurred. Otherwise, the instrumentation performed very reliably. Since for the calculation of the nutrient input a complete data set of chemical analysis and the respective deposition data are required, small gaps in the data set were filled by the help of a artificial neural network (section 4.2.2.2) (Figure 4.4). The correlation between the originally measured fogwater flux data and the simulated flux data was examined using the Pearson's correlation test. That test showed a significant correlation ($r = 0.73$) on the $p < 0.05$ level.

We did not find any systematic differences in liquid water content concerning the trajectories or advection regime.

In the same time period, 1150 mm were deposited by precipitation (wet deposition).
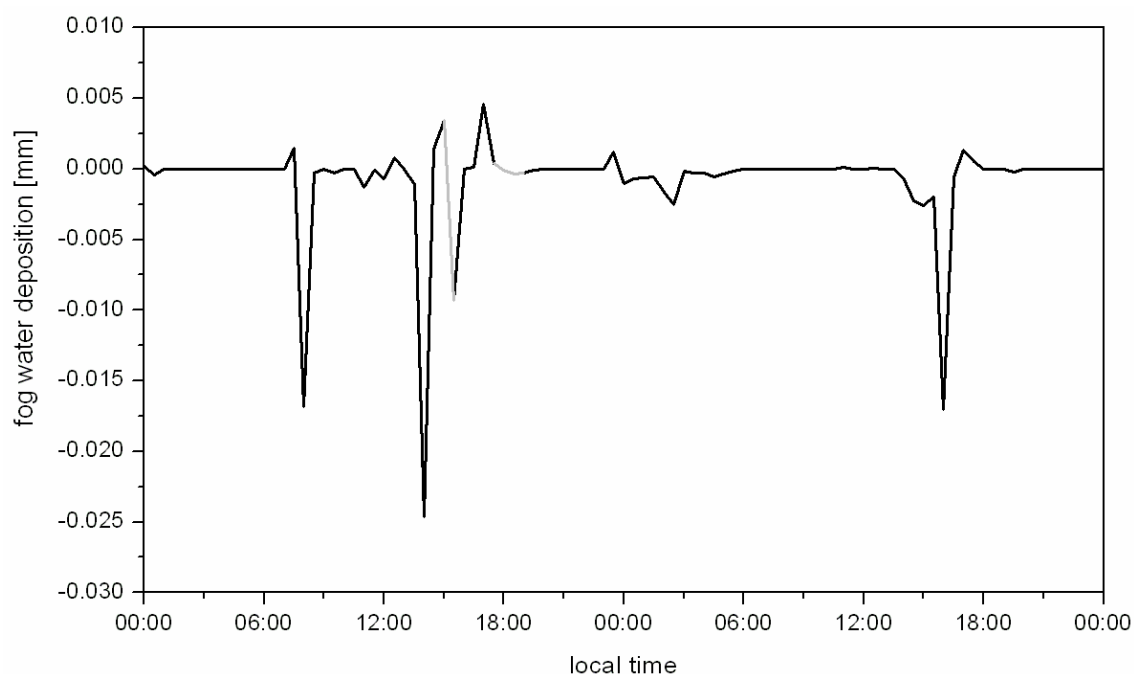
Figure 4.4: Pattern of fog water deposition [mm] during 27 August and 28 August 2006 as an instance for gap filling by using a neural network. The black line represents the originally measured fog water deposition and the grey line is the reproduced fog water deposition.

4.3.3 Nutrient input through occult and wet deposition

The nutrient input through occult and wet deposition was calculated on the basis of 217 fog water and 20 rainwater samples, both completely covered the experimental phase. For the consideration of the sample based input of H^+, NH_4^+, Na^+, K^+, Ca^{2+}, Mg^{2+}, Cl^-, NO_3^-, PO_4^{3-}, SO_4^{2-} and F^-, the quantity of water deposition and the chemical analysis of the respective water sample were regarded. Figure 4.5 and Figure 4.6 show the event based nutrient input through occult and wet deposition. The total nutrient input during the study period is shown in Table 4.6. The dominating ions were NH_4^+, NO_3^-, and SO_4^{2-} (and Cl^- for wet deposition, respectively). The total input of nitrogen by means of occult deposition was 18 mg m^{-2} (10 mg m^{-2} through NH_4^+ and 8 mg m^{-2} through NO_3^-). The sulfur input was 17 mg m^{-2}. For wet deposition, the input of nitrogen was 167 mg m^{-2} (77 mg m^{-2} through NH_4^+ and 90 mg m^{-2} through NO_3^-). The total input of sulfur was 244 mg m^{-2}.
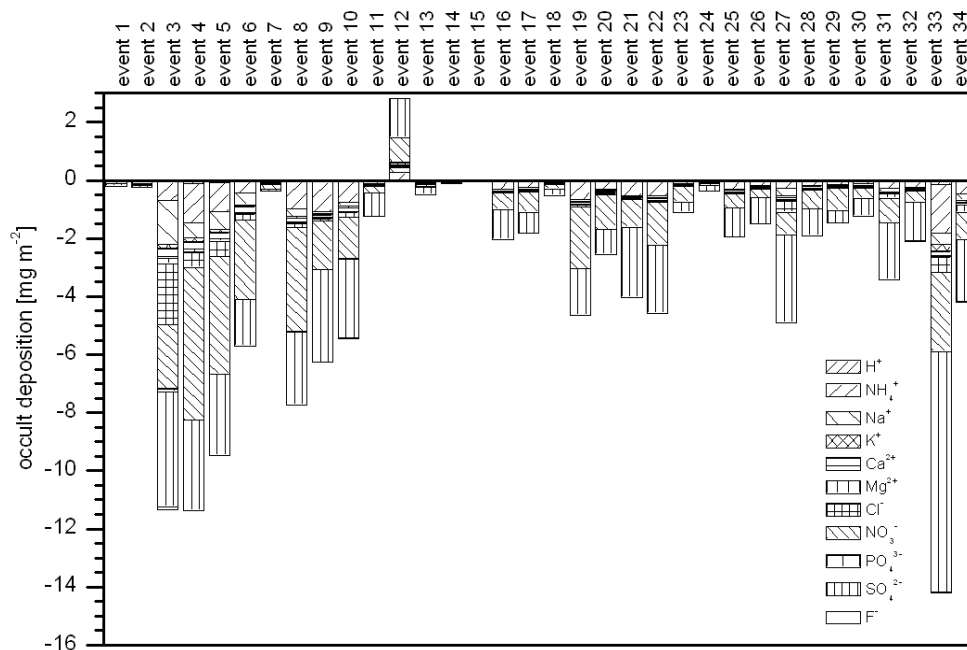
Figure 4.5: Nutrient input through occult deposition [mg m^{-2}] subdivided into 34 single fog events. A negative deposition means nutrient input into the ecosystem and positive deposition means emission of nutrients as a result of positive fog water fluxes.
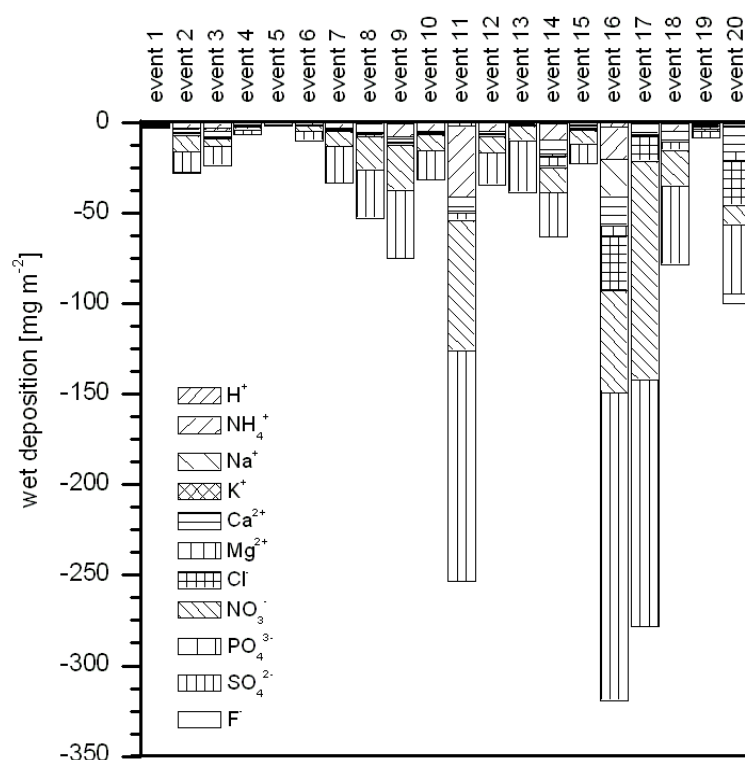
Figure 4.6: Nutrient input through wet deposition [mg m^{-2}] subdivided into 20 single rain events.

Table 4.6: Total nutrient input through occult and wet depsition [mg m^{-2}] measured from 04 August to 20 September 2006 at the Chilan site ("n.d." means no data).

Ion	Occult deposition [mg m^{-2}]	Wet deposition [mg m^{-2}]	Ratio [wet deposition/occult deposition]
H^+	0.8	10.3	13.3
NH_4^+	12.5	98.7	7.9
Na^+	5.0	23.6	4.8
K^+	1.2	1.8	1.5
Ca^{2+}	2.3	77.7	33.1
Mg^{2+}	0.8	19.3	23.7
Cl^-	5.8	96.2	16.5
NO_3^-	36.6	398.9	10.9
PO_4^{3-}	0.2	n.d.	n.d.
SO_4^{2-}	50.2	732.3	14.6
F^-	0.2	5.3	33.4

4.4   Discussion

4.4.1   The influence of air mass history on the chemical composition of fog water

Large differences of ion concentrations were found between the groups of fogwater samples. Statistical tests proved that the classification of the fogwater samples on the basis of the backward trajectories was mostly appropriate and plausible. The differentiation between class I and class III as well as between class II and class III was statistically significant. However, the differences between class I and class II were not significant although the concentrations of ions associated with anthropogenic activity (H^+, NH_4^+, NO_3^-, and SO_4^{2-}) were found to be higher for class II. Thus, it is confirmed that the advection regime of an air mass plays an important role for the chemical concentration of the respective fogwater sample. We interpret these differences in terms of air mass histories of the three classes, and differences of uptake of ions and their precursors during their travel before reaching the sampling site (Klemm et al. 1994; Tago et al. 2006). The base ion charge due to the industrialized region in the western part of Taiwan and the urban agglomeration of the capital Taipei is assumed to be identical for all classes. Air masses classified as class I travel exclusively over the Pacific Ocean and the Taiwan Strait before reaching the study site. Therefore, the fogwater samples of class I exhibit the lowest ion concentrations of ions that are related to anthropogenic activity such as NH_4^+, NO_3^-, and SO_4^{2-}. The maritime impact plays an important role since the concentration of the sea salt related ions Na^+, Cl^-, Mg^{2+}, and Ca^{2+}, are relatively high (although NH_4^+, NO_3^-, and SO_4^{2-} are still higher concentrated) (see also Munger et al. 1989; Gundel et al. 1994). Air masses categorized as class II were advected from the south and passed the Philippines during their last 120 hours. The samples of class II exhibit a similar pattern as class I concerning chemical composition so that those air masses are assumed to be principally influenced by the Pacific Ocean. The anthropogenic influence by means of industry plays a minor role since the

agriculture (cultivation of sugar cane, rice, corn, and manioc) is predominant on the Philippines. The differences between of chemical composition between class I and class II were found to be not statistically significant for any parameter. Class III represents air masses that were transported from mainland China. The fogwater samples of class III show high concentrations of ions attributed to anthropogenic activites. Some trajectories pass directly over the heavily industrialized urban agglomerations of Beijing and Shanghai so that the continental influence can clearly be explained. The differences between class I and class III are significant for all analyzed parameters revealing a distinct air mass history of each class. The statistical analysis showed that class II adopts a mid-position. For most parameters (pH, conductivity, H^+, NH_4^+, Ca^{2+}, Mg^{2+}, SO_4^{2-}) the differences between class II and class III are significant except for Na^+, K^+, Cl^-, and NO_3^- for which the classes do not differ from each other.

The sample number involved a methodological problem since the class II included only 20 fogwater samples (with very low concentrations that were partly below the detection limit), and an analysis of variance did not yield a positive result. Thus, the differences between the classes for F^- and PO_4^{3-} could not be statistically verified.

The pH, electric conductivity, concentration of NH_4^+ as well as SO_4^{2-} were found to be the most differentiating parameters that express the grade of the continental or anthropogenic influence, respectively. The distribution of these four parameters for class I, class II, and class III are plotted in Figure 4.7.
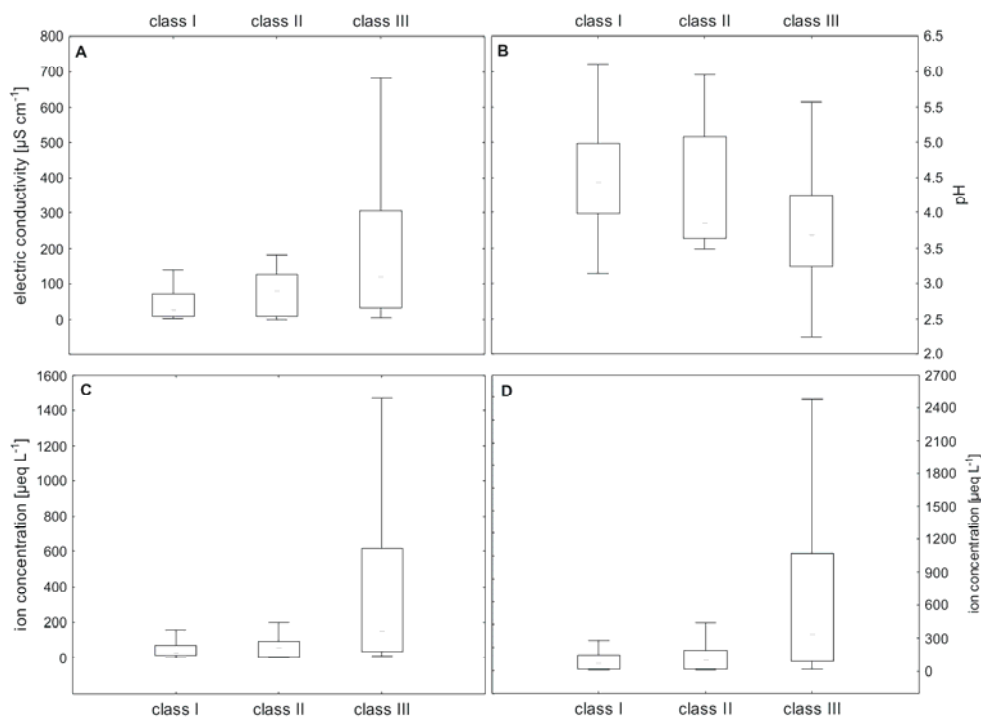

Figure 4.7: Box-Whisker-plots showing the 5 % percentile, 25 % percentile, 50 % percentile (median), 75 % percentile, and the 95 % percentile of the electric conductivity [μS cm^{-1}] (A), pH (B), the concentration of NH_4^+ [μeq L^{-1}] (C), and the concentration of SO_4^{2-} [μeq L^{-1}] (D) for class I, class II, and class III.

4.4.2 Contribution of occult and wet deposition to nutrient input

The differences between the fog and rainwater samples were found to be statistically significant for most analyzed parameters. The mean absolute ion concentrations [μeq L^{-1}] were roughly about 5 to 20 times higher in the fog water than in the rain water. Our results agree well with studies from other experimental sites (Schemenauer et al. 1995; Igawa et al. 1998; Bridges et al. 2002; Beiderwieden et al. 2005). Klemm and Wrzesinsky (2007) report of enrichment factors for NH_4^+, NO_3^-, and SO_4^{2-} in fog versus rain water of 18.1, 12.7, and 11.8, respectively, at a mountainous site in central Europe. The enrichment factors found in our study are 17.8 for NH_4^+, 14.6 for NO_3^-, and 14.0 for SO_4^{2-}, respectively. The differences between fog and rain water may result from the altitude of formation. Fog water represents lower layers of the atmosphere that are more strongly influenced by continental emissions, whereas rain droplets originate at higher altitudes where the atmosphere is less polluted by ground-based emissions (Bridges et al. 2002). Moreover, the rain droplets are much larger and may therefore be more diluted than the fog droplets.

The input of ions through wet deposition has been found to be substantially larger than through occult deposition (Table 4.6). The ratio between both types of input is as high as 33.4 for F$^-$ and 33.1 for Ca^{2+}. The smallest differences exist for K^+. Geogenic origin and industrial processes are the main sources for potassium, so the concentrations in rain water are relatively low.

Although the ion concentrations of the fog water were notably higher than those of the rain water, the absolute nutrient input originated principally from wet deposition. That discrepancy between the measured ion concentrations and the actual relevance for the ecosystem is solely explained by the net amount of water input. During the experimental period, 5.77 mm water was deposited through fog water, and 1150 mm were precipitated through rain. Although the fogwater deposition was rather high, in comparison with rain it accounted for about 0.5 % of the total. For the Yuan Yang Lake site (about 2 km from the Chilan station), Chang et al. (2002) estimated the fog deposition by exposure experiments with epiphytic bryophytes. They report stand-scale deposition rates of 0.17 mm h^{-1}. This calculates to an estimated daily amount of fog deposition of 4.08 mm. The discrepancy between our measurements and the findings from Chang et al. (2002) may be due to the different characteristics of the respective experimental periods concerning the influencing parameters such as the liquid water content of the foggy air and wind velocity. During the experimental period, the mean wind velocity was very low (< 1 m s^{-1} for 57.7 % of the time). During 18.7 % of the time, the friction velocity $u*$ was < 0.1 m s^{-1} indicating that the turbulence regime was not fully developed. Consequently, the eddy covariance method, measuring the turbulent fog water flux, detected only small fluxes. Especially at night, when atmospheric layering was stabile, the fog water fluxes were very small.

Another reason for the relatively low fog water depositions measured in this study may be due to the strong seasonal variation of the occurrence of fog. Chang et al. (2002) found out that during the summer months, the average daily fog duration is 4.7 hours while it was 11.0 hours during the rest of the year. Since this study was carried out in August and September, we possibly did not measure during a period typical for the entire year. Only during 22.1 % of the experimental period, the visibility was < 1000 m (foggy conditions), which corresponds to a daily fog duration of 5.3 hours.

During the summer month, typhoons play an important role for the ecosystem and are a major source of rainfall (Chang et al. 2002; Chang et al. 2006). On the 9th August and the 16th September 2006, typhoons fell on the study site and caused heavy precipitation for several days. The measured amount of rainfall of 1150 mm within 47 days is not representative, either. Depending on number and strength of typhoons, the annual rainfall is highly variable and varies between 2000 mm and 5000 mm. In any case, our experimental period was dominated by high precipitation amounts. For May 2003, Chang et al. (2006) report that the contribution of fog reached 35 % of the total water input, while in September 2003 the fog/rain ratio reduced to only 5 % due to the high precipitation brought by a typhoon.

We consequently suppose that the contribution of fog water to the nutrient input has been overestimated so far. We alternatively assume that the important ecological factor influencing the vegetation structure and thereby the growth of the cypress forest, is the reduction of incoming shortwave solar radiation through fog (Lai et al. 2005). Fog reflects about 90 % of incoming short wave radiation (Häckel 1999). The mean daily sunshine duration is drastically reduced during foggy conditions. As a consequence, the biological activity, or rather the rate of photosynthesis, is diminished. Additionally, the fog water itself influences the physiological conditions and may be a stress factor due to the direct and persistent contact of the acidic solution with the plant surface (Paoletti et al. 1989; Kohno et al. 2001).

Our results of the fog and rain chemistry agree very well with the data given in Chang et al. (2002) for the adjacent measuring station. Compared to other sites, the ion concentrations of the fog water at the Chilan site are relatively low (*e.g.,* Olivier and de Rautenbach 2002; Burkard et al. 2003). The study site is situated in a rural area. The maritime influence is evident due to the comparatively high concentrations of Na^+ and Cl^-. However, the prevalent weather situation has strong impact on the ion loading and thus, the air chemistry. Advection of air masses from mainland China implies a significant nutrient input for the ecosystem. The contribution of ions attributable to anthropogenic activity, such as NH_4^+, NO_3^-, and SO_4^{2-}, is significantly correlated with the air mass transport from China. The most intensive interrelation between advection and nutrient input exists for SO_4^{2-}. During the experimental period, 31 mg m^{-2} SO_4^{2-} were deposited through occult deposition with air masses originating from China, whereas only 19 mg m^{-2} were deposited during air mass advection from the Philippines and the Pacific Ocean.

Due to the requirement of a complete data set of chemical analysis and the respective deposition data for the calculation of the nutrient input, small gaps in the data set were filled using an artificial neural network. The pattern of the simulated flux data reproduced by the artificial neural networks and of the originally measured flux data conformed well. Hence, the closing of the data gaps with MLP networks by means of the corresponding climate data from a nearby station seems to provide a good approximation for otherwise lost data intervals. Our correlation coefficient of $r = 0.73$ expresses a high correlation between the originally measured fog water flux data and the simulated flux data. We consequently conclude that the gap filling by using artificial neural networks was justified.

4.5   Conclusions

The appearance of both endemic *Chamaecyparis* species is assumed to be deeply coupled with the occurrence of fog. Our results indicate that the pertinence of fog for the forest ecosystem is not due to the relevant nutrient input. The nutrient input through wet deposition exceeded the input through occult deposition by far. During our experimental period of 47 days, we found that the input of nutrients through wet deposition was about 13 times higher than through occult deposition. 93 % of total nutrient input originated from rain, and just 7 % entered the ecosystem through fogwater deposition. These large differences result from the different magnitudes of water input. The ecosystem gained about 200 times more water input by the means of rain than by fog deposition. The examination of the meteorological conditions shows that our experimental period was characterized by exceptionally high rainfall and relatively low fog frequency. The occurrence of typhoons in the summer months is therefore an important ecological factor for the nutrient budget of the cypress forest, even though the runoff water is assumed to play an important role in the hydrological budget of a typhoon event as well. We conclude that the contribution of fog water to the nutrient budget of the ecosystem has been overestimated so far.

The median pH of all fogwater samples was 4.13, and the events of class III (air masses originating from mainland China) exhibited a median pH of 3.69. During weather situations with advection of air masses from north-northwest, an enhanced nutrient input was observed. The nutrient input was substantially lower during air mass transport from westerly and southerly directions. The chemical composition of the fogwater samples was led back to the origin of the air mass and the subsequent pathway. We conclude that the weather conditions have an influence on the nutrient input through occult deposition into the ecosystem.

Acknowledgements

Chapter 5

Turbulent fogwater fluxes throughout fog events at a subtropical montane cloud forest in Taiwan

E. Beiderwieden[*1], Y.-J. Hsia[2], and O. Klemm[1]

[1]Institute for Landscape Ecology, University of Münster, Robert-Koch-Str. 26, 48149 Münster, Germany.

[2]Graduate Institute of Natural Resources, National Dong Hwa University, Shoufeng, Hualien 974, Taiwan.

[*]corresponding author

Abstract

An eddy covariance setup was installed within a subtropical montane cypress forest to study the turbulent vertical fluxes of fog water. The occurrence of fog at the Chilan research site was frequent with an average fog duration of 5.3 hours per day. The fog events were found to proceed in a typical pattern with fogwater deposition during the event and emission of medium size fog droplets towards the end of a fog event. The emission of the fog droplets corresponded with the onset of a negative energy balance and radiation balance. Special effort was undertaken to examine the quality of the flux data.

5.1   Introduction

In the present study, we characterize the interactions between turbulent fog water fluxes and the energy budget at the Chilan research site in NE Taiwan, with special focus on the quality of eddy covariance data. Only few studies of direct fogwater flux measurements in montane ecosystems exist so far (*e.g.*, Burkard et al. 2003; Eugster et al. 2006). Particularly in humid environments, the application of the eddy covariance method is related to large difficulties since the sensitive sensing devices of the optical and sonic techniques may often be obstructed by water droplets.

To our knowledge, the study presents the only measurements of turbulent fogwater fluxes by means of the eddy covariance method available for Southeast Asia. This study is imbedded in several research activities with the overall scope to enlighten the ecological processes of the endemic cypress forest within the Yuan Yuang Lake Nature Preserve (*e.g.*, Chou et al. 2000; Chang et al. 2002; Chang et al. 2006). Fog is assumed to be a key factor determining the vegetation structure and thus for the appearance of the endemic cypress forest at that altitude range. With this study, we improve the understanding of the hydrological processes and the subtropical montane cloud forest.

5.2   Methods

5.2.1   Site description

The study took place at the Chilan research site within the Yuan Yuang Lake Nature Preserve in northeastern Taiwan (1650 m about sea level). The Chilan site is characterized by a temperate heavy moist climate with high annual rainfall of more than 4000 mm (Chou et al. 2000). The annual frequency of fog occurrence often exceeds 350 days (Chang et al. 2006), and the fog duration is 4.7 to 11 hours per day (Chang et al. 2002). The wind regime shows a pronounced diurnal cycle. During daytime, uphill winds from SE and S prevail and are strongly coupled with the occurrence of fog. After sunset, the advection regime changes and downhill winds from N and NW predominate that lead to the dissipation of the fog.

The measurements were carried out within a partly managed cypress forest. It comprises an area of about 300 ha and is situated within a valley on a relatively flat section which slopes with an angle of 15° towards SE. The canopy layer is considerably closed and uniform. The average height of the cypress plantation is 13.7 m. Due to the homogenous canopy layer, the study site is well suitable for micrometeorological measurements. The instrumental setup for the fogwater flux measurements was mounted at an experimental tower (24°35'27.4''N and 121°29'56.3''E) at 23.4 m above ground level and thus approximately 10 m above the average canopy height.

5.2.2   Experimental setup

The turbulent fogwater fluxes were measured using the eddy covariance method. The experimental setup consisted of a FM-100 fog droplet spectrometer[3] in combination with a Young 81000 ultrasonic anemometer[4]. The fog droplet spectrometer detected the number and size of fog droplets by scattering of a laser beam. The spectra of fog droplets with mean diameters from 1.5 µm to 49.25 µm within 40 channels were recorded. Further meteorological data were taken from the standard instrumentation available at the meteorological station.

5.2.3   Data processing

The sample frequency of the eddy covariance measurements was 12.5 Hz and the averaging interval was 30 min. The wind vector coordinates were double rotated to align the main axis with the streamlines and to yield a zero average v and w wind component, respectively. The fog water flux data were not de-trended to prevent distortion of the data. The quality criteria were therefore applied to the original data. The steady-state condition of the time series was tested using the stationarity test by Foken and Wichura (1996). The variances of the 30-min intervals were compared with the variances of the six 5-min intervals (within the same 30-min interval). The deviation [%] expresses the dimension of the steady state condition.

The extent of the atmospheric turbulence can be characterized using the friction velocity u_* and the integral turbulence characteristic *ITC* (Foken 2003). The friction velocity u_*, calculated after

$$u_* = \sqrt{- \overline{w' \cdot u'}}$$ (5.1)

is a measure for the vertical exchange of momentum and thus, the turbulent flow field was less developed if u_* was low. The degree of the development of the turbulence regime was also determined by comparing the measurement result (left hand side of Formula 5.2) with the theoretical value (right part of Formula 5.2). The relation between *ITC* of the vertical wind w and the stability was parameterized after

$$\frac{\sigma_w}{u_*} = c_1 \cdot \left(\frac{z}{L} \right)^{c_2}$$ (5.2)

The coefficients c_1 and c_2 depend on the stability z/L and are given in Foken (2003).

The gravitational deposition was determined after Stokes' settling velocity (Beswick et al. 1991). The total fogwater flux was calculated by adding the turbulent and the gravitational flux.

---

[3] Droplet Measurement Technologies, Boulder, USA

[4] R.M. Young Company, 2801 Aeropark Drive, Traverse City, Michigan, USA

5.3   Results and discussion

5.3.1   Turbulent fogwater flux

During the experimental period from August 04 through September 20 in 2006, the total fogwater deposition into the ecosystem by means of turbulent and gravitational deposition was 5.8 mm. The total fogwater fluxes ranged between +31.7 mg m^{-2} s^{-1} (fogwater emission) and -56.6 mg m^{-2} s^{-1} (fogwater deposition). The mean total fog water flux was -4.1 mg m^{-2} s^{-1}, and the mean liquid water content averaged over foggy conditions (visibility < 1000 m) was 83.9 mg m^{-3}. During 22.5 % of the experimental period, the visibility was < 1000 m (corresponding to daily mean fog duration of 5.3 hours).

We found a bimodal pattern of the median normalized droplet size distribution. Figure 5.1 shows that fog droplets with mean droplet diameters d with 3 µm < d < 6 µm and 10 µm < d < 15 µm were the most frequent. The larger fog droplets with mean diameters of 15 µm < d < 25 µm contributed most to the total fog water flux.

The sedimentation velocity ranged between 0.007 cm s^{-1} for mean droplet diameters of 1.5 µm and 7.2 cm s^{-1} for mean droplet diameters of 49.25 µm.
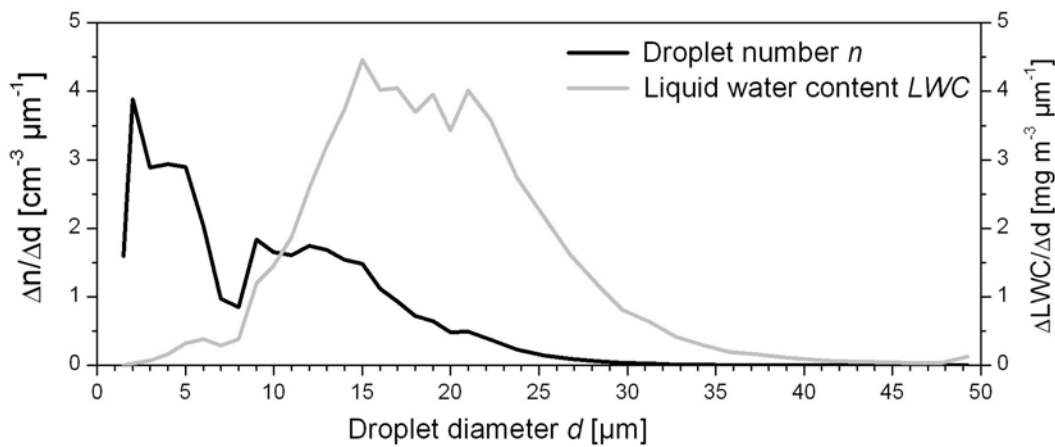
Figure 5.1: Median droplet size distribution of droplet number n (black line) and liquid water content LWC (grey line) on the basis of the medians of all 30-min intervals with foggy conditions (visibility < 1000 m).

5.3.2   Pattern of fog events

The interactions between the turbulent fogwater flux and the energy fluxes within the fog events were examined on the basis of the 30-min intervals. Figure 5.2 shows the averages of nine representative individual fog events. We found a typical pattern with fog water deposition during the event and emission of medium scale fog droplets at the end of the fog event (Figure 5.3). The emission of fog droplets corresponded with the onset of a negative energy balance of the ecosystem and a negative radiation balance.
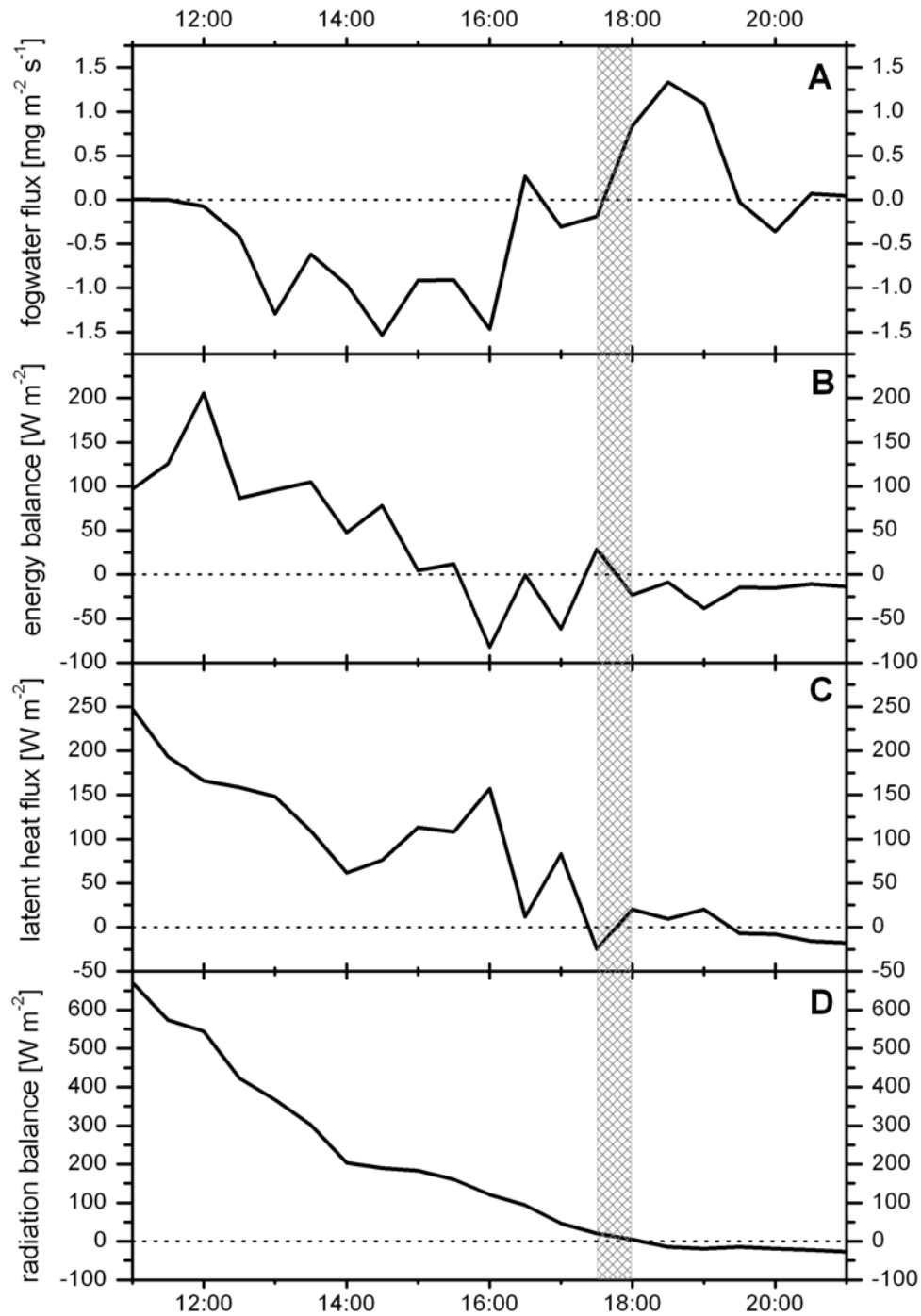
Figure 5.2: Pattern of a representative fog event representing the turbulent fogwater flux (A), the energy balance (B), the latent heat flux (C), and the radiation balance (D) during a fog event.

After noon, the advection of warm and water vapor saturated air masses from SE led to the formation of orographic fog as a result of forced lifting and adiabatic cooling during the uphill transport. The turbulent fogwater flux was negative, *i.e.* fog droplets deposited into the ecosystem (panel A in Figure 5.2). In the afternoon, the energy balance decreased (panel B) along with the radiation balance (panel D) as a result of the daily course as well as the absorption and reflection of shortwave radiation by fog; the air

temperature dropped accordingly (not shown in Figure 5.2). During the time period from 17:30 to 18:00 hrs local time (grey shaded area in Figure 5.2), a change of the meteorological conditions induced. The energy balance as well as the radiation balance turned negative due to the reduction of incoming solar radiation by fog and the decrease of solar radiation at sundown. Simultaneously, the turbulent fogwater flux became positive and fog droplets were emitted out of the ecosystem. We assume that the previously intercepted fog water evaporated from the leaf surfaces as a result of a temperature gradient between forest and atmosphere. Throughout the fog events, the air temperature within the forest was higher than outside. The evaporated water vapor condensed outside the canopy layer and fog originated locally. The course of the latent heat flux leads to the observation that evaporation occurred despite the presence of fog (panel C).

After 19:00 hrs local time, the mean wind direction changed from SE to N/NW (not shown in Figure 5.2) and the advection of drier air by those down-slope winds led to dissipation of the fog.
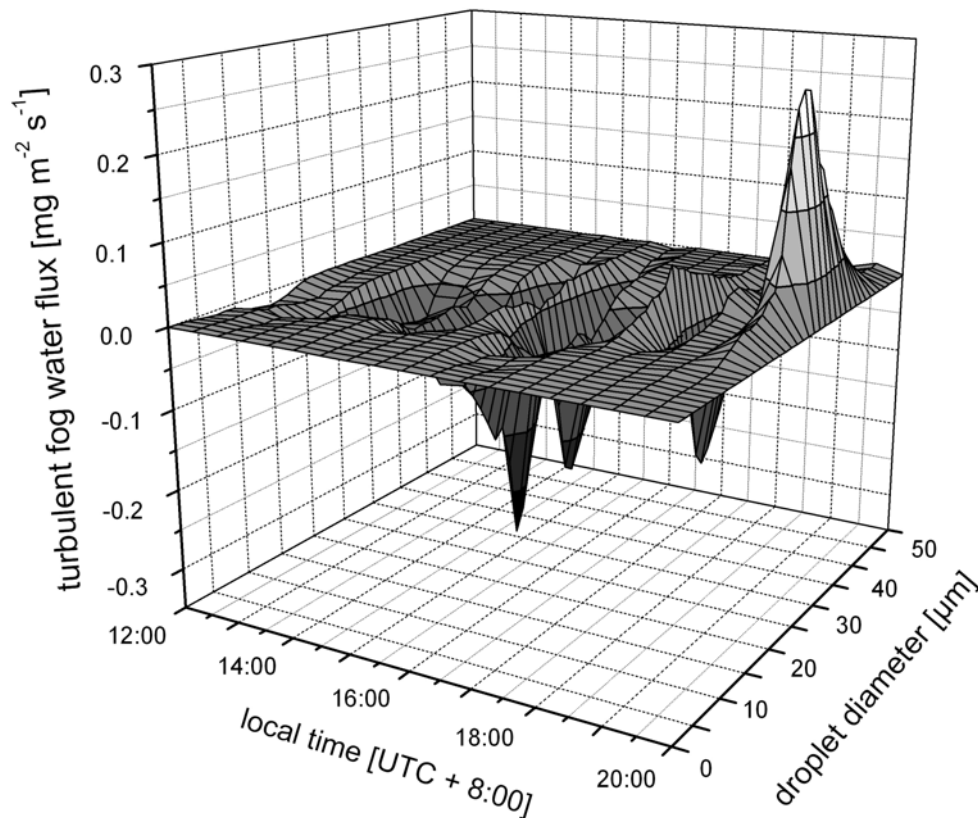
Figure 5.3: Relationship between the turbulent fogwater flux and the droplet diameter over time for an exemplary fog event, using 30-min intervals of data measured by means of the eddy covariance method at the Chilan site (2006/08/18, 12:00 to 20:00 hours local time).

5.3.3   Data quality of eddy covariance data

For an unbiased evaluation of the application of the eddy covariance method, the data was quality checked. The examination of steady-state conditions during the experimental period showed that 88 % of the data can be classified as class 1 to class 3 (Table 5.1). The deviation between the measured and the theoretical value for the integral turbulence characteristic of the vertical wind indicated that 78 % of the data belong to class 1 to class 3 (Table 5.1). After Foken (2003), the classes 1 to 3 (for steady-state conditions and ITC_w) exhibit a high accuracy and are suitable for fundamental research. Class 4 and class 5 are appropriate for continuous research without restriction.

Table 5.1: *Relative distribution of the steady-state conditions and the integral turbulence characteristic of the vertical wind during the experimental period (classification after Foken [2003]). Classes 1 to 3 exhibit the highest data quality.*

Class	Range [%]	Relative distribution [%]	
		stationarity	ITC_w
class 1	0 - 15	64	7
class 2	16 - 30	12	22
class 3	31 - 50	12	49
class 4	51 - 75	10	21
class 5	76 - 100	2	1

The distribution of the friction velocity u_* is shown in Table 5.2. For $u_* > 0.1$ m s^{-1}, turbulent conditions were assumed. The fluxes corresponding to low friction velocities were small but appeared plausible. In 19 % of the data, that condition was not fulfilled. Particularly during nighttime, when the atmospheric layering is stable, the turbulence regime was not very pronounced and u_* was low. Overall, the mean wind speed was quite low during the experimental period; about 58 % of the time, the wind velocity was < 1 m s^{-1}.

Table 5.2: *Relative distribution of the friction velocity during the experimental period.*

Class	Range [m s^{-1}]	Relative distribution [%]
		u_*
class 1	0.00 - 0.1	19
class 2	0.11 - 0.3	61
class 3	0.31 - 0.5	16
class 4	0.51 - 0.7	3
class 5	0.71 - 1.0	1

5.4   Conclusions

During a 47-day period, we measured the turbulent fog water flux by means of the eddy covariance method within a montane cloud forest in southeastern Taiwan. The data were checked concerning the stationarity of the time series and the development of the turbulent atmospheric conditions.

After application of the quality criteria, the Chilan research site was found to be suitable for micrometeorological measurements. Overall, the quality of the flux data measured during daytime was of better quality that those during nighttime due to a better developed flow field over the day. The relatively homogeneous canopy layer of the cypress plantation minimized the generation of additional turbulence elements. The one-dimensional approach appeared appropriate to study the turbulent fog water fluxes and its relevance for the ecosystem. Earlier studies turned out that the energy balance was closed by 17 to 22 %. However, the advection of air masses is assumed to play a role in the local energy budget and further research is needed to study this topic in detail.

Chapter 6

The influence of fog on the turbulent vertical fluxes of CO_2 and water vapor at a subtropical montane cloud forest ecosystem in Taiwan

K. Mildenberger[*1], E. Beiderwieden[1], Y.-J. Hsia[2], and O. Klemm[1]

[1]Institute for Landscape Ecology, University of Münster, Robert-Koch-Str. 26, 48149 Münster, Germany.

[2]Graduate Institute of Natural Resources, National Dong Hwa University, Shoufeng, Hualien 974, Taiwan.

[*]corresponding author

Abstract

The turbulent vertical fluxes of CO_2 and water vapor were quantified above a subtropical mountain cloud forest in NE Taiwan during a seven week experimental field study. The study site is characterized by a high frequency of orographic fog. At daytime, humid air masses are transported uphill, cool down so that condensation leads to fog formation. The CO_2 flux in August and September 2006 ranged between -80 µmol m^{-2} s^{-1} (deposition) and +51 µmol m^{-2} s^{-1} (emission), with an average of -4.7 µmol m^{-2} s^{-1}. The fluxes show a diurnal cycle with CO_2 deposition during daytime representing photosynthetic CO_2 uptake by plants and positive fluxes during night resulting from respiration. The diurnal pattern of the water vapor flux showed maximum positive values (evapotranspiration) at daytime, and minor positive fluxes during nighttimes. It ranged between –7.3 mmol m^{-2} s^{-1} and +16 mmol m^{-2} s^{-1}, the average was +1.7 mmol m^{-2} s^{-1}. The limited solar radiation during fog led to a reduction of the CO_2 flux by 21 % and to a reduction of the water vapor flux by 45 %, as compared to clear situations. However, even though the reduction of solar radiation is high, the *Chamaecyparis* species are able to perform photosynthesis at a high rate. Under foggy conditions, the water vapor flux is still positive, which is a sign for transpiration under saturated conditions.

6.1   Introduction

The water and carbon budgets of subtropical mountain cloud forests are not well examined at this time. Micrometeorological setups are difficult to operate in terrain with steep slopes and a high frequency of rain and fog (*c.f.,* Klemm et al. 2006). It is not clear so far why *Chamaecyparis* species perform extraordinarily well in some sub-tropical mountain cloud forest, and what their ecological limiting factors are. High frequency of fog throughout the year certainly plays an important role in the hydrological cycle of the associated cloud forest ecosystems. In light of the high precipitation rates throughout the year, this is not likely to be a key factor in the eco-physiology of *Chamaecyparis*. The occurrence of fog strongly affects the light environment, which is one of the important ecological factors for plant growth and performance. Limitation of the short wave radiation during fog events might be a factor in the ecological competition of plants, particularly of forest trees. Little is known about the specific physiology of these trees within the mountain cloud forest. We investigate the response of the forest ecosystem CO_2 and water vapor exchange fluxes as a function of light conditions, which are governed by fog.

6.2   Materials and methods

6.2.1   Study Site

Investigations were carried out for seven weeks in August and September 2006 in a subtropical mountain cloud forest in northern Taiwan. The study site is located near the Yuan Yang Lake ecosystem (YYL) at 24°35' N, 121°24' E, at an altitude of 1683 m a.s.l. It was declared a nature preserve in 1986 by the Council of Agriculture. The climate is temperate heavy moist with a mean annual temperature of 13 °C, a low solar radiation and high annual rainfall (> 4000 mm) (Klemm et al. 2006). The humidity is high and there is a high frequency of fog, which accounted for 38 % of the total time 2003 (Chang et al. 2006). The wind regime is influenced by the topography and time of day. There are uphill winds from SE at daytime and downhill winds from NW at night. The fog at the site is formed orographic due to cooling of air during their uphill transport (Klemm et al. 2006). Fog occurs mostly between 12:00 and 21:00 hrs local time, when the wind is from the valley (SE winds).

The measurements were made in a plantation of *Chamaecyparis* species near the YYL by a slope of 15 % towards SE at an experimental tower of 23.7 m height (24°35′27.4′′ N, 121°29′56.3′′ E, 1683 m a.s.l.) (Figure 6.1). The dominant species are *Chamaecyparis* var. *formosana* and *Chamaecyparis formosensis*. The average tree height ranged between 11 m and 13 m and the canopy is rather dense and uniform. In the understory, *Rhododendron formosanum* dominates. Due to the high frequency of fog, there are a lot of epiphytes, mosses and liverworts. Klemm et al. (2006) described the study site as well suited for micrometeorological measurements.
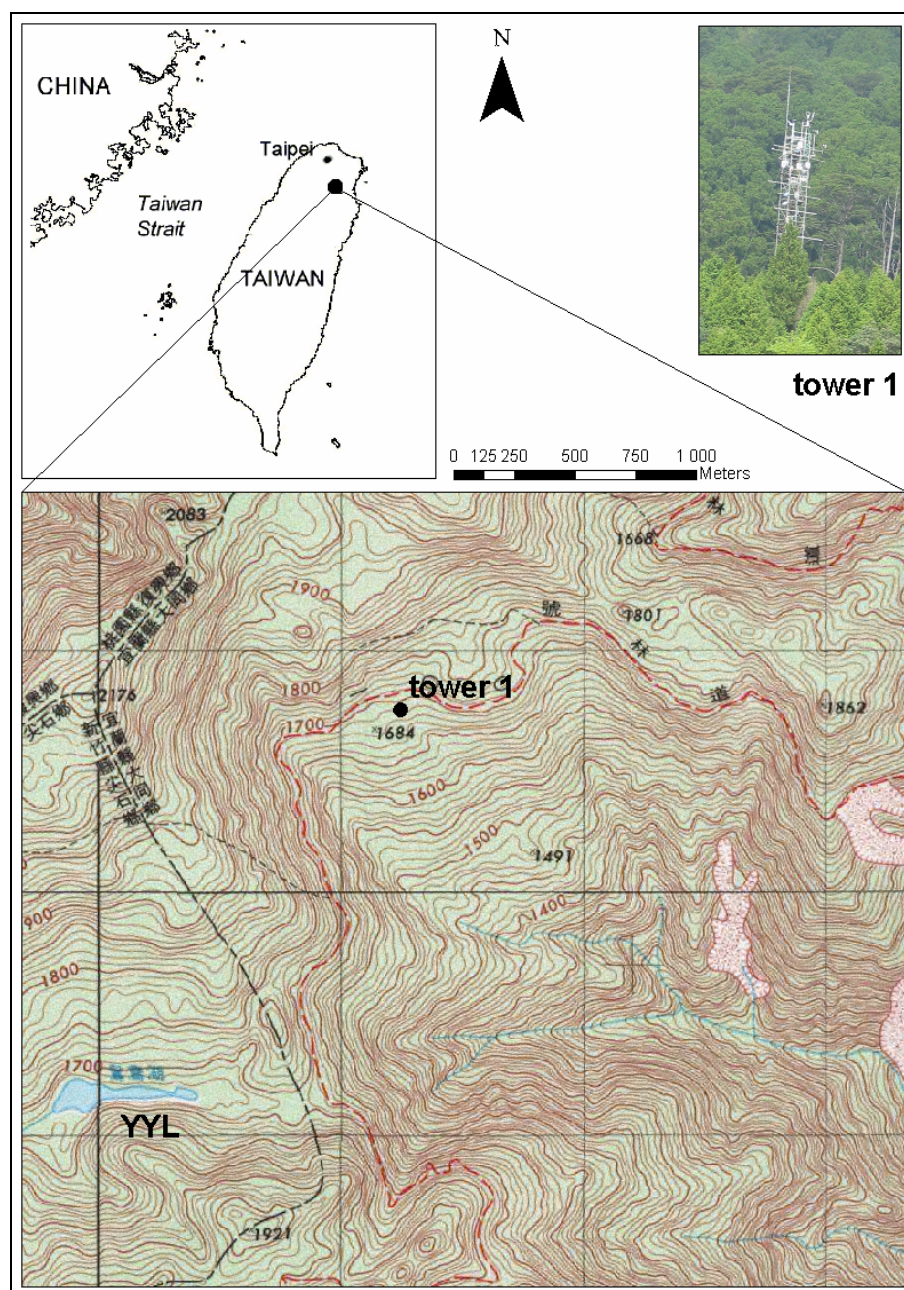
Figure 6.1 Map of the study site with the experimental tower (at 1683 m a.s.l.; 24°35′27.4″ N, 121°29′56.3″ E).

6.2.2 Instrumentation and experimental setup

From the 4th August through 20th September 2006, we operated an experimental setup for measuring the vertical turbulent fluxes of CO_2, water vapor and fog at the tower above the *Chamaecyparis* plantation. For CO_2 and water vapor concentration, the LI-COR 7500 open path infrared gas analyzer was used. The temperature and the wind vectors were measured by using a Young 81000 ultrasonic anemometer. The data were collected with a frequency of 12.5 Hz with a computer. In addition, there were setups for measuring visibility, fog droplet fluxes, solar radiation, relative humidity, and rain.

Conditions with visibility < 1000 m were considered fog according to the World Meteorological Organisation (WMO) definition.

The vertical turbulent fluxes were calculated by using the eddy covariance method

$$F_c = \overline{w'\cdot c'} \qquad\qquad (6.1)$$

where $\overline{w}$ is the mean vertical velocity during a 30 minute time period, w' the deviation of individual readings from $\overline{w}$, $\overline{c}$ the mean concentration of the measured parameter (CO_2 or water vapor), and c' its deviation, respectively.

The planar fit method following Wilczak et al. (2001), divided into four different wind sectors, was used to rotate the coordinate system and to force $\overline{w}$ to zero. Subsequently, the data were WPL corrected (Webb et al. 1980) and 30-min averages of all parameters were calculated. The data were quality checked in a two step procedure. First, periods with instrument malfunction were identified. These data were excluded from further analysis. Secondly, data were tested for stationarity and integral turbulence characteristic ITC_w. Only intervals with well developed turbulence regime (friction velocity $u_* > 0.1$ m s^{-1}; $ITC_w < 30$ %) and stationarity (for CO_2 and water vapor concentration, temperature) were used. Plausible (but not necessarily high quality) 30-min averages were used for gap filling. Overall, the data quality is good. Generally, the daytime data, associated with winds from SE, are of higher quality than the night time data, which are often associated with stable conditions.

For statistical analyses, the time scale was tested for normal distribution and students t-test was performed for describe the significance of the difference between foggy and clear meteorological situations.

6.3   Results and discussion

Averaged meteorological and flux data are shown in Figure 6.2 and Figure 6.3. The mean CO_2 and water vapor flux in the study period (Figure 6.2 and Figure 6.3) are -4.7 µmol m^{-2} s^{-1} and +1.7 mmol m^{-2} s^{-1}, respectively, between 06:30 hrs and 17:00 hrs local time. The CO_2 flux is negative, indicating ecosystem take up of CO_2 due to plant photosynthesis. Under foggy conditions, the CO_2 flux is reduced, as the fog reduces the solar radiation. At night, the CO_2 flux is positive due to respiration of plants and soil. By contrast, the water vapor flux is positive almost throughout the entire day. There is always evapotranspiration, including night time and foggy periods.

During the experimental period, fog occurred between 12:00 and 21:00 hrs local time, when the wind direction was SE (valley winds). At this time the high humidity lead to condensation, while the air masses were cooled down during orographic lifting. But it is interesting that there was still evapotranspiration under foggy conditions although the air was saturated (Beiderwieden et al. *submitted*). During some of the days, there were meteorological situations without fog and wind from SE.

We compare conditions for the time period between 12:00 hrs and 21:00 hrs for foggy with clear situations of the same period of day. During foggy conditions, the mean CO_2 flux was –4.2 μmol m^{-2} s^{-1}, and the mean water vapor flux was +0.83 mmol m^{-2} s^{-1}. In contrast, the CO_2 flux at non foggy conditions during the same time period is -5.3 μmol m^{-2} s^{-1}, and the water vapor flux 1.5 mmol m^{-2} s^{-1} (Table 6.1). In other words, the CO_2 flux under foggy conditions is 21 % less and the water vapor flux is 45 % less than during clear situations. At the same time, the solar radiation was reduced by 64 % during fog. The specific humidity is similar during foggy and not foggy situations. The temperature is reduced by just 1.5 °C during fog.

The reduction of the CO_2 and water vapor fluxes under foggy conditions (21 % and 45 %, respectively), is not statistically significant, despite a reduction of the solar radiation by 64 % (meaning a statistically significant reduction). This leads to the hypothesis that the *Chamaecyparis* species are able to perform photosynthesis at a high rate even under reduced light conditions. Apparently, their light use efficiency is high. This hypothesis is supported by results of Lai et al. (2005), who found in greenhouse experiments that the two cypress species have their highest growth rate under medium light conditions (75 μmol m^{-2} s^{-1} to 100 μmol m^{-2} s^{-1} photosynthetic photon flux density corresponding to 18 W m^{-2} to 24 W m^{-2} photosynthetic active radiation).

With sundown at 18:00 hrs local time, the wind regime changes. At fogless days, the wind direction turns from valley winds (SE) to downhill winds (NW). During foggy days, the wind turns later, just after 21:00 hrs.

Table 6.1: *Averaged fluxes, radiation, specific humidity, temperature, and wind direction from 12:00 to 21:00 hrs local time during the experimental period from 4th August through 20th September 2006.*

	CO$_2$ flux [μmol m^{-2} s^{-1}]	H$_2$O flux [mmol m^{-2} s^{-1}]	short wave radiation [W m^{-2}]
fog	–4.17	0.83	68.78
no fog	–5.25	1.49	185.02
	specific humidity [mmol m^{-3}]	**temperature** [°C]	**wind direction**
fog	1036.78	19.71	SE
no fog	1044.53	21.18	NW / SE
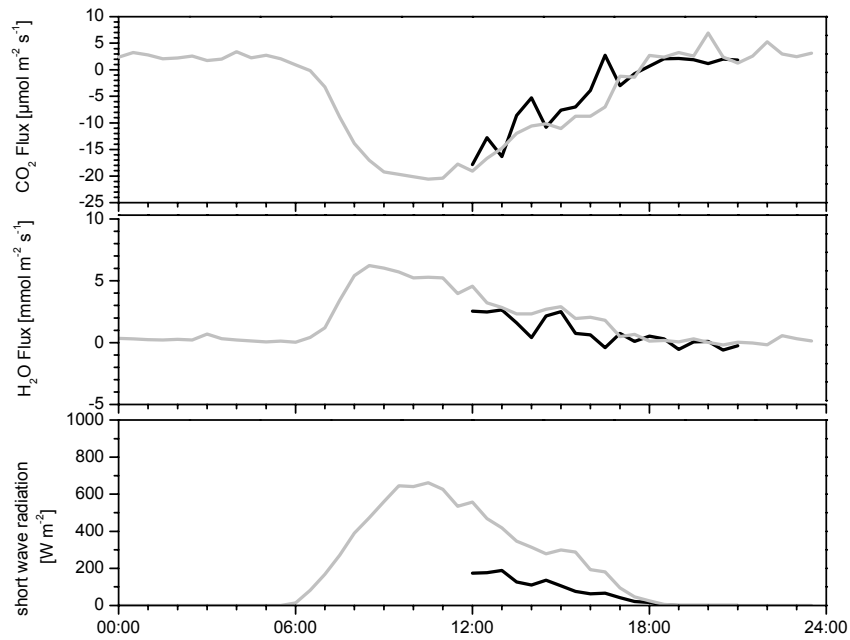
Figure 6.2: Averaged day course for CO_2 flux, water vapor flux, and short wave radiation between 4th August and 20th September 2006 at the YYL site under foggy (black line) and clear (grey line) conditions.
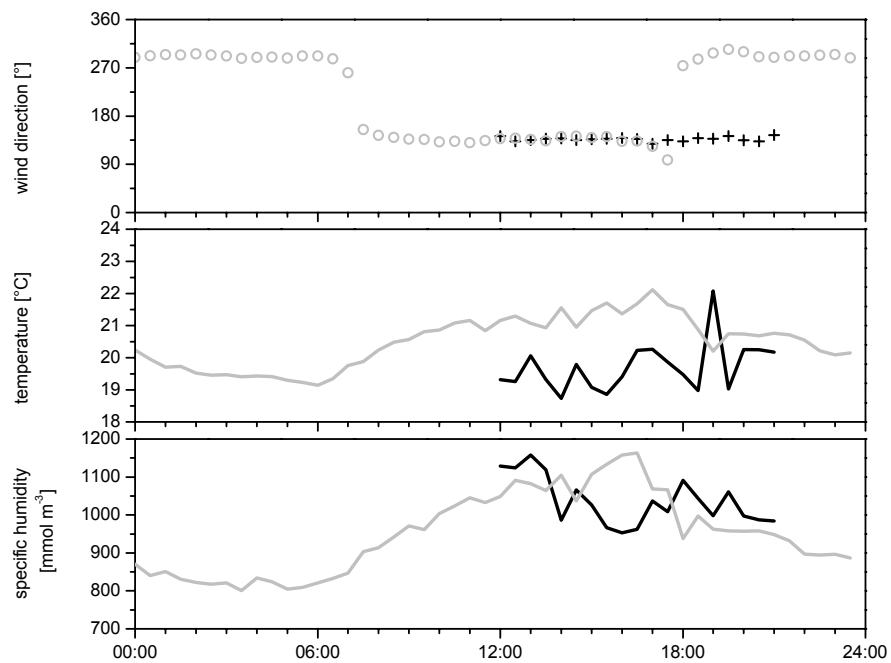
Figure 6.3: Averaged day course for wind direction, temperature, and specific humidity between the 4th August and 20th September 2006 at the YYL site under foggy (black line / cross) and clear (grey line / circle) conditions.

6.4 Conclusions

Solar radiation is one of several key factors limiting plant uptake of CO_2 from the atmosphere. Therefore, it is suspected that the reduction of radiation due to the occurrence of fog limits CO_2 fluxes and photosynthesis. However, our study supports the results of Lai et al. (2005) from greenhouse experiments that the two *Chamaecyparis* species at our site are well adapted to medium light conditions. The photosynthesis rates are only marginally reduced under foggy conditions, as compared to clear conditions. Note there are positive water vapor fluxes under foggy conditions. Such fluxes were also found the same site employing the Bowen ratio method (Beiderwieden et al. *submitted*). This leads to the conclusion that there is confirmed evapotranspiration even under situations where the air masses are saturated. We suspect that it is the plants' transpiration that leads to the positive water vapor fluxes. More experiments to examine this phenomenon are needed.

Chapter 7

Synthesis and concluding remarks

This thesis consists of five interrelated papers. This section links the results of the individual papers and presents the final conclusions. Each of the three field campaigns (in total about six months) was focused on a different research question and thus, a comprehensive study on the impact of fog on the ecology of the cypress forest at the Chilan research station was performed.

We developed and installed an eddy covariance setup at the Chilan research station in northeastern Taiwan to measure the fogwater fluxes above a forest canopy. To our knowledge, our study provides the only measurements of fogwater fluxes by means of the eddy covariance method existing for Southeast Asia. Despite the difficult meteorological conditions, the instrumental setup worked very reliably. After the classification of Foken (2003), the data is of high quality and suitable for fundamental research. We applied an artificial neural network to fill small gaps in the data set. Statistical tests ensured that the pattern of our originally measured flux data and the flux data simulated by artificial neural networks conformed well.

Within this study, we discussed how the energy budget is influenced by fog water. We found that the energy balance of the ecosystem was negative during foggy conditions (-15 W m^{-2}), *i.e.* the ecosystem lost energy and cooled down. In contrast, the energy balance was positive during clear weather periods (26 W m^{-2}) indicating a surplus of energy for the ecosystem. We thus corroborate the hypothesis that the energy budget of the cypress forest is influenced by the presence of fog.

The reduction of the net radiation during foggy conditions was found to be the result of the reflection and absorption of solar radiation by fog. On average, the amount of solar radiation was reduced by 64 %. Since less energy was available during foggy conditions, the biogeochemical processes of the ecosystem were less pronounced. We revealed that the presence of fog affects both the fluxes of CO_2 and water vapor. During foggy conditions, the CO_2 flux was reduced by 21 % and the water vapor flux was 45 % less compared to clear weather conditions. However, the water vapor flux was always positive. For example, evapotranspiration occurred even under foggy (saturated) conditions. The *Chamaecyparis* species (red cypress and yellow cypress) are well adapted to these conditions since they are the predominant tree species for at least 4000 years (Chen and Wu 1999). Former studies found that both *Chamaecyparis* species have their optimal growth rate under medium light conditions from 18 W m^{-2} to 24 W m^{-2} photosynthetically active radiation (Lai et al. 2005). Hence, we conclude that the occurrence of fog implies an advantage for *Chamaecyparis* species in inter-specific

competition because they are able to perform photosynthesis very effectively even under foggy conditions.

We emphasized in this study that positive water vapor fluxes were measured despite the presence of fog. This is a novel aspect because the simultaneous occurrence of evapotranspiration and the deposition of fog droplets contradicts the conventional assumption under the water vapor saturated conditions. However, the existence of these fluxes was shown by two different and independent methods, the Bowen ratio method and the eddy covariance method. Using Monte Carlo type simulations in combination with a single value t-test, we showed that statistically significant evapotranspiration in conjunction with fog droplet deposition occurred during foggy conditions.

We observed a typical pattern of fog droplet deposition during a fog event and emission of fog droplets at the end of the fog event in the evening hours. The emission of fog droplets coincided with the onset of a negative energy balance and radiation balance. We attribute the upward flux of fog droplets to the re-evaporation of the previously intercepted fog water from the leaf surfaces as the result of a temperature gradient between the forest and the atmosphere. Outside the forest canopy, the evaporated water vapor condensed and fog originated locally. This interrelation between hydrological processes and the energy budget was exemplified by presenting a representative fog event. We found a median Bowen ratio of 1.06, indicating that the sensible heat flux and the latent heat flux are nearly balanced. We conclude that the wind regime plays an important role in the local energy budget. The wind regime is characterized by a pronounced diurnal cycle at the study site. During the day, upslope winds from the SE associated with the occurrence of fog prevailed. The advection of warm and saturated air masses to the study area was found to be an important factor for the energy balance of the ecosystem. After sunset, winds from the NW predominated and led to the dissipation of fog.

The analysis of the chemical composition of fog and rainwater confirmed our initial working hypothesis. The ion concentrations of fog water were about 5 to 20 times higher than those of the corresponding rain samples; the total mean equivalent concentration was about 15 times higher. The differences between the concentrations of fog and rain water were found to be significant for most parameters. We attribute the differences to the altitude of fog or rain droplet formation. Fog arises in the lower layers of the atmosphere that are strongly influenced by anthropogenic emissions, whereas rain originates at higher altitudes where the atmosphere is less polluted from ground-based emissions. The size of the droplets is also likely to influence the chemical properties as the rain droplets are larger and may therefore be more diluted than the fog droplets.

We further support our primary hypothesis that the chemical composition of the fog water is characterized by the origin or rather the pathway of the air mass. The analysis of backward trajectories showed that three different advection regimes existed. The air masses of class I were transported exclusively over the Pacific Ocean, class II traveled over the Philippines, and the air masses of class III were advected from mainland China.

A relationship between the ion concentrations and the air masses was verified as we found explicit differences of the ion concentrations between the individual advection classes. The differences between class I and class III as well as between class II and class III were demonstrated to be statistically significant. These differences were attributed to the uptake of ions and their precursors during the transport before reaching the study site. The electric conductivity, pH, and the concentrations of NH_4^+ and SO_4^{2-} were identified to be the key parameters to differentiate the grade of the anthropogenic influence. Weather conditions with advection of air masses from China accounted for an enhanced nutrient input into the ecosystem through occult deposition.

However, the nutrient deposition through wet deposition was substantially larger than through occult deposition (about 13 times). The nutrient input through occult deposition contributed only 7 % to the total nutrient input whereas the nutrient input through wet deposition was 93 %. Our result contradicts the estimation of the nutrient input through occult deposition by Chang et al. (2002) for the same site. They report that more than 50 % of the ecosystem input was through fog water deposition. The discrepancy between our results and the findings of Chang et al. (2002) is explained to be mainly due to the seasonal variation of the amount of fogwater deposition. The contribution of fog to the total water input was reported to be up to 35 % for May and only 5 % for September (Chang et al. 2006) due to the high precipitation brought by typhoons in the summer season. Our experimental period in August and September 2006 was characterized by exceptionally high rainfall and a relatively low fog frequency. The ecosystem gained about 200 times more water through rain (a total of 1150 mm) than through fog water deposition (5.77 mm). The typhoons are identified to be the major source of rainfall and thus play an important role in the hydrology of the cypress forest (Chang et al. 2006). The high amount of water delivered by rain reduces the significance of fog for the nutrient supply to the ecosystem. We conclude that the contribution of fog water to the nutrient budget has been overestimated so far and we negate our hypothesis that occult deposition provides a relevant contribution to the nutrient budget of the ecosystem on an annual average.

Finally, we conclude that the occurrence of fog is the ecological key factor for the functioning of the montane cypress forest within the Yuan Yuang Lake nature preserve. Its relevance for the ecosystem was found to be primarily due to a reduction of the solar radiation. The *Chamaecyparis* species were found to be adapted to the medium light conditions.

Nevertheless, further research is needed to study the influence of the presence of fog on the plant physiology of the *Chamaecyparis* species. A more detailed study of the influence of fog on the CO_2 fluxes and the evaporation processes during foggy conditions would improve the understanding of the biogeochemical cycles of the cypress forest. As forest ecosystems are considered to be important worldwide carbon pools, they strongly impact the atmospheric CO_2 concentration. We have currently started a project to study the net ecosystem exchange of CO_2 between the forest and the atmo-

sphere at the Chilan research site. Within this context, we also intend to install multi-dimensional eddy covariance setups to research the advective transport processes at the study site. Particularly within the framework of global warming, long term measurements of CO_2 as well as water vapor fluxes will yield relevant information about the principal feedback mechanisms affecting the future development of cloud forest ecosystems.

Summary

This thesis is focused on the role of fog water in the hydrological and nutrient cycle of a subtropical montane cloud forest ecosystem in Taiwan. The fogwater fluxes from the atmosphere to the forest canopy were determined by means of the eddy covariance method. In particular, the influence of fog on the energy budget of the ecosystem was investigated. The chemical composition of fog water and rain was studied in order to quantify the nutrient input through occult and wet deposition. The relevance of both deposition pathways for the nutrient budget of the ecosystem was evaluated.

Paper 1: The impact of fog on the energy budget of a subtropical cypress forest in Taiwan

The results of two experimental periods (11 days with clear weather and 5 days with foggy conditions) carried out at the same study site were compared with regard to the influence of fog on the energy balance of the ecosystem. Under clear conditions, the energy balance was positive (26 W m^{-2}), *i.e.* the ecosystem gained energy. During foggy conditions, the energy balance was negative (-15 W m^{-2}) indicating a loss of energy. The incoming shortwave radiation was reduced notably during foggy conditions (up to 95 %) and thus, less energy was available for the ecosystem. The ratio of available energy and the sum of the sensible heat flux, the latent heat flux, and the soil heat flux was studied for daytime and night time conditions for both the clear and foggy periods. At daytime during clear conditions, the net radiation exceeded the sum of the sensible heat flux, latent heat flux, and soil heat flux. In contrast, at daytime under foggy conditions, the net radiation was slightly lower than the sum of the sensible heat flux, latent heat flux, and soil heat flux. The imbalance of the energy budget of the cypress forest was most pronounced at night due to the negative net radiation as a result of the absence of solar radiation and net upward longwave radiative cooling. For both periods, the energy balance was not completely closed. The energy balance closure was -22 % under clear conditions and 17 % under foggy conditions.

Paper 2: It goes both ways: measurements of simultaneous evapotranspiration and fog droplet deposition at a montane cloud forest

By means of the Bowen ratio method and the eddy covariance method, positive water vapor fluxes were measured despite foggy (saturated) conditions. A Monte Carlo simulation confirmed that the evapotranspiration in conjunction with fog droplet deposition was statistically significant. The relationship between the observed water fluxes and the energy budget of the ecosystem is shown by a representative fog event. The vertical gradients of temperature and water vapor pressure measured at two levels (15.05 m and 23.12 m) peaked around noon during days without fog. During foggy conditions, the

gradients dropped to a minimum. The median Bowen ratio was found to be 1.06 for the cypress forest. The median water vapor flux determined with the Bowen ratio method was $+5.2 \times 10^{-5}$ kg m^{-2} s^{-1} and $+6.5 \times 10^{-6}$ kg m^{-2} s^{-1} calculated with the eddy covariance method. At daytime, the sensible heat flux was larger than the latent heat flux. At night, the sensible heat flux was negative whereas the latent heat flux was still positive. The sensible heat flux, the latent heat flux, and the water vapor fluxes associated with wind directions from S to SE were found to be considerably higher than those from N to NW.

Paper 3: Nutrient input through occult and wet deposition into a subtropical montane cloud forest

During a 47-day experimental period, 217 fogwater and 20 rain samples were collected. The differences of ion concentrations between fog water and rain were significant for most ions. The mean ion concentrations were about 5 to 20 times higher in the fog water than in the rain water. For each fogwater sample, a backward trajectory was calculated representing the path of the air mass during the last 120 hours before reaching the study site. The trajectories showed that three advection regimes existed. The air masses of class I traveled exclusively over the Pacific Ocean, class II air masses were transported over the Philippines, and class III air masses were advected from mainland China. Significant differences of ion concentrations between the respective classes were found. An eddy covariance setup was installed to study the fogwater fluxes above the cypress forest. During the experimental period, 5.77 mm fog water was deposited by means of turbulent and gravitational deposition. The mean liquid water content as averaged during foggy conditions was 83.9 mg m^{-3}. An artificial neural network was used to fill small data gaps in the fogwater flux time series. The event based nutrient input was calculated by multiplying the water deposition by the ion concentration of the simultaneously collected water sample. The nutrient input through wet deposition was found to be substantially larger than for occult deposition. About 93 % of the total nutrient input originated from rain and only 7 % were from occult deposition.

Paper 4: Turbulent fogwater fluxes throughout fog events at a subtropical montane cloud forest in Taiwan

The interactions between turbulent fog water fluxes and the energy budget throughout fog events were analyzed. A characteristic pattern was found over the course of fog events with deposition of fog droplets during the event and emission of fog droplets at the end. Fog droplet emission corresponded to the onset of a negative energy and radiation balance. It is assumed that the intercepted fog water evaporated due to a temperature gradient between the forest and the atmosphere. Outside the canopy layer, the water vapor condensed and fog originated. The study was also focused on the quality of the eddy covariance data. The friction velocity u_* and the integral turbulence characteristic of the vertical wind component ITC_w were used to characterize the

development of the atmospheric turbulence. For 81 % of the data, the friction velocity was larger than 0.1 m s^{-1}, *i.e.* the flow field was well-developed. The examination of the steady-state conditions and the *ITC$_w$* parameter showed that 88 % and 78 %, respectively, of the data are of high quality and suitable for fundamental research.

Paper 5: The influence of fog on the turbulent vertical fluxes of CO$_2$ and water vapor at a subtropical mountain cloud forest ecosystem in Taiwan

The study of turbulent CO$_2$ fluxes showed a typical diurnal cycle with deposition fluxes during daytime indicating the photosynthetic uptake of CO$_2$ by plants, and positive fluxes during the night resulting from respiration. The diurnal pattern of the water vapor fluxes showed maximum positive fluxes at daytime, *i.e.* evapotranspiration, and minor positive fluxes during nighttime. The response of the CO$_2$ and water vapor fluxes as a function of the light conditions of the cypress forest was studied. During foggy conditions, the CO$_2$ flux was reduced by 21 % and the water vapor flux by 45 % as compared to clear weather situations. The reduction of the CO$_2$ and water vapor fluxes was obvious but not statistically significant. During foggy conditions, the solar radiation was reduced by 64 % and the air temperature was reduced by 1.5 °C. The cypress species were thus assumed to perform photosynthesis at a high rate even under reduced light conditions. Their light use efficiency was found to be high.

Zusammenfassung

Inhalt dieser Arbeit ist die Untersuchung der Bedeutung von Nebel im Wasser- und Nährstoffhaushalt eines subtropischen Bergnebelwaldes in Taiwan. Zur Bestimmung der Nebelwasserflüsse zwischen Atmosphäre und Wald wurde die Eddy-Kovarianz-Methode verwendet. Besonderer Schwerpunkt der Untersuchung war der Einfluss von Nebel auf den Energiehaushalt des Ökosystems. Zudem wurde die chemische Zusammensetzung von Nebel- und Regenwasser untersucht, um den Nährstoffeintrag über nasse und feuchte Deposition zu quantifizieren. Die Relevanz beider Eintragspfade für den gesamten Nährstoffhaushalt des Ökosystems wurde bewertet.

Paper 1: The impact of fog on the energy budget of a subtropical cypress forest in Taiwan

Der Einfluss von Nebel auf den Energiehaushalt eines Ökosystems wurde in zwei Messkampagnen (elf Tage bei klaren Wetterbedingungen und fünf Tage unter nebeligen Bedingungen) im gleichen Untersuchungsgebiet untersucht. Im Zeitraum ohne Nebel war die Energiebilanz positiv ($26\,\mathrm{W\,m^{-2}}$), so dass das Ökosystem einen Energieüberschuss erhielt. Unter nebeligen Bedingungen war dagegen die Energiebilanz negativ ($-15\,\mathrm{W\,m^{-2}}$), was einen Energieverlust des Ökosystems bedeutet. Bei Nebel war die kurzwellige Sonneneinstrahlung um bis zu 95 % reduziert, so dass dem Ökosystem weniger Energie zur Verfügung stand. Das Verhältnis von verfügbarer Energie zur Summe aus sensiblem Wärmefluss, latentem Wärmefluss sowie dem Bodenwärmefluss wurde für Tag und Nacht sowohl unter klaren als auch unter nebeligen Wetterbedingungen untersucht. Tagsüber bei klarem Wetter war die Energie der Netto-Strahlung höher als die Summe aus sensiblem Wärmefluss, latentem Wärmefluss und Bodenwärmefluss. Bei Tage unter nebeligen Bedingungen war die Summe aus sensiblem Wärmefluss, latentem Wärmefluss und Bodenwärmefluss etwas größer als die NettoStrahlung. Die Energiebilanz war nachts aufgrund der negativen Strahlungsbilanz (Fehlen von kurzwelliger Einstrahlung und gleichzeitiger Energieverlust durch langwellige Ausstrahlung) am wenigsten ausgeglichen. Während der beiden betrachteten Messzeiträume war die Energiebilanz nicht komplett geschlossen. Bei klaren Wetterbedingungen war die Energiebilanz bis auf -22 % geschlossen und bei nebeligem Wetter bis auf 17 %.

Paper 2: It goes both ways: measurements of simultaneous evapotranspiration and fog droplet deposition at a montane cloud forest

Anhand der Bowen-Ratio-Methode und der Eddy-Kovarianz-Methode wurden positive Wasserdampfflüsse trotz nebeliger Wetterbedingungen (gesättigte Verhältnisse) gemessen. Durch eine Monte-Carlo-Simulation wurde nachgewiesen, dass die Evapotrans-

piration und die gleichzeitige Deposition von Nebelwasser statistisch signifikant waren. Das Verhältnis zwischen den beobachteten Wasserflüssen und dem Energiehaushalt des Ökosystems wird anhand eines repräsentativen Nebelereignisses erklärt. Die vertikalen Gradienten von Temperatur und Wasserdampf (gemessen auf 15,05 m und 23,12 m Höhe) zeigten an Tagen ohne Nebel ihr Maximum zur Mittagszeit. Bei Nebel waren die Gradienten am geringsten. Im Rahmen dieser Studie wurde für den Zypressenwald ein Medianwert des Bowen-Verhältnisses von 1,06 ermittelt. Die Medianwerte der Wasserdampfflüsse waren $+5,2 \cdot 10^{-5}$ kg m^{-2} s^{-1} (gemessen mit der Bowen-Ratio-Methode) bzw. $+6,5 \cdot 10^{-6}$ kg m^{-2} s^{-1} (gemessen mit der Eddy-Kovarianz-Methode). Tagsüber war der sensible Wärmestrom größer als der latente Wärmestrom. Bei Nacht wurden negative Werte für den sensiblen Wärmefluss gemessen, während der latente Wärmefluss weiterhin positiv war. Es wurde festgestellt, dass der sensible Wärmefluss, der latente Wärmefluss sowie die Wasserdampfflüsse, die mit südlichen bis südöstlichen Windrichtungen in Verbindung gebracht wurden, wesentlich höher waren als bei Winden aus Norden bis Nordwesten.

Paper 3: Nutrient input through occult and wet deposition into a subtropical montane cloud forest

Im Rahmen einer 47-tägigen Messkampagne wurden insgesamt 217 Nebel- und 20 Regenwasserproben gesammelt. Die Ionenkonzentrationen der Nebel- bzw. Regenwasserproben waren für fast alle untersuchten Ionen signifikant verschieden, im Nebelwasser waren sie durchschnittlich 5 bis 20 mal höher als im Regenwasser. Es wurde für jede Nebelprobe eine Rückwärtstrajektorie berechnet, die den Verlauf der Luftmasse während der letzten 120 Stunden vor Erreichen des Untersuchungsgebiets darstellt. Daraufhin wurden drei verschiedene Advektionsregimes identifiziert. Luftmassen der Klasse I strömten ausschließlich über den Pazifischen Ozean, die Luftmassen der Klasse II wurden über die Philippinen transportiert und die Luftmassen der Klasse III wurden aus China advehiert. Die Ionenkonzentrationen der einzelnen Klassen waren signifikant unterschiedlich. Mittels der Eddy-Kovarianz-Methode wurden die Nebelwasserflüsse über dem Zypressenwald gemessen. Insgesamt wurden während der Messperiode 5,77 mm Nebelwasser durch sedimentative und turbulente Deposition ins Ökosystem eingetragen. Der mittlere Flüssigwassergehalt bei nebeligen Wetterbedingungen war 83,9 mg m^{-3}. Kleine Datenlücken in den Nebelflussdaten wurden mit Hilfe eines künstlichen neuronalen Netzes geschlossen. Durch Multiplikation der Wasserdeposition mit der chemischen Zusammensetzung der entsprechenden Probe wurde der ereignisbezogene Nährstoffeintrag berechnet. Der Nährstoffeintrag durch nasse Deposition war wesentlich höher als der durch feuchte Deposition. Nährstoffe wurden zu etwa 93 % über nasse Deposition und 7 % über feuchte Deposition eingetragen.

Paper 4: Turbulent fogwater fluxes throughout fog events at a subtropical montane cloud forest in Taiwan

Schwerpunkt der Untersuchung war die Interaktion zwischen den turbulenten Nebelwasserflüssen und dem Energiehaushalt im Verlauf der Nebelereignisse. Es wurde ein typischer Verlauf mit Nebelwasserdeposition während des Ereignisses und Emission von Nebeltropfen am Ende des Ereignisses beobachtet. Die Tropfenemission begann zu dem Zeitpunkt, an dem die Energiebilanz und die Strahlungsbilanz negativ wurden. Dieses Phänomen wird so erklärt, dass das zuvor interzipierte Nebelwasser aufgrund des Temperaturgradienten zwischen Atmosphäre und Wald evaporiert. Außerhalb des Kronendachs kondensiert der Wasserdampf wieder und es entsteht Nebel. Im Rahmen dieser Untersuchung wurde zudem die Qualität der Eddy-Kovarianz-Daten bewertet. Die Ausprägung der atmosphärischen Turbulenz wurde mit Hilfe der Schubspannungsgeschwindigkeit u_* sowie der integralen Turbulenzcharakteristik der vertikalen Windkomponente ITC_w beschrieben. Für 81 % der Daten war die Schubspannungsgeschwindigkeit größer als $0,1 \, \mathrm{m \, s^{-1}}$, was auf eine gute Entwicklung der Turbulenz schließen lässt. Nach Betrachtung der Stationarität und der ITC_w wurde die Qualität von 88 % bzw. 78 % der Daten als hoch und somit für Grundlagenforschung geeignet eingestuft.

Paper 5: The influence of fog on the turbulent vertical fluxes of CO_2 and water vapor at a subtropical mountain cloud forest ecosystem in Taiwan

Die Untersuchung der turbulenten CO_2-Flüsse zeigte den erwarteten Tagesgang mit Deposition von CO_2 am Tage (Aufnahme von CO_2 durch photosynthetische Aktivität der Pflanzen) und positiven Flüssen bei Nacht (Respiration der Pflanzen). Der Verlauf der Wasserdampfflüsse zeigte tagsüber die größten positiven Werte (Evapotranspiration) und nachts kleinere positive Werte. Die Betrachtung der Reaktion der CO_2- und Wasserdampfflüsse auf die Lichtbedingungen des Zypressenwaldes zeigte, dass der CO_2-Fluss bei nebeligen Bedingungen um 21 % geringer und der Wasserdampffluss um 45 % geringer als bei klaren Wetterbedingungen war. Diese Reduzierung war deutlich zu beobachten, jedoch statistisch nicht nachweisbar. Bei Nebel war die Strahlung um 64 % und die Lufttemperatur um 1,5 °C vermindert. Es wird daher vermutet, dass die Zypressen das vorhandene Licht optimal ausnutzen und ihre Photosyntheserate daher auch bei Nebel hoch ist.

References

Aldrich, M. (1998). Tropical Montane Cloud Forests. *Planning and Advisory Workshop Report*. World Conservation Monitoring Centre, Cambridge, UK, 23 pp.

Aldrich, M., Bubb, P., and Hostettler, S. (2000). *Tropical Montane Cloud Forests*. Time for Action. Arborvitae. WWF International, IUCN, Gland and Cambridge, 36 pp.

Arya, S.P. (2001). *Introduction to Micrometeorology*. Academic Press, San Diego, 415 pp.

Aubinet, M., Grelle, A., Ibrom, A., Rannik, Ü., Moncrieff, J., Foken, T., Kowalski, A.S., Martin, P.H., Berbigier, P., Bernhofer, C., Clement, R., Elbers, J.A., Granier, A., Grünwald, T., Morgenstern, K., Pilegaard, K., Rebmann, C., Snijders, W., Valentini, R., and Vesala, T. (2000). Estimates of the annual net carbon and water exchange of European forests: the EUROFLUX methodology. *Advances in Ecological Research*, **30**, 113-75.

Beiderwieden, E., Wrzesinsky, T., and Klemm, O. (2005). Chemical characterization of fog and rain collected at the eastern Andes cordillera. *Hydrology and Earth System Sciences*, **9**, 185-191.

Beiderwieden, E., Wolff, V., Hsia, Y.-J., and Klemm, O. (submitted). It goes both ways: measurements of simultaneous evapotranspiration and fog droplet deposition at a montane cloud forest.

Benzing, D.H. (1998). Vulnerabilities of tropical forests to climate change: the significance of resident epiphytes. *Climatic Change* **39,** 519-540.

Beswick, K.M., Hargreaves, K.J., Gallagher, M.W., Choularton, T.W., and Fowler, D. (1991). Size-resolved measurements of cloud droplet deposition velocity to a forest canopy using an eddy correlation technique. *Quarterly Journal of the Royal Meteorological Society*, **117**, 623-645.

Bishop, C. (1995). *Neural Networks for Pattern Recognition*. University Press, Oxford, 482 pp.

Bridges, K.S., Jickjells, T.D., Davies, T.D., Zeman, Z., and Hunova, I. (2002). Aerosol, precipitation and cloud water chemistry on the Czech Krusne Hory plateau adjacent to a heavily industrialised valley. *Atmospheric Environment,* **36**, 353-360.

Bruijnzeel, L.A. and Proctor, J. (1995). Hydrology and biogeochemistry of tropical montane cloud forests: what do we really know? In: Hamilton, L.S., Juvik, J. O., and Scatena, F. N. (Eds.). *Tropical montane cloud forests*. Proceedings of an international symposium. East-West Center, Honolulu, Hawaii, USA.

Bruijnzeel, L.A. and Veneklaas, E.J. (1998). Climatic conditions and tropical montane forest productivity: the fog has not lifted yet. *Ecology* **79**, 3-9.

Bruijnzeel, L.A. and Hamilton, L.S. (2000). *Decision Time for Cloud Forests*. Humid Tropics Programme Series No 13, IHO-UNESCO, Paris.

Bruijnzeel, L.A. (2001). Hydrology of tropical montane cloud forests: A Reassessment. *Land Use and Water Resources Research*, **1**, 1.1-1.18.

Bruijnzeel, L.A. (2004). Hydrological functions of a tropical forest: not seeing the soil for the trees? *Agriculture, Ecosystems and Environment*, **104**, 185-228.

Bubb, P., May, I., Miles, L., and Sayer, J. (2004). Cloud forest agenda. In *UNEP-WCMC Biodiversity Series*, Cambridge, UK, 32 pp.

Burkard, R., Eugster, W., Wrzesinsky, T., and Klemm, O. (2002). Vertical divergences of fogwater fluxes above a spruce forest. *Atmospheric Research*, **64**, 133-145.

Burkard, R., Bützberger, P., and Eugster, W. (2003). Vertical fogwater flux measurements above an elevated forest canopy at the Lägeren research site, Switzerland. *Atmospheric Environment*, **37**, 2979-2990.

Cayuela, L., Glicher, D.J., and Rey-Benayas, J.M. (2006). The Extent, Distribution, and Fragmentation of Vanishing Montane Cloud Forest in the Highlands of Chiapas, Mexico. *Biotropica*, **38**, 544-554.

Cavelier, J., Solis, D., and Jaramillo, M.A. (1996). Fog interception in montane forests across the Central Cordillera of Panamá. *Journal of Tropical Ecology*, **12**, 357-369.

Cavelier, J., Jaramillo, M., Solis, D., and de León, D. (1997). Water balance and nutrient inputs in bulk precipitation in tropical montane cloud forest in Panama. *Journal of Hydrology*, **193**, 83-96.

Chang, S.-C., Lai, I.-L., and Wu, T. (2002). Estimation of fog deposition on epiphytic bryophytes in a subtropical montane forest ecosystem in northeastern Taiwan. *Atmospheric Research*, **64**, 159-167.

Chang, S.-C., Yeh, C.-F., Wu, M.-J., Hsia, Y.-J., and Wu, J.-T. (2006). Quantifying fog water deposition by in situ experiments in a mountainous coniferous forest in Taiwan. *Forest Ecology and Management*, **224**, 11-18.

Chapin, F.S., Matson, P.A., and Mooney, H.A. (2002). *Principles of Terrestrial Ecosystem Ecology*. Springer Verlag, New York, 436 pp.

Chen, S.-H. and Wu, J.-T. (1999). Paleolimnological environment indicated by the diatom and pollen assemblages in an alpine lake of Taiwan. *Journal of Paleolimnology*, **22**, 149-159.

Chen, J.-S. and Chiu, C.-Y. (2000). Effect of topography on the composition of soil organic substances in a perhumid sub-tropical montane ecosystem in Taiwan. *Geoderma*, **96**, 19-30.

Chou, C.-H., Chen, Y.-T., Liao, C.-C., and Peng, C.I. (2000). Long-term ecological research in the Yuen-yang Lake forest ecosystem I. Vegetation composition and analysis. *Botanical Bulletin of Academia Sinica*, **41**, 61-72.

Clark, K.L., Nadkarni, N.M., Schaefer, D., and Gholz, H.L. (1998). Cloud water and precipitation chemistry in a tropical montane forest, Monteverde, Costa Rica. *Atmospheric Environment*, **32**, 1595-1603.

Culf, A.D., Foken, T., and Gash, J.H.C. (2004). The energy balance closure problem. In Kabat, P. et al. (Eds.). Vegetation, water, humans and the climate. A new perspective on an interactive system. Springer, Berlin, Heidelberg. pp 159-166.

Dawson, T.E. (1998). Fog in the California redwood forest: ecosystem input and use by plants. *Oecologie*, **117**, 476-485.

DeFelice, T.P. (2002). Physical attributes of some clouds amid a forest ecosystem's trees. *Atmospheric Research*, **65**, 17-34.

Dollard, G.J., Unsworth, M.H., and Harve, M.J. (1983). Pollutant transfer in upland regions by occult precipitatios. *Nature*, **302**, 241-243.

Doumenge, C., Gilmour, D.A., Ruiz Perez, M., and Blockhus, J. (1995). Tropical montane forests: conservation status and management issues. In: Hamilton, L.S., Juvik, J.O., and Scatena, F.N. (Eds.). *Tropical Montane Cloud Forests. Ecological Studies* 110, Springer Verlag, New York 407 pp.

Draxler, R.R. and Rolph, G.D. (2003): HYSPLIT (Hybrid Single Particle Lagrarian Integrated Trajectory) Modell access via NOAA ARL READY Website (http://www.arl.noaa.gov/ready/hysplit4.htm). NOAA Air Resources Laboratory, Silver Spring, MD.

Elias, V., Tesar, M., and Buchtele, J. (1995). Occult precipitation: sampling, chemical analysis and process modelling in the Sumava Mts. (Czech Republic) and the Taunus Mts. (Germany). *Journal of Hydrology*, **166**, 409-20.

Eugster, W., Burkard, R., Holwerda, F., Scatena, F., and Bruijnzeel, L.A. (2006). Characteristics of fog and fogwater fluxes in a Puerto Rican elfin cloud forest. *Agricultural and Forest Meteorology,* DOI:10.1016/j.agrformet.2006.07.008.

Foken, T. and Oncley, S.P. (1995). Results of the workshop "Instrumental and methodical problems of the land surface flux measurements". *Bulletin of the American Meteorological Society*, **76**, 1191-1193.

Foken, T. and Wichura, B. (1996). Tools for quality assessment of surface-based flux measurements. *Agricultural and Forest Meteorology*, **78**, 83-105.

Foken, T. (2003). *Angewandte Meteorologie, Mikrometeorologische Methoden*. Springer-Verlag, Berlin, 289 pp.

Foken, T., Göckede, M., Mauder, M., Marth, L., Amiro, B.D, Munger, J.W. (2004). Post field data quality control. In Lee, X., Massman, W., and Law, B. (Eds.). *Handbook of Micrometeorology: A Guide for Surface Flux Measurement and Analysis*. Kluwer, Dordrecht, 81-108 pp.

Gallagher, M.W., Beswick, K., and Choularton, T.W. (1992). Measurements and Modelling of Cloudwater Deposition to Moorland and Forests. *Environmental Pollution*, **75,** 97-107.

Gu, J., Smith, E.A., and Merrit, J.D. (1999). Testing energy balance closure with GOES-retrieved net radiation and in situ measured eddy correlation fluxes in BOREAS. *Journal of Geophysical Research*, **104** (D22), 27881-27893.

Gundel, L.A., Benner, W.H., and Hansen, A.D.A. (1994). Chemical composition of fog water and interstitial aerosol in Berkeley, California. *Atmospheric Environment*, **28**, 2715-2725.

Häckel, H. (1999): *Meteorologie*. Ulmer-Verlag, Stuttgart, 448 pp.

Hamilton, L.S., Juvik, J.O., Scatena, F.N. (1995). The Puerto Rico Tropical Cloud Forest Symposium: Introduction and Workshop Synthesis. In: Hamilton, L.S., Juvik, J.O., and Scatena, F.N. (Eds.). *Tropical Montane Cloud Forests. Ecological Studies* 110, Springer Verlag, New York 407 pp.

Heusinkveld, B.G., Jacobs, A.F.G., Holtslag, A.A.M., and Berkowicz, S.M. (2004). Surface energy balance in an arid region: role of soil heat flux. *Agricultural and Forest Meteorology*, **122**, 21-37.

Holder, C.D. (2003). Fog precipitation in the Sierra de las Minas Biosphere Reserve, Guatemala. *Hydrological Processes*, **17**, 2001-2010.

Holder, C.D. (2004). Rainfall interception and fog precipitation in a tropical montane cloud forest of Guatemala. *Forest Ecology and Management*, **190,** 373-384.

Holwerda, F., Burkard, R., Eugster, W., Scatena, F.N., Meesters, A.G.C.A., Bruijnzeel, L.A. (2006). Estimating fog deposition at a Puerto Rican elfin forest site: comparison of the water budget and eddy covariance methods. *Hydrological Processes*, **20,** 2669-2692.

Houghton, D.D. (1985). *Handbook of Applied Meteorology*. Wiley-Interscience, New York, 1461 pp.

Hsia, Y.-J., Chang, S.-C., and Klemm, O. (2004). Fog deposition and evaporation at a mountain cloud forest in Taiwan. In: Sidle, R.C., Tani, M., Abdul Rahim, N., and Tewodros Ayele, T. (Eds). Forest and water in warm, humid Asia. *Proceedings of a IUFRO Forest Hydrology Workshop*, 10-12 July 2004, Kota Kinabalu, Malaysia, Disaster Prevention Research Institute, Uji, Japan. 274 pp.

Hutley, L.B., Doley, D., Yates, D.J., and Boonsaner, A. (1997). Water Balance of an Australian Subtropical Rainforest at Altitude: the Ecological and Physiological Significance of Intercepted Cloud and Fog. *Australian Journal of Botany*, **45**, 311-329.

Hwang, Y.H., Fan, C.W., Yin, M.H. (1996). Primary production and chemical composition of emergent aquatic macrophytes, *Schoenoplectus mucronatus* ssp. *Robustus* and *Sparganium fallax*, in the Yuang-Yang Lake, Taiwan. *Botanical Bulletin of Academia Sinica*, **37**, 265-273.

Igawa, M., Tsutsumi, T. M., and Hiroshi, O. (1998). Fogwater chemistry at a mountainside forest and the estimation of the air pollutant deposition via fog droplets based on the atmospheric quality at the mountain base. *Environmental Science & Technology*, **36**, 1-6.

Jen, I.-A. (1995). Expectation and historical review of cypress (*Chamaecyparis* ssp.) timber production in Taiwan. *Bulletin of the Taiwan Forest Research Institute*, **10**, 227-234.

Klemm, O., Bachmeier, A. S., Talbot, R.W., and Klemm, K.I. (1994). Fog chemistry at the New England Coast: Influence of air mass history. *Atmospheric Environment*, **28**, 1181-1188.

Klemm, O., Chang, S.-C., and Hsia, Y.-J. (2006). Energy Fluxes at a Subtropical Mountain Cloud Forest. *Forest Ecology and Management,* **224**, 5-10.

Klemm, O. and Wrzeseinsky, T. (2007). Fog deposition fluxes of water and ions to a mountainous site in central Europe. Accepted for publication in *Tellus.*

Kohno, Y., Matsuki, R., Nomura, S., Mitsunari, K., and Nakao, M. (2001). Neutralization of acid fog droplets on plant leaf surfaces. *Water, Air, and Soil Pollution*, **130**, 977-982.

Kowalski, A.S. and Vong, R.J. (1999). Near-surface fluxes of cloud water evolve vertically. *The Quarterly Journal of the Royal Meteorological Society*, **125,** 2663-2684.

Kuo, Y.-H., Chen, C.-H., Chien, S.-C., and Lin, H.C. (2004). Novel diterpenes from the heartwood of Chamaecyparis obtusa var. formosana. *Chemical & Pharmaceutical Bulletin*, **52**, 764-766.

Lai, I.-L., Scharr, H., Chavarria-Krauser, A. Wu, J.-T., Schurr, U., and Walter, A. (2005). Leaf growth dynamics of two congener gymnosperm species reflect the heterogeneity of light intensities given in their natural ecological niche. *Plant Cell and Environment*, **28**, 1496-1505.

Lawton, R.O., Nair, U.S., Pielke, R.A., and Welch, R.M. (2001). Climatic Impact of Tropical Lowland Deforestation on Nearby Montane Cloud Forests. *Science*, **294**, 584-587.

Legendre, P. and Legendre, L. (1998). Numerical Ecology. In *Developments in Environmental Modelling.* Elsevier, Scientific Publishing, Amsterdam, 853 pp.

León-Vargas, Y., Engwald, S., and Proctor, M. C. F. (2006). Microclimate, light adaption and desiccation tolerance of epiphytic bryophytes in two Venezuelan cloud forests. *Journal of Biogeography*, **33**, 901-913.

Liao, C.-C., Chou, C.-H., and Wu, J.-T. (2003a). Regeneration patterns of yellow cypress on down logs in mixed coniferous-broadleaf forest of Yuangyuang Lake Nature Preserve, Taiwan. *Botanical Bulletin of Academia Sinica*, **44**, 229-238.

Liao, C.-C., Chou, C.-H., and Wu, J.-T. (2003b). Population structure and substrates of Taiwan Yellow False Cypress (*Chamaecyparis obtusa* var. *formosana.* in Yuangyuang Lake Nature Reserve and nearby Szumakuszu, Taiwan. *Taiwania*, **48**, 6-21.

Liljequist, G.H. und Cehak, K. (1990). Allgemeine Meteorologie. Viehweg, Braunschweig, 396 pp.

Liu, W.-J., Meng, F.-R., Zhang, Y.-P., Liu, Y.-H., and Li, H. M. (2004). Water input from fog drip in the tropical seasonal rain forest of Xishuangbanna, South-West China. *Journal of Tropical Ecology*, **20**, 517-524.

Lovett, G.M. (1984). Rates and Mechanisms of Cloud Water Deposition to a Subalpine Balsam Fir Forest. *Atmospheric Environment*, **18**, 361-371.

Marth, L. (1998). Flux sampling errors for aircrafts and towers. *Journal of Atmospheric and Oceanic Technology*, **15**, 416-429.

Monteith, J.L. and Unsworth, M. (1990). Evaporation and Environment. *Symposium of the Society for Experimental Biology*, **19**, 205-234.

Munger, J.W., Colett, J., Daube, B., and Hoffmann, M.R. (1989). Chemical composition of coastal stratus clouds – dependence on droplet size and distance from the coast. *Atmospheric Environment*, **23**, 2305-2320.

Ohmura, A. (1982). Objective Criteria for Rejecting Data for Bowen Ratio Flux Calculations. *Journal of Applied Meteorology*, **21**, 595-598.

Oke, T.R. (1987). *Boundary Layer Climates*. Second Edition. Methuen, New York, 435 pp.

Olivier, J. and de Rautenbachn C.J. (2002). The implementation of fogwater collection systems in South Africa. *Atmospheric Research*, **64**, 227-238.

Pahl, S. (1996). Feuchte Deposition auf Nadelwälder in den Hochlagen der Mittelgebirge. *Berichte des Deutschen Wetterdienstes*, **198**, 137 pp.

Panin, G.N., Tetzlaff, G., and Raabe, A. (1998). Inhomogeneity of the land surface and problems in the parameterization of surface fluxes in natural conditions. Journal *of Applied Meteorology and Climatology*, **60**, 163-178.

Paoletti, E., Gellini, R., and Barbolani, E. (1989). Effects of acid fog and detergents on foliar leaching of cations. *Water, Air, and Soil Pollution*, **45**, 49-61.

Papale, D. and Valentini, R. (2003). A new assessment of European forest carbon exchanges by eddy fluxes and artificial neural network spatialization. *Global Change Biology*, **9**, 525-535.

Patterson, D. (1996). *Artificial Neural Networks*. Prentice Hall, Singapore, 477 pp.

Payero, J.O., Neale, C.M.U., Wright, J.L., and Allen, R.G. (2003). Guidelines for Validating Bowen Ratio Data. *American Society of Agricultural Engineers*, **46**, 1051-1060.

Peacock, C.E. and Hess, T.M. (2004). Estimating evapotranspiration from a reed using the Bowen ratio energy balance method. *Hydrological Processes*, **18**, 247-260.

Pounds, J.A., Fogden, M.P.A., and Campbell, J.H. (1999). Biological response to climate change on a tropical mountain. *Nature*, **398**, 611-615.

Raabe, A., Arnold, K., and Ziemann, A. (2002). Horizontal turbulent fluxes of sensible heat and horizontal homogeneity in Micrometeorological experiments. *American Meteorological Society*, **19**, 1225-1230.

Rolph, G.D. (2003). Real-time Environmental Applications and Display sYstem (READY) Website (http://www.arl.noaa.gov/ready/hysplit4.html). NOAA Air Resources Laboratory, Silver Spring, MD.

Schatzmann, M. (1999). Wind tunnel modelling of fog droplet deposition on cylindrical obstacles. *Journal of Wind Engineering and Industrial Aerodynamics*, **83**, 371-380.

Schemenauer, R.S., Banic, C.M., and Urquizo, N. (1995). High elevation fog and precipitation chemistry in Southern Quebec, Canada. *Atmospheric Environment*, **29**, 2235-2252.

Setiono, R. and Hui, L.C.K. (1995). Use of a quasi-Newton method in a feedforward neural network construction algorithm. *IEEE Transactions on Neural Networks*, 273-277.

Stadtmüller, T. (1987). *Cloud Forests in the Humid Tropics*. A Bibliographic Review. The United Nations University, Tokyo and Centro Agronomico Tropical de Investigacion y Ensenanza, Turrialba, Costa Rica, 81 pp.

Stauch, V. and Jarvis, J. (2006). A semi-parametric gap-filling model for eddy covariance CO_2 flux time series data. *Global Change Biology*, **12**, 1707-1716.

Stull, R.B. (1988*). An Introduction to Boundary Layer Meteorology*. Dordrecht, Boston, London, Kluwer Academic Publishers. 666 pp.

Stull, R.B. (2000). Meteorology today for scientists and engineers: A technical companion book. West Publishing Company, 502 pp.

Su, H.J. (1984). Studies on the climate and vegetation types of the natural forest in Taiwan (II) Altitudinal vegetation zones in relation to temperature gradient. *Quarterly Journal of Chinese Forestry*, **17**, 57-73.

Tago, H., Kimura, H., Kozawa, K., and Fujie. K. (2006). Long-term observation of fogwater composition at two mountainous sites in Gunma Prefecture, Japan. *Water, Air, and Soil Pollution*, **175**, 375-391.

Thalmann, E. (2001). Comparison of wet and occult deposition. Diploma thesis, University of Bern.

Thalmann, E., Burkard, R., Wrzesinsky, T., and Klemm, O. (2002). Ion fluxes from fog and rain to an agricultural and a forest ecosystem in Europe. *Atmospheric Research*, **64**, 147-158.

Trautner, F. (1988). Die Entwicklung und Anwendung von Messsystemen zur Untersuchung der chemischen und physikalischen Eigenschaften von Nebelwasser und dessen Deposition auf Fichten. Dissertation, University of Bayreuth.

Trautner, F. and Eiden, R. (1988). A measureing device to quantify deposition of fog water and ionic input by fog on small spruce trees. *Trees*, **2**, 92-95.

Vermeulen, A.T., Wyers, G.P., Romer, F.G., Van Leeuwen, N.F.M., Draaijers, G.P.J., and Erisman, J.W. (1997). Fog deposition on a coniferous forest in The Netherlands. *Atmospheric Environment*, **31**, 375-386.

Vong, R.J. and Kowalski, A.S. (1995). Eddy correlation measurements of size-dependent cloud droplet turbulent fluxes to complex terrain. *Tellus*, **47** B, 331-352.

Weathers, K.C. and Likens, G.E. (1997). Clouds in southern Chile: an important source of nitrogen to nitrogen-limited ecosystems? *Environmental Science and Technology*, **31**, 210-213.

Weathers, K.C., Lovett, G.M., Likens, G.E., and Caraco, N.F.M. (2000). Cloudwater inputs of nitrogen to forest ecosystems in southern Chile: forms, fluxes, and sources. *Ecosystems*, **3**, 590-595.

Webb, E., Pearman, G.I., and Leuning, R. (1980). Correction of flux measurements for density effects due to heat and water vapor transfer. *Quarterly Journal of the Royal Meteorological Society*, **106**, 85-100.

Wilson, K., Goldstein, A., Falge, E., Aubinet, M., Baldocchi, D., Berbigier, P., Bernhofer, C., Ceulemans, R., Dolman, H., Field, C., Grelle, A., Ibrom, A., Law, B.E., Kowalski, A., Meyers, T., Moncrieff, J., Monson, R., Oechel, W., Tenhunen, J., Valentini, R., and Verma, S. (2002). Energy balance closure at FLUXNET sites. *Agricultural and Forest Meteorology*, **113**, 223-43.

Wilczak, J., Oncley, S., and Stage, S. (2001). Sonic anemometer tilt correction algorithms. *Boundary Layer Meteorology*, **99**, 127-150.

Wrzesinsky, T. and Klemm, O. (2000). Summertime fog chemistry at a mountainous site in central Europe. *Atmospheric Environment*, **34**, 1487-1496.

Wrzesinsky, T. (2004). Direkte Messung und Bewertung es nebelgebundenen Eintrags von Wasser und Spurenstoffen in ein montanes Waldökosystem. Dissertation, University of Münster. (URN: nbn:de:bvb:703-opus-784).

Zadroga, F. (1981). The hydrological importance of a montane cloud forest area of Costa Rica. In: Lal, R. and Russel, E. W. (Eds.). *Tropical Agricultural Hydrology*. John Wiley and Sons, New York, p 59-73.

Zimmermann, L., Frühauf, C., and Bernhofer, C. (1999). The role of interception in the water budget of spruce stands in the Eastern Ore Mountains/Germany. *Physics and Chemistry of the Earth*, **24**, 809-812.

Danksagung

Curriculum Vitae

Eva Beiderwieden, born on 25th February 1980 in Mülheim an der Ruhr, Germany

1986 - 1990	Grundschule an der Saarner Str., Mülheim an der Ruhr
1990 - 1999	BMV Mädchengymnasium, Essen
1999 - 2001	Student of Landscape Ecology, University of Münster
2001 - 2002	ERASMUS-student, University of Alicante, Spain
2002 - 2004	Student of Landscape Ecology, University of Münster
2004 - 2007	PhD-student at the Institute for Landscape Ecology, University of Münster